GEOSCIENCE CANADA

JOURNAL OF THE GEOLOGICAL ASSOCIATION OF CANADA
JOURNAL DE L'ASSOCIATION GÉOLOGIQUE DU CANADA

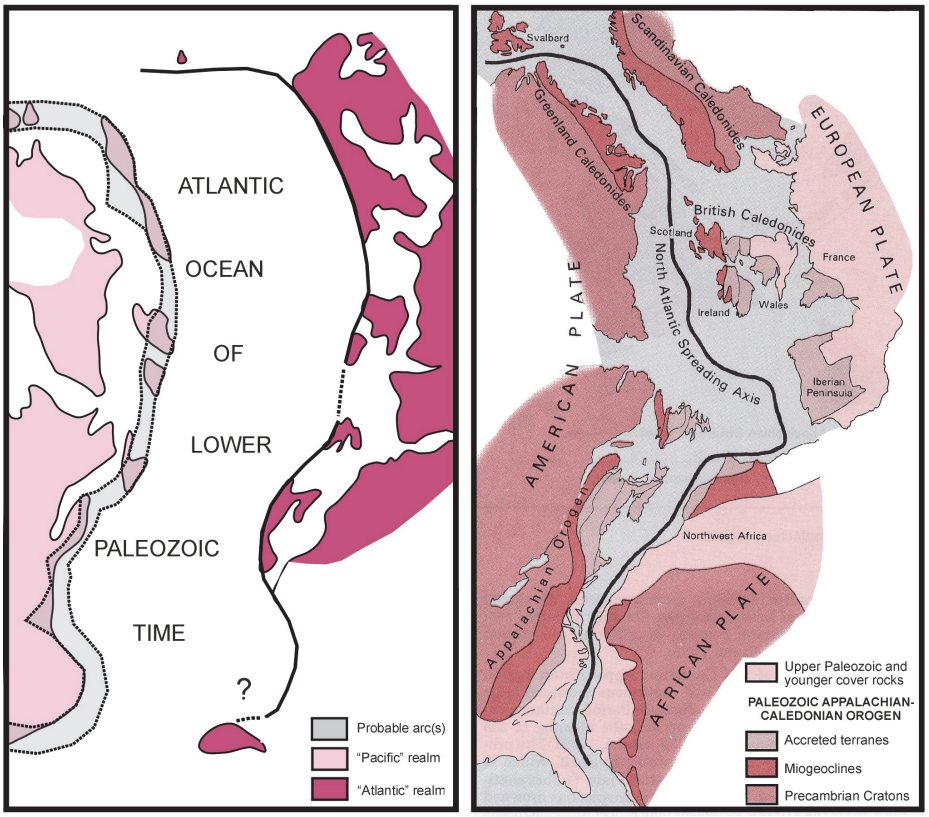

Do simmering hot spots influence entire orogenic zones?

Himalayan basalts – is there a LIP in the air?

The growing state of Winesconsin

The Wilson Cycle turns 50 – thoughts from the delivery room

GAC–MAC 2017: Back to where it began – Field trip previews

Review: Gold modelling – questioning the vein gangue

2016 VOLUME 43

Publisher/Éditeur
Geological Association of Canada
c/o Department of Earth Sciences
Memorial University of Newfoundland
St. John's NL Canada A1B 3X5
Tel: (709) 864-7660
Fax: (709) 864-2532
gacpub@mun.ca
gac@mun.ca
www.gac.ca

Print Edition: ISSN 0315-0941
Online Edition: ISSN 1911-4850

Volume 43

A journal published quarterly by the Geological Association of Canada, incorporating the Proceedings.
Une revue trimestrielle publiée par l'Association géologique du Canada et qui en diffuse les actes.

Those wishing to submit material for publication in Geoscience Canada should refer to the Instructions to Authors on the journal's website, www.geosciencecanada.ca

AUTHORS PLEASE NOTE:
Please use the web address http://journals.hil.unb.ca/index.php/GC/index for submissions; please do not submit articles directly to the editor.

The Mission of the Geological Association of Canada is to facilitate the scientific well-being and professional development of its members, the learned discussion of geoscience in Canada, and the advancement, dissemination and wise use of geosciences in public, professional and academic life. Articles in Geoscience Canada are freely available two years after their publication date, unless authors have arranged for immediate open access. Opinions expressed and interpretations presented are those of the authors and do not necessarily reflect those of the editors, publishers and other contributors. Your comments are welcome.

Cover Image: The changing views of the North Atlantic borderlands.
On the left is a redrawn coloured version of the hand-drawn Figure 3 from Tuzo's 1966 paper in Nature showing the concept of his 'Atlantic Ocean of Lower Paleozoic time.' On the right is a later reconstruction of the Appalachian - Caledonian Orogen by Hank Williams, from the Decade of North American Geology volume (Williams 1995), showing the spreading axis of the modern North Atlantic.

PRESIDENTIAL ADDRESS

Commitment, Collaboration and Communication: The Backbones of Geoscience*

Victoria Yehl, M.Sc., P.Geo.

Senior Geologist, British Columbia Securities Commission
Vancouver, British Columbia, Canada
Email: vyehl@hotmail.com

*Adapted from the Geological Association of Canada Presidential Address, as given June 1st, 2016 in Whitehorse at GAC–MAC 2016: Margins through Time.

This work, whether it be in the form of my original oral presidential address with a few slides for emphasis, or this later transition to a publication in the Association's flagship journal Geoscience Canada, is truly the most daunting part of being President of the Geological Association of Canada (GAC®). I have pondered on what topic to speak to, and how I would present it, ever since I made the decision to accept the Vice-President role – I did know that this was coming. The past-presidents on the nominating committee do not make it any easier – their advice that "you can speak about anything you want" did not help at all! Good grief! To address peers, colleagues, mentors and students to speak about anything; why would anyone take this on? I knew, however, from almost the first moment that I wanted to address the dynamic nature of geoscience and the things that are needed to preserve it – hence, the three C's in my title: Commitment, Collaboration and Communication. This idea inadvertently answered the question of why anyone would actually take on the presidency of GAC. Such things are done by those who are truly passionate about geoscience, and care about these ideas. I have been honoured to serve in this way.

The title and the messages have come from a place in my mind that struggles to share what it is we do and how we keep up with the ever-evolving hypotheses, ideas and technologies in our dynamic vocation. How do we as geoscientists, or as a wider organization, ever keep up with advances? I think the answer is simply put – being a geoscientist is not just a job or a career path – it is truly a lifestyle (choice) and those of us who are truly passionate about geoscience ('lifers,' as I call us), have a very real and heart-felt commitment to what we do and how we do it. We miss birthdays, anniversaries, weddings, funerals, and much more, leading some around us to suggest that we do not care, but that could not be further from the truth. Geoscientists are passionate folk who are so extremely focused on what they are doing that they often forget that there are other things besides their samples, drills, rocks, laboratories, classrooms or stock prices. Fortunately, there are many things we can do to accentuate our knowledge and many forums through which we can improve, evolve and be successful together as geoscientists. The passion we hold for our calling is an important part of this, but there are more specific things that are essential to the success and future of our profession.

I feel that success in the geosciences is highly dependent on Commitment, Collaboration and Communication. Without these, discoveries are not made, understanding is not advanced and the building blocks of our resource-based lives will not exist. Those who contribute to associations such as the Geological Association of Canada, the Society of Economic Geologists (SEG) or the Prospectors and Developers Association of Canada (PDAC), to name just a few, help all of us to stay current and achieve success in our work. The people who serve in these kinds of organizations truly do this out of a sense of unstated duty – that is, Commitment – and it is this that defines the 'lifers' I have already alluded to. No one is making money offering a short course or writing a textbook, or writing a scientific article for that matter; you do these things because you are fully committed to your passion, your chosen field. In mineral exploration or scientific research, or any aspect of geoscience, Collaboration is a vital part of how we approach things – we can achieve far more working together than alone. This in itself depends on Communication, not just within our discipline, but beyond it. There is more often than not a misconception as to what geoscientists actually do, and we all should feel the need to educate others.

Many people think that what we do is very adventurous, bordering on cavalier or even like the exploits of Indiana Jones – but the truth is very different. Geoscientists actually act with great planning and precision after doing lots of background work and research, and results may take many years to create minor advancements. Also, what we do varies widely (in location, accommodation and activity) and it changes over time – from field or laboratory-based work, to interpretation and presentation, to modelling and mining and beyond. It is far broader than most realize. Geoscience is a dynamic field, and never static. We are involved in mineralogy, climatology, materials supply, chemistry, construction, conservation, paleontol-

Geoscience Canada, v. 43, http://www.dx.doi.org/10.12789/geocanj.2016.43.106 pages 227–230

ogy, energy, forensics and even in medicine. But why should we try to communicate the breadth of what we do? The answer is simple – because we find and provide the materials that give us things, from space shuttles and supercomputers to mobile phones, and from posh jewellery to simple forks, knives and spoons. The value of geoscience is generally poorly explained to anyone other than those we work most closely with, even though we would not have our 21st century technological society without geoscience. As the saying goes, "If it cannot be grown, it must be mined," and the latter part always requires geoscience in some way. Nevertheless, mining is often construed as a negative by current society and its merits remain often unsung. Many associations, including the GAC, have geoscience outreach programs that focus on communicating to the public, to foster collaborations with other branches of geoscience, and provide information to government, educational institutions and others explaining what geoscience is, what it does, and why it is needed. This effort must continue! Particularly if organizations such as GAC are to continue to provide the hub, the nexus, the coalescence point that we all utilize.

Why should or would anyone want to be a geoscientist in the first place and why should geoscientists volunteer and/or get involved? There is a marvellous, unattributed quote that explains this well:

> "*Geology is a magnificent and unique science. What makes geoscience unique, you may rightly ask; well, a good geologist has to know something of everything: physics, chemistry, geography, math, biology, engineering, and many, many more. But it's worth it, oh how it's worth it!*" [1]

Geoscience of any type is not a 'sit still' career; there are always new things to apply, to do, to test and to explore. These things are done through working with our colleagues and peers and sharing our ideas, theories and geoscience knowledge. We do not do our work alone, nor do we do it without some kind of unrelenting drive to discover and achieve. We geoscientists also have tremendous capacity to deal with economic cycles, extreme conditions, weather, changing cultures, a great variety of languages and customs, and much more. All of this comes from the first of the C's – the Commitment that I have alluded to as defining the 'lifers' of geoscience. There is so much we can do, and so many areas where we can contribute in our varying specialty fields, but all require a strong focus, and a drive to achieve, discover and advance. In other words, they demand Commitment.

As we all know, geoscience is always evolving; it can be truly exciting and inspiring as there are a multitude of techniques, theories, technological advancements and innovations that can help us grow and to develop as geoscientists. We need to be aware of all of these new things and committed to undertaking the work to grasp them. As John Thompson stated at the Association for Mineral Exploration's (AME) annual Mineral Roundup conference:

> *"Making quality discoveries is, however, harder than ever and, in addition to technical challenges, exploration is complicated by social, legal and other non-technical issues. Over the last 50 years, major step changes in exploration have resulted from radical advances in our understanding of ore-forming processes; new geophysical, geochemical and remote sensing technologies; and new ways to integrate and interrogate data."* [2]

All geoscientists need to adapt to and solve progressively greater challenges to make those next discoveries, identifications and develop new understanding. Keeping our discipline up-to-date and meeting these challenges brings me to the other two C's – Collaboration and Communication. The ways in which we collaborate and communicate include field schools, field trips, tours, visits, focused workshops, short courses, and writing papers and articles. Much like geoscience discoveries or developments, these things do not happen in a vacuum. Other aspects of Collaboration and Communication include mentorship and our participation in conferences, trade shows, short courses and colloquia. Most of these ways to work together require a host, a venue or a champion that provides a mechanism to share our knowledge as it grows. Annual conferences, regularly published journals and newsletters, and maintained networks, including those on social media such as Facebook and LinkedIn, provide outlets for us to achieve this collaboration. Organizations such as GAC, MAC, CSPG, PDAC, SEG, AME, and many others consistently provide these venues and pathways. So in the end, Collaboration and Communication depend vitally upon the Commitment of those who keep such entities viable.

However, over the past 10–20 years most of these organizations have experienced dwindling sponsorships, decreasing memberships and even further contractions in the number of volunteers that help them survive, thrive and provide us with these crucial opportunities. We all have used, and keep on our shelves, important key reference volumes, such as *Facies Models, Minerals Deposits of Canada* and the *Atlas of Alteration*. These are just a few examples of widely-known geoscience contributions that have had an influence well beyond Canadian borders. Such contributions do not write themselves, but come from those who are willing to give both their time and their knowledge so that the rest of us can benefit. Diminishing participation in geoscience organizations will, over time, limit our development as scientists and will reduce what we provide back to the world around us. What we do as geoscientists and how we share it truly matters to the world. We should be proud of what we do and the importance of our work. When journalist Rex Murphy spoke at AME's Roundup 2016, he reminded geoscientists to not be ashamed of what we do, as it is critical to the way of life we have come to want, need, and increas-

[1] Sourced from ZME Science at www.zmescience.com
[2] Dr. John Thompson, AME Roundup 2016, Vancouver, BC

ingly expect. We mitigate hazards, identify and foster the supply of the raw materials that we need, work to protect the environment by better understanding our surroundings, and we do much more besides those 'mere' things. The dissemination and sharing of this knowledge helps society respond to natural hazards, manage our water and air, and in the end manage all of our resources. It also encourages a wider understanding of how the world around us works, what benefits not only geoscientists, but all of society.

The comic strip *Frank and Ernest* [3] has a published panel that shows three apparent expeditionists (complete with pith helmets and rock hammers), and one says to the other two: "I'm an internationally renowned geologist. Would you two stop referring to me as a Rock Star?" I believe we geoscientists should embrace the term 'Rock Star' and work hard to bring our science and its benefits to our peers and to the rest of the world – we have a lot to offer. To do this we need to be adept at all of my three C's. Commitment means that we need to keep up with our profession, support it and stay current; Collaboration means that we need to work with our peers and others to make discoveries and advancements; and, last but not least, Communication means that we need to share what we do within our profession, and with the public.

It is especially vital that more of us engage with those professional associations and organizations that we have benefited from in the past – these organizations need our contributions if they are to continue to be the repositories and forums that we have all come to depend upon. These organizations are both the foundation and the back bone of what we do; they give us access to the knowledge, information, ideas and the people that we need to succeed, both individually and collectively.

Commitment, Collaboration and Communication are the reasons why anyone would want to be the president of, or actively participate in, an organization such as the GAC. With fewer individuals willing to give their time and energy to such organizations, there is a real danger that we may lose them and also the knowledge they make accessible to all geoscientists. So in closing, I wish to challenge all geoscientists – be Committed, Collaborate and Communicate well. And above all, become involved in geoscience organizations, if you are not already doing so, and please stay involved if you are already part of this vital framework. Your colleagues and your profession need you, and we will always achieve more together than we can as individuals.

I wish you all the best for continued success in your pursuits, and it has been an honour to have served as your *GAC president.*

Cheers,
Vicki

[3] As created by Bob and Tom Thaves © 2000

http://www.dx.doi.org/10.12789/geocanj.2016.43.106

GEOLOGICAL ASSOCIATION OF CANADA
(2016-2017)

CORPORATE MEMBERS

PLATINUM

MEMORIAL UNIVERSITY

GOLD

AngloAmerican

Anglo American Exploration (Canada) Ltd.

Northwest Territories Geological Survey

SILVER

ROYAL TYRRELL MUSEUM

BRITISH COLUMBIA GEOLOGICAL SURVEY

OFFICERS

President
Graham Young

Vice-President
Stephen Morison

Past President
Victoria Yehl

Secretary-Treasurer
James Conliffe

COUNCILLORS

Ihsan Al-Aasm
Alwynne Beaudoin
Oliver Bonham
James Conliffe
Louise Corriveau
Andy Kerr
Stephen Morison
David Pattison
Sally Pehrsson
Liz Stock
Dène Tarkyth
Chris White
Victoria Yehl
Graham Young

STANDING COMMITTEES

Communications: Sally Pehrsson

Finance: Dène Tarkyth

GAC Lecture Tours: Alwynne Beaudoin

Publications: Chris White

Science Program: Louise Corriveau

ANDREW HYNES SERIES: TECTONIC PROCESSES

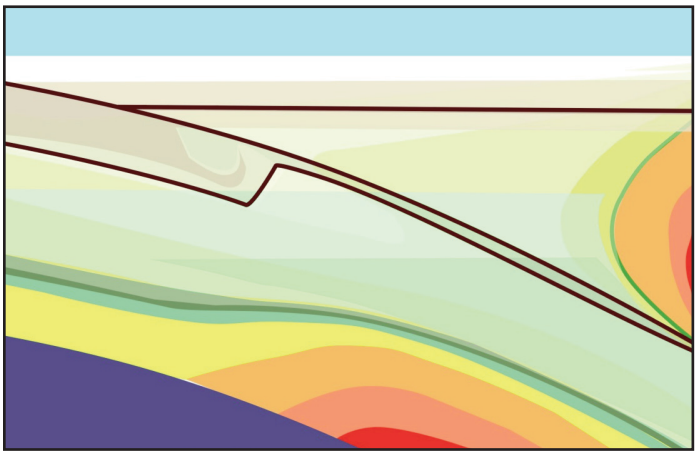

The Role of the Ancestral Yellowstone Plume in the Tectonic Evolution of the Western United States

J. Brendan Murphy

Department of Earth Sciences
St. Francis Xavier University
Antigonish, Nova Scotia, B2G 2W, Canada
E-mail: bmurphy@stfx.ca

SUMMARY

Plate reconstructions indicate that if the Yellowstone plume existed prior to 50 Ma, then it would have been overlain by oceanic lithosphere located to the west of the North American plate (NAP). In the context of models supporting long-lived easterly directed subduction of oceanic lithosphere beneath the NAP, the Yellowstone plume would have been progressively overridden by the NAP continental margin since that time, the effects of which should be apparent in the geological record. The role of this 'ancestral' Yellowstone plume and its related buoyant swell in influencing the Late Mesozoic–Cenozoic tectonic evolution of the southwestern United States is reviewed in the light of recent field, analytical and geophysical data, constraints provided by more refined paleogeographic constructions, and by insights derived from recent geodynamic modelling of the interaction of a plume and a subduction zone.

Geodynamic models suggesting that the ascent of plumes is either stalled or destroyed at subduction zones have focused attention on the role of gaps or tears in the subducted slab that permit the flow of plume material from the lower to the upper plate during subduction. These models imply that the ascent of plumes may be significantly deflected as plume material migrates from the lower to the upper plate, so that the connection between the hot spot track calculated from plate reconstructions and the manifestations of plume activity in the upper plate may be far more diffuse compared to the more precise relationships in the oceanic domain. Other geodynamic models support the hypothesis that subduction of oceanic plateau material beneath the NAP correlates with the generation of a flat slab, which has long been held to have been a defining characteristic of the Laramide orogeny in the western United States, the dominant Late Mesozoic–Early Cenozoic orogenic episode affecting the NAP.

Over the last 20 years, a growing body of evidence from a variety of approaches suggests that a plume existed between 70 and 50 Ma within the oceanic realm close to the NAP margin in a similar location and with similar vigour to the modern Yellowstone hot spot. If so, interaction of this plume with the margin would have been preceded by that of its buoyant swell and related oceanic plateau, a scenario which could have generated the flat slab subduction that characterizes the Laramide orogeny.

Unless this plume was destroyed by subduction, it would have gone into an incubation period when it was overridden by the North American margin. During this incubation period, plume material could have migrated into the upper plate via slab windows or tears or around the lateral margins of the slab, in a manner consistent with recent laboratory models. The resulting magmatic activity may be located at considerable distance from the calculated hot spot track.

The current distribution of plumes and their buoyant swells suggests that their interaction with subduction zones should be common in the geological record. If so, the Late Mesozoic–Cenozoic evolution of western North America may represent a relatively modern analogue for such processes.

RÉSUMÉ

Les reconstitutions de plaques montrent que si le panache de Yellowstone avait existé avant 50 Ma, il aurait été recouvert par la lithosphère océanique située à l'ouest de la plaque nord-américaine (PNA). Dans le contexte de modèles de subduction de longue durée vers l'est de la lithosphère océanique sous la PNA, avec le temps, la marge continentale de la PNA aurait

progressivement neutralisé le panache de Yellowstone, et on devrait en voir les effets dans le registre géologique. Le rôle de ce panache de Yellowstone « ancestral » et de son renflement de surface régional associé sur l'évolution tectonique du Sud-ouest des États-Unis au Mésozoïque–Cénozoïque tardif est reconsidéré ici à la lumière de données récentes, de terrain, analytiques et géophysiques, de contraintes découlant de constructions paléogéographiques affinées, et d'idées nouvelles découlant d'une modélisation géodynamique récente de l'interaction d'un panache et d'une zone de subduction.

Les modèles géodynamiques suggérant que l'ascension des panaches soient bloquée ou détruite dans les zones de subduction ont attiré l'attention sur le rôle d'hiatus ou de déchirures dans la plaque subduite qui permettent le passage du matériau du panache de la plaque inférieure à la plaque supérieure pendant la subduction. Ces modèles impliquent que le flux ascendant des panaches peut être sensiblement dévié alors que le matériau du panache migre de la plaque inférieure à la plaque supérieure, de sorte que la connexion entre la trace du point chaud calculée à partir des reconstructions de la plaque et les manifestations de l'activité du panache dans la plaque supérieure peut être bien plus diffuse que sa contrepartie du domaine océanique. D'autres modèles géodynamiques appuient l'hypothèse selon laquelle la subduction du matériau de plateau océanique sous la PNA correspond à la génération d'une plaque plate, particularité qui a longtemps été considérée comme caractéristique déterminante de l'orogenèse de Laramide dans l'ouest des États-Unis, épisode orogénique dominante de la fin du Mésozoïque au début du Cénozoïque affectant la PAN.

Au cours des 20 dernières années, un nombre croissant d'éléments de preuve provenant d'une variété d'approches suggèrent qu'un panache existait bien entre 70 et 50 Ma dans le domaine océanique près de la marge la PNA, en un endroit et avec une vigueur similaires au point chaud de Yellowstone moderne. Le cas échéant, l'interaction de ce panache avec la marge aurait été précédée de celle de son renflement de surface et du plateau océanique connexe, scénario qui aurait pu générer la subduction de la plaque plate qui caractérise l'orogenèse Laramide.

À moins que ce panache n'ait été détruit par subduction, il serait entré dans une période d'incubation lorsqu'il a été recouvert par la marge nord-américaine. Au cours de cette période d'incubation, le matériau du panache aurait pu migrer dans la plaque supérieure par des fenêtres ou déchirures de la plaque ou autour des marges latérales de la plaque, conformément aux modèles récents de laboratoire. La trace de l'activité magmatique résultante pourrait se trouver alors à une distance considérable de la trace du point chaud calculée.

La distribution actuelle des panaches et de leurs renflements de surface suggère que leur interaction avec les zones de subduction devrait être un phénomène courant dans le registre géologique. Si tel est le cas, l'évolution du Mésozoïque–Cénozoïque tardif de l'Amérique du Nord occidentale peut représenter un analogue relativement moderne pour de tels processus.

Traduit par le Traducteur

INTRODUCTION

Although not universally accepted (e.g. Anderson 1994; Foulger and Natland 2003; King 2007), hot spots are considered to reflect upwelling of sub-lithospheric mantle plumes (Morgan 1971, 1972). In a classical sense, a sub-oceanic mantle plume is envisaged to have a central conduit which can underplate a 400–1000 km diameter area of the lithosphere, creating an oceanic plateau above a buoyant swell (Richards et al. 1988; Sleep 1990). This buoyant swell develops a pronounced asymmetry as it becomes elongated 'downstream,' in some instances by as much as 2500 km, by the motion of the overriding plate (McKenzie 1983; Sleep 1990; Geist and Richards 1993; Ribe and Christiansen 1994). Estimates for the area of oceanic plateaus that might have been overridden by the North American plate (NAP) range up to 0.48 million km^2 (comparable in size to the state of California; Liu et al. 2010), and imply that the plateaus are significantly smaller in areal extent than the swell.

Although plumes may rise from different boundary layers in the mantle (Courtillot et al. 2003), recent tomographic images and geodynamic models suggest that many emanate from the edges of regions known as Large Low Shear Velocity Provinces (LLSVPs) which are located near the core–mantle boundary (e.g. Williams et al. 1996; Torsvik et al. 2006; Burke et al. 2008; Tan et al. 2011; Hassan et al. 2015). Instabilities within the mantle result in plumes that can be entrained, deformed and displaced by large-scale subduction-induced mantle flow (Steinberger and O'Connell 1998, 2000; Davaille et al. 2003; Steinberger et al. 2004; Davaille and Vatteville 2005). As a result, hot spots above the plumes move relative to one another, although inter-hot spot motion is much less than the motion of the lithospheric plates (O'Neill et al. 2005).

Assuming that their present distribution is representative of the past, overriding of plumes at convergent margins should be common in the geological record. Fletcher and Wyman (2015) noted that 29% of mantle plumes have been located within 1000 km of a subduction zone over the past 60 Ma (Fig. 1), a statistic that also implies interaction between the subduction zone, buoyant swell and oceanic plateau should precede that of the plume itself. Plumes may vary in their buoyancy flux and the dimensions of their topographic swell (Sleep 1990). As the features of individual plumes and subduction zones are both highly variable, the features produced by plume–slab interactions may also be highly variable, and therefore difficult to decipher in the geologic record.

Oppliger et al. (1997) and Murphy et al. (1998, 2003) proposed that the Mesozoic–Cenozoic orogenic activity in western North America was profoundly influenced by plume–slab interactions, in which the ancestral Yellowstone plume, preceded by an oceanic plateau and its buoyant swell, were progressively overridden by the westerly migrating margin of the NAP (Fig. 2a, b). This style of 'plume-modified orogenesis' has also been used to explain the origin of the Karoo–Ferrar flood basalts (Dalziel et al. 2000), as well as Mesoproterozoic orogenesis in eastern and central Australia (Betts et al. 2007, 2009).

The model as applied to western North America has two fundamental requirements: (i) that the Yellowstone plume

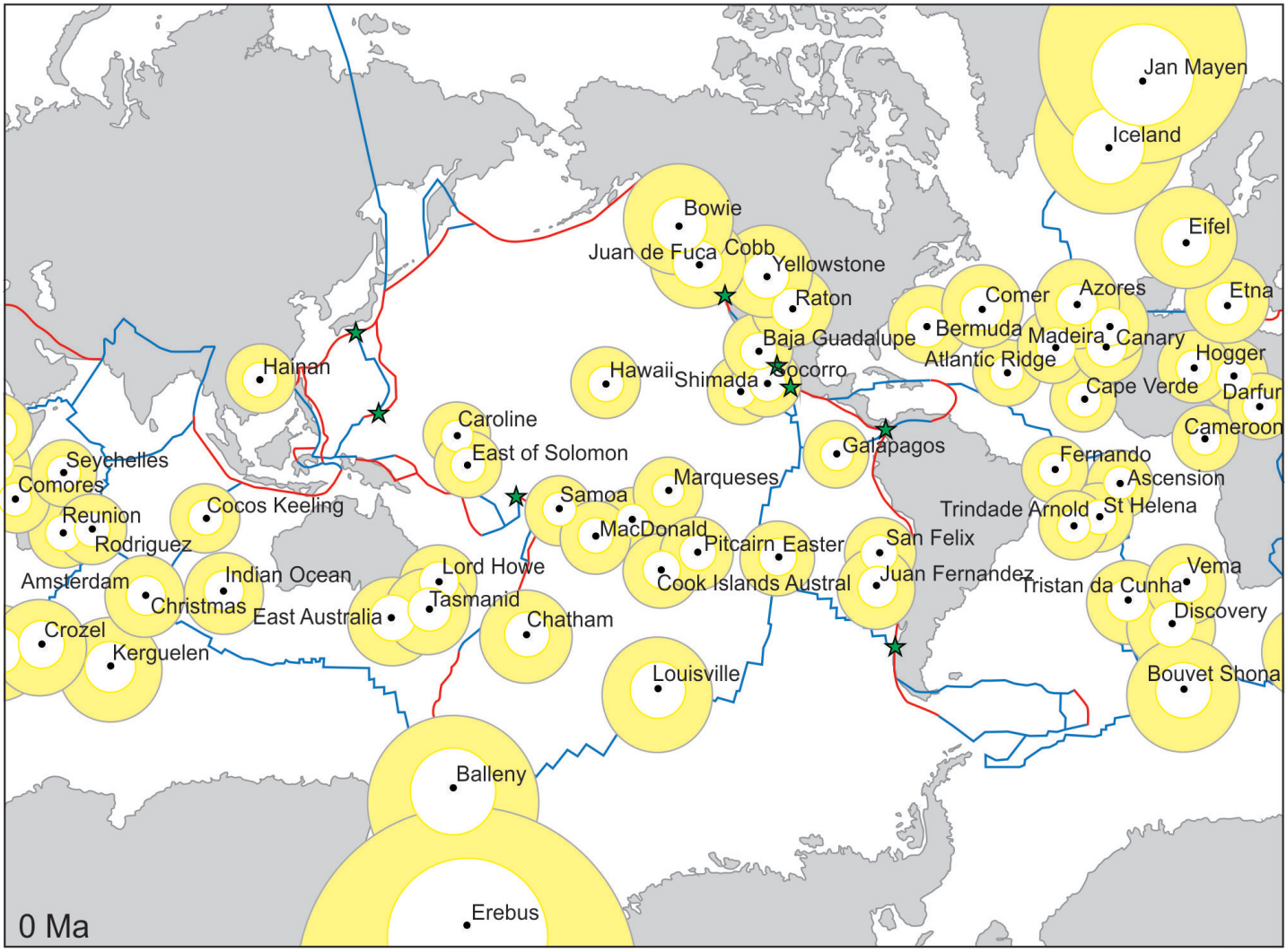

Figure 1. After Fletcher and Wyman (2015) showing zone of potential (500 km, 1000 km) for modern plumes to interact with modern subduction zones (red lines; after Seton et al. 2012). Green stars denote slab windows where a ridge intercepts a subduction zone.

existed prior to ca. 50 Ma, before which reconstructions indicate the plume would have been located beneath oceanic lithosphere (Engebretson et al. 1985; O'Neill et al. 2005; Seton et al. 2012), and (ii) that plumes maintain their integrity where they are affected by subduction processes.

If the Yellowstone plume existed prior to ca. 50 Ma, then plate reconstructions indicate that its buoyant swell, plateau, as well as hot spot oceanic islands with plume-type chemistry, would have collided with the convergent margin of western North America. Such events should be recorded in the geological evolution of western North America.

With regard to the second requirement, recent laboratory studies suggest that the integrity of plumes may be severely affected by subduction processes in that their ascent may be stalled, severely distorted or even destroyed by slab-driven subduction processes (e.g. Kincaid et al. 2013; Druken et al. 2014). On the other hand, 3D numerical models (Betts et al. 2012, 2015) identify combinations of plume and slab properties that may facilitate the transfer of plume material from the lower to the upper plate especially via gaps or tears that may develop in the slab.

The purpose of this article is to re-assess the viability of the underlying requirements for plume–slab interaction to have influenced the Mesozoic–Cenozoic evolution of the western United States in the light of recent laboratory and numerical models, tomographic data, improved plate tectonic reconstructions, as well as more recent field-based studies.

MESOZOIC–EARLY CENOZOIC OROGENESIS

It is widely recognized that episodic accretionary orogenic events have dominated the tectonic evolution of the western margin of the NAP since the Late Paleozoic, resulting in the Antler (Mississippian), Sonoma (Permian–Triassic), Nevadan (Jurassic) and Sevier (Early Cretaceous) orogenies. These events are widely interpreted to reflect predominantly eastward-dipping subduction of the Farallon oceanic plate beneath North America, which at various times in the Mesozoic also produced the voluminous ca. 130–85 Ma Cordilleran

http://www.dx.doi.org/10.12789/geocanj.2016.43.105

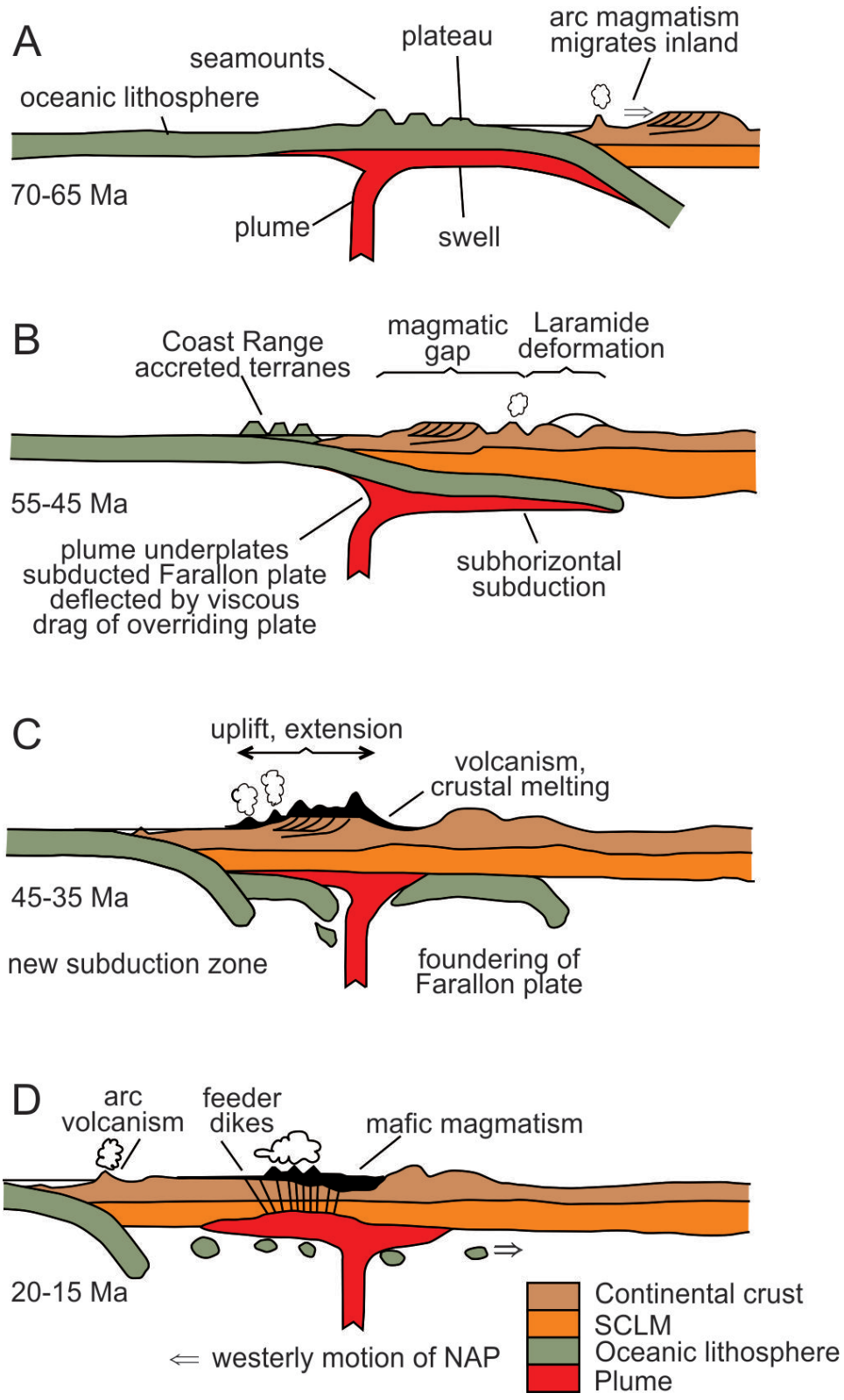

Figure 2a. Schematic diagram (after Murphy et al. 1998) showing late Mesozoic–Tertiary evolution of the southwestern United States at about 40°N (current latitude)and its proposed relationship to the ancestral Yellowstone plume. The plume is stationary, and the North American plate (NAP) moves progressively westward. (A) Plume is beneath oceanic crust where it creates oceanic terranes that subsequently accrete to NAP (Duncan 1982; Johnston et al. 1996). NAP begins to override the oceanic plateau and buoyant swell. (B) NAP continues to override the plateau and swell, resulting in flat-slab subduction, and eventually overrides the plume. (C) Assimilation of subducted portion of Farallon slab by plume, leading to generation of voluminous intracrustal melts, brittle deformation and reestablishment of dipping subduction zone at periphery of NAP. (D) 20–15 Ma breakthrough of plume-related bimodal magma, formation of dike complexes and flood basalts. SCLM: Sub-continental lithospheric mantle.

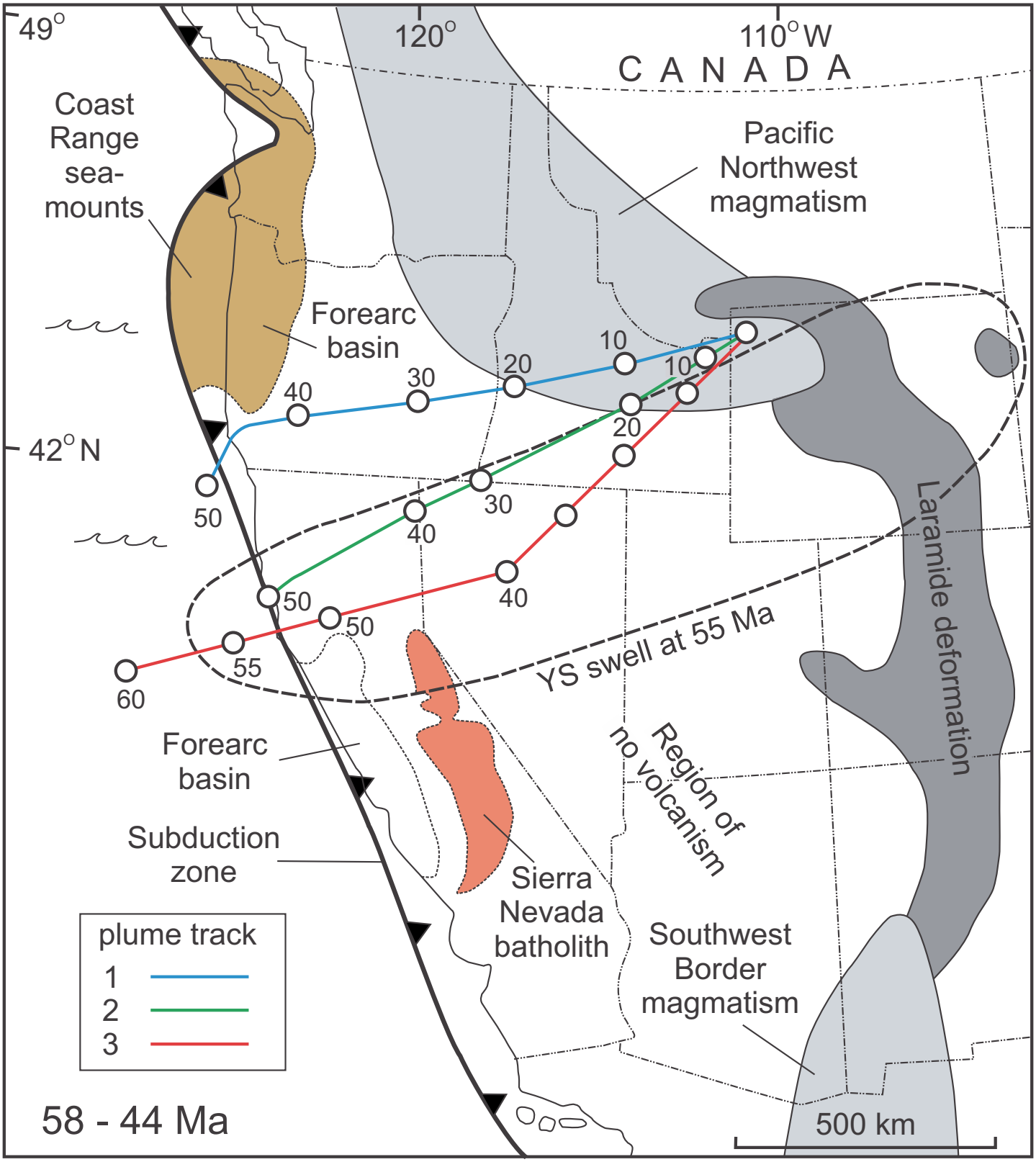

Figure 2b. Simplified mid-Eocene tectonic map of the Cordillera (modified after Dickinson 1991; Burchfiel et al. 1992; Murphy et al. 1998) showing three potential tracks of Yellowstone plume from its oceanic position before 50 Ma to its present position beneath Yellowstone (see Wells et al. 2014). Track 1 derived from O'Neill et al. 2005; Track 2 from Müller et al. 1993; Track 3 from Murphy et al. 1998. Dashed line indicates approximate region of a proposed buried plume-related swell ca. 55 Ma for Yellowstone plume following Track 3 (YS swell at 55 Ma).

http://www.dx.doi.org/10.12789/geocanj.2016.43.105

batholiths (e.g. Hamilton 1969; Dewey and Bird 1970; Lipman et al. 1972; Kistler and Peterman 1973, 1978; Dickinson and Snyder 1978; Coney et al. 1980; DePaolo 1981; Livaccari et al. 1981; Severinghaus and Atwater 1990; Burchfiel et al. 1992; Dickinson and Lawton 2001; Saleeby 2003; Busby 2004, 2012; Dickinson 2004; Monger 2014).

A rival model (see discussion in Hoffman 2013), supported by tomographic images of a vertical slab wall extending to a depth of 2000 km in the mantle (Sigloch and Mihalynuk 2013), holds that the earlier orogenic events reflect westerly dipping intra-oceanic subduction and episodes in the assembly of a superterrane (or ribbon continent) located to the west of North America (e.g. Johnston 2001, 2008; Hildebrand 2009; Hildebrand and Whalen 2014) that collided with the passive margin of North America at either ca. 150 Ma (SAYBIA; Johnston 2001, 2008; Johnston and Borel 2007) or between 125 and 100 Ma (RUBIA; Hildebrand 2009). There are variants within this model. According to Johnston (2001, 2008), the collision of SAYBIA resulted in extensive oroclinal development in the Canadian Cordillera, whereas Hildebrand and Whalen (2014) claimed that the westward subduction produced the oldest (ca. 130–100 Ma) phases of the Cordilleran batholiths as well as collision with NAP at ca. 100 Ma, which was followed by slab failure and consequent asthenospheric upwelling that resulted in the younger (100–85 Ma) Cordilleran batholiths.

In both models, there is widespread agreement that (i) most terranes had accreted to North America by ca. 80 Ma, and (ii) the Late Cretaceous to Eocene evolution of the Cordillera was influenced by interactions between the North American, Farallon, and Kula plates, and especially by the northward migration of the triple junction between them and the consequent northward propagation of subduction (Atwater 1970, 1989; Kelley and Engebretson 1994). These interactions may be even more complicated if the more recently hypothesized Resurrection plate, which would have been completely subducted by ca. 50 Ma, is verified (Haeussler et al. 2003; McCrory and Wilson 2013; Wells et al. 2014; Fig. 3). Terranes that accreted during the Tertiary include Siletzia (Fig. 4), which is exposed for 600 km along the Pacific Northwest (e.g. Snavely et al. 1968; Wells et al. 1984, 2014; Babcock et al. 1992, 1994). These terranes were translated northwards within the Kula plate and the collision of Siletzia with the NAP is interpreted to be responsible for the South Vancouver Orocline (Johnston et al. 1996; Johnston and Acton 2003). Eastward-dipping subduction then initiated along the western margin of the accreted Siletzia, producing a north–south Cascade volcanic arc, beginning at ca. 42 Ma (Fig. 3).

Between ca. 80 Ma and 45 Ma, a series of enigmatic events occurred in the southwestern United States that are traditionally assigned to the Laramide orogeny (Burchfiel et al. 1992). These events include widespread thick-skinned deformation, basement uplifts as much as 1500 km (Black Hills, South Dakota) from the continental margin, as well as simultaneous contraction and crustal thickening in both the foreland and hinterland. Voluminous magmatism ceased, and relatively minor magmatism with subduction-related geochemistry migrated inland. These features have been attributed to 'flat-slab subduction,' a region where a gently inclined subduction zone ca. 500 km wide extended about 700 km into the continental interior (Coney and Reynolds 1977; Dickinson and Snyder 1978; Livaccari et al. 1981; Severinghaus and Atwater 1990; Burchfiel et al. 1992; Saleeby 2003). According to Bird (1988), traction associated with subduction of the shallow slab could have stripped away the mantle lithosphere beneath the North American crust and transmitted the stress capable of causing the thick-skinned deformation in the foreland. In this context, the resumption of voluminous magmatism in the Eocene is attributed to the breakup and foundering of the Farallon slab (Humphreys 1995) and the re-initiation of normal-angle subduction, followed in the late Eocene by voluminous ignimbrite associated with localized extension and emplacement of metamorphic core complexes (Coney 1979; Davis and Coney 1979; Gans et al. 1989).

The flat-slab model is supported by *P–T* studies of lawsonite-bearing eclogite xenoliths in Oligocene kimberlite pipes that intrude the Colorado Plateau. These xenoliths are thought to have originated in the Farallon slab, and equilibrated at depths between 90 and 160 km and at temperatures between 500 and 700°C (Usui et al. 2003). In the Canadian and Mexican portions of the Cordillera, however, coeval development of a magmatic arc within 300 km of the trench indicates that the effects of flat-slab subduction were limited to the southwestern United States (English et al. 2003), a feature that implies segmentation of the Farallon slab into flat and steep zones (Saleeby 2003).

Rival models for the Laramide orogeny include the collision of a superterrane at ca. 125 Ma, with North America on the lower plate, followed by voluminous ca. 100–85 Ma magmatism associated with slab break-off (e.g. Hildebrand 2009, 2014; Hildebrand and Whalen 2014). As these events would have occurred before the classic Laramide events, they do not preclude the shallow-slab subduction model, which could have been initiated in the aftermath of this collision. English and Johnston (2004) pointed out, however, that fold and thrust belts in Canada and Mexico are coeval with those within the putative flat-slab region, and that a viable explanation for synchronous contraction along the entire length of the orogen remains enigmatic.

The 'hit-and-run' model of Maxson and Tikoff (1996), which attributes Laramide orogenesis to the Late Cretaceous collision followed by northward translation of the colliding terranes would refute the flat-slab model because of the timing of these hypothesized events. This model builds on the controversial Baja–BC hypothesis (Irving 1985; Irving et al. 1985, 1995, 1996), in which a wealth of paleomagnetic data implies up to 3000 km of northward (i.e. dextral) translation of terranes relative to cratonic North America since 70 Ma (Beck 1992; Wynne et al. 1995; Johnston et al. 1996; Kent and Irving 2010). Although plate reconstructions (Atwater 1970; Engebretson et al. 1985) and field evidence for dextral transpression (Oldow et al. 1989; Maxson and Tikoff 1996) are consistent with dextral translation along the North American margin of terranes embedded in the Kula plate, identifying the structures that might accommodate such a large displacement remains

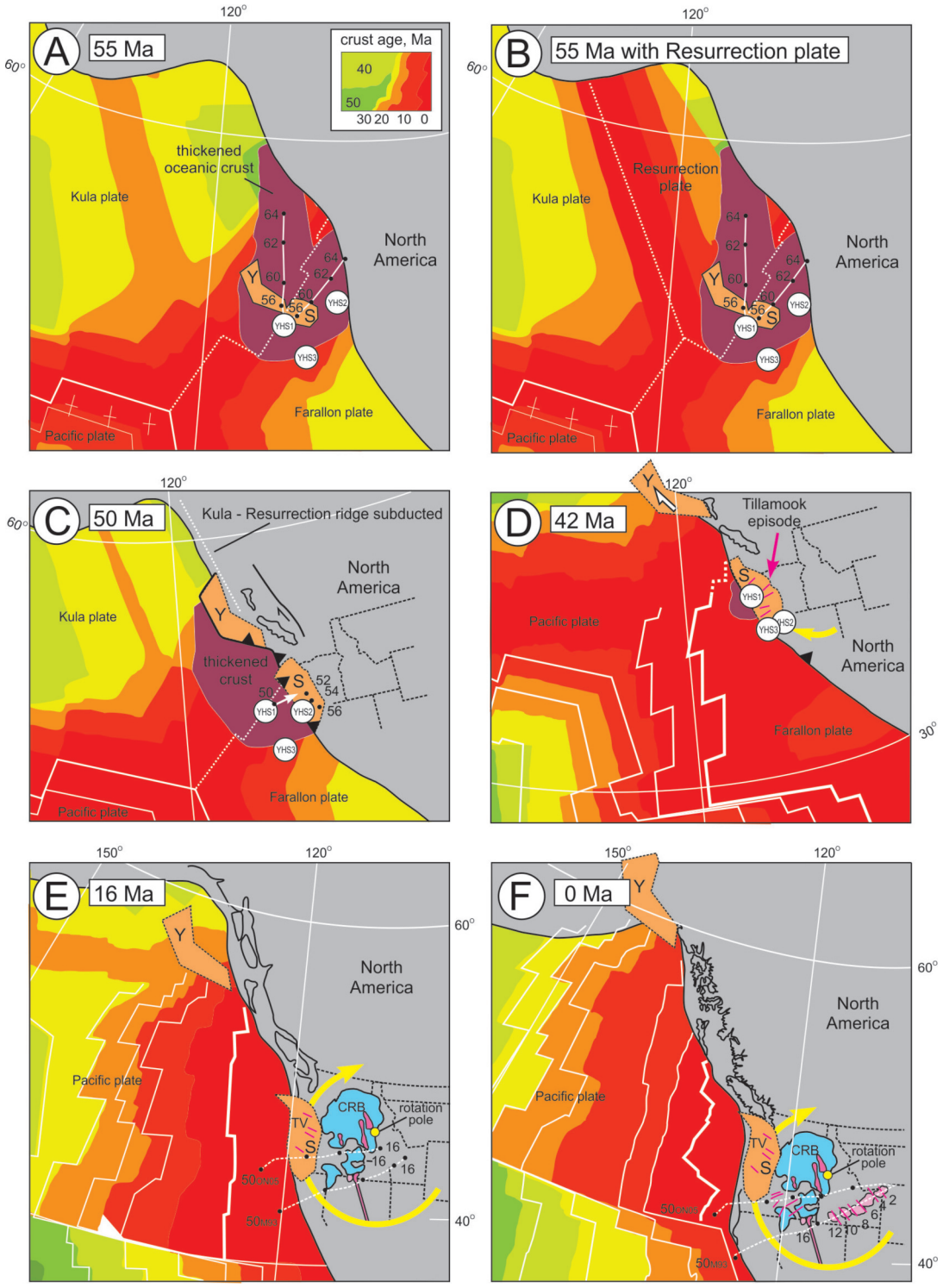

Figure 3. Schematic reconstruction of the Paleogene–Recent reconstruction of the Pacific Northwest (after Wells et al. 2014). (A) examines Pacific–Kula–Farallon–North American plate interactions, and (B) examines the additional effects of the putative Resurrection plate. Plate reconstruction model of Seton et al. (2012) showing three possible locations for the ancestral Yellowstone hot spot (YHS) as shown by Wells et al. (2014). YHS1 is the location relative to North American plate (NAP) derived from the moving hot spot reference frame (O'Neill et al. 2005; ON05); YHS2 from the plate circuit reference frame of Müller et al. (1993; M93) and YHS3 from a reference frame defined by moving hot spots in the Pacific, Atlantic, and Indian oceans (Doubrovine et al. 2012). Hot spot reference frame paths for YH1 (ON05; O'Neill et al. 2005) and YH2 (M93; Müller et al. 1993) shown in E and F by dotted lines; small dots on path show location every 10 m.y.

YHS is centered at or near the Kula–Farallon Ridge in (A) and the Resurrection–Farallon Ridge in (B). Oceanic (Siletzia, S, and the conjugate Yakutat, Y) terranes form at ridge-centred hot spot at ca. 55 Ma. (C) Accretion of oceanic terranes by 50 Ma. (D) Progressive overriding of the YHS by NAP, producing northwest-directed extension magmatism in the forearc. (E) CRB – Steens and Columbia River Basalt provinces. Yellow arrow (E and F) shows potential clockwise rotation of Coast Range which moves plume products progressively away from the hot spot track. (F) YHS under Yellowstone; age progression of Snake River Plain from 16 Ma to 0 Ma shown in pink.

http://www.dx.doi.org/10.12789/geocanj.2016.43.105

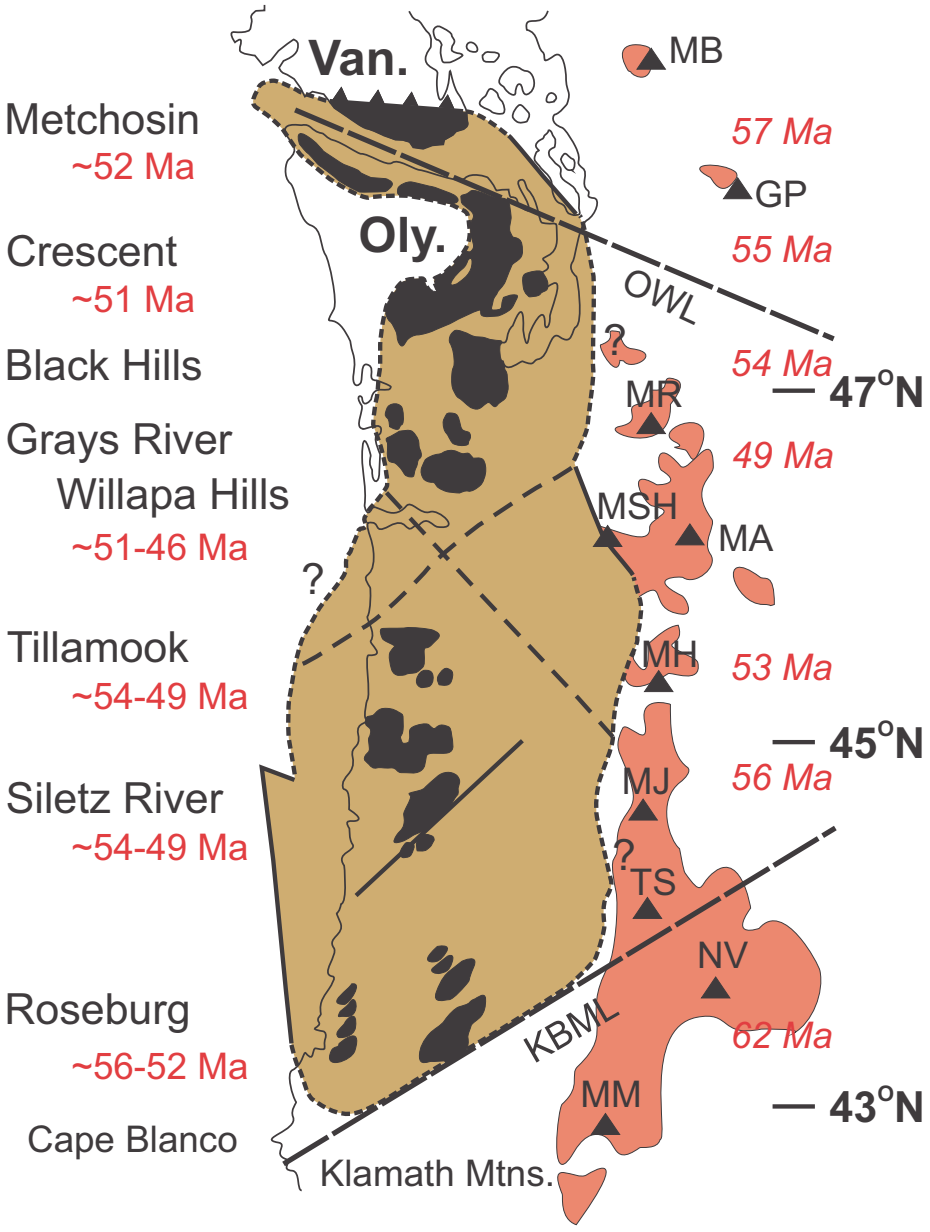

Figure 4. Outcrop (black) and inferred subsurface distribution (pink) of Siletz and Crescent mafic rocks (also known as Siletzia and as the Coast Range Basalt Province) along with age estimates for selected mafic rocks (compiled by McCrory and Wilson 2013), and for the Cascade Arc volcanoes (black triangles) from Duncan (1982). OWL – Olympic–Wallowa Lineament; KBML – Klamath–Blue Mountains Lineament. Modified from original figure by Duncan (1982).

elusive (Price and Carmichael 1986; Cowan 1994; Monger et al. 1994; Monger 2014). Recently, however, Hildebrand (2015) proposed a reconstruction in which the Texas Lineament and the Lewis and Clarke transverse zone, now 1300 km apart, were formerly contiguous, but were offset during the 80–58 Ma Laramide orogeny along N–S faults within the Cordilleran fold and thrust belt. According to Hildebrand (2015) the entire width of the Cordillera was translated northwards. By uniting two belts of plutonic rocks, the reconstruction eliminates the magmatic gap between them, and is therefore a first-order challenge to the flat-slab model. A magmatic gap could still exist between 58 and 43 Ma, but the existence of a flat slab at that time would not match the earliest stages of Laramide thick-skinned deformation.

This article assesses the potential effects of plume–slab interaction in the context of the more widely accepted model in which the Mesozoic–Cenozoic evolution of the western United States is dominated by long-lived easterly subduction. The effects of plume–slab interaction in the context of the rival models of Johnston and Hildebrand will be discussed in a separate contribution.

MODERN YELLOWSTONE PLUME

Plume versus non-plume models for the origin of the Yellowstone hot spot have been debated ever since Morgan (1972) and Armstrong et al. (1975) related the diachronous onset of magmatism in the Snake River Plain to the migration of the NAP over a stationary plume (e.g. Humphreys et al. 2000; Pierce and Morgan 2009; Fouch 2012). Alternative 'non-plume' models include the edge effects of cratonic lithosphere (King and Anderson 1998) and 'hot-lines' (Christiansen et al. 2002). The region around the hot spot is characterized by high heat flow, pronounced hydrothermal activity, a topographic bulge 600 m high and ca. 600 km wide, and a 10–12 m positive geoid anomaly (Smith and Braile 1994).

The potential relationship between magmatism and the modern Yellowstone plume development, beginning at about 17 Ma, has been suggested on the basis of geochronological, geophysical, structural and petrological data (e.g. Armstrong et al. 1975; Hadley et al. 1976; Geist and Richards 1993; Smith and Braile 1994; Camp 1995; Glen and Ponce 2002; Hooper et al. 2007; Ito and van Keken 2007; Graham et al. 2009; Smith et al. 2009). These studies show the age progression of magmatism along the Yellowstone–Snake River Plain which matches the calculated trajectory of the hot spot track derived from plate reconstructions.

Over the past decade, the plume model has been supported by a variety of geophysical techniques. Although some studies imply a shallow source for the Yellowstone hot spot (e.g. Montelli et al. 2006), in general, the results of teleseismic tomography reveal an inclined low velocity anomaly 100 km wide within the upper mantle beneath Yellowstone that is interpreted as

the thermal effects of the Yellowstone plume (Fig. 5). This anomaly extends 400 km along the length of the Yellowstone–Snake River Plain (YSRP), dips about 60 degrees WNW and can be detected to a depth of about 500 km, deflecting the 410 km discontinuity downward by as much as 12 km (Yuan and Dueker 2005; Waite et al. 2006; Smith et al. 2009). The anomaly has been modelled to reflect about 1% of partial melting at an ambient temperature of 200°C above normal (Schutt and Humphreys 2004). As a further example of the potential complexity, a *P*-wave model (Obrebski et al. 2010) shows a gap in the Juan de Fuca subducted slab in the region above the Yellowstone plume and below the YSRP.

Magnetotelluric surveys fail to detect magma directly beneath the Yellowstone hot spot and may not have the sensitivity to detect such deep structural features (Kelbert et al. 2012). These surveys do, however, detect a zone of low mantle resistivity beneath the eastern segment of the Snake River Plain, consistent with small degrees of partial melt at depths between 40 and 80 km (Zhdandov et al. 2011; Kelbert et al. 2012).

P to *S* body-wave tomography models imply an even deeper origin for the Yellowstone plume. Porritt et al. (2014) showed images of the plume to a depth of 1000 km. Other tomographic images suggest that this thermal anomaly may be connected to a much broader low-velocity anomaly in the uppermost portion of the lower mantle (e.g. Allen et al. 2008; Schmandt and Humphreys 2010; Obrebski et al. 2010; Sigloch 2011). These images also indicate that the 660 km discontinuity is deflected upwards by 12–18 km beneath Yellowstone, interpreted to reflect the presence of a plume-like upwelling (Schmandt et al. 2012). Zhao (2007) identified anomalies in both the upper and lower mantle and speculated that the complex distribution of anomalies may be due to interaction of the Yellowstone plume with the Farallon slab (see Fletcher and Wyman 2015). In addition to tomographic studies, Pierce and Morgan (2009) proposed that some of the large-scale tectonic features require a mantle plume extending to a depth of at least 1000 km.

The oldest widely accepted surface expression of the Yellowstone plume includes the main phase of the ca. 17 Ma Steen and Columbia River flood basalt provinces as well as voluminous contemporaneous silicic volcanism and is widely attributed to the initial impingement of the Yellowstone plume beneath North American lithosphere (e.g. Hooper et al. 2007; Coble and Mahood 2012; Fig. 6). The geochemistry of the basaltic rocks is complex and includes primary components typical of MORB, OIB and older mantle components (Carlson 1984; Draper 1991; Hooper and Hawkesworth 1993; Bryce and DePaolo 2004), interpreted to reflect the interaction of plume-derived material with sub-continental lithospheric mantle and overlying crust (Hooper et al. 2007; Coble and Mahood 2012). However, the volcanic centres lie on a N–S trend with the youngest centres and largest volumes occurring well to the north of the putative Yellowstone hot spot track (Barry et al. 2010). These trends have been variously explained by (i) a deflection of the Yellowstone plume by the Juan de Fuca slab (Geist and Richards 1993), (ii) exploitation by the plume of the

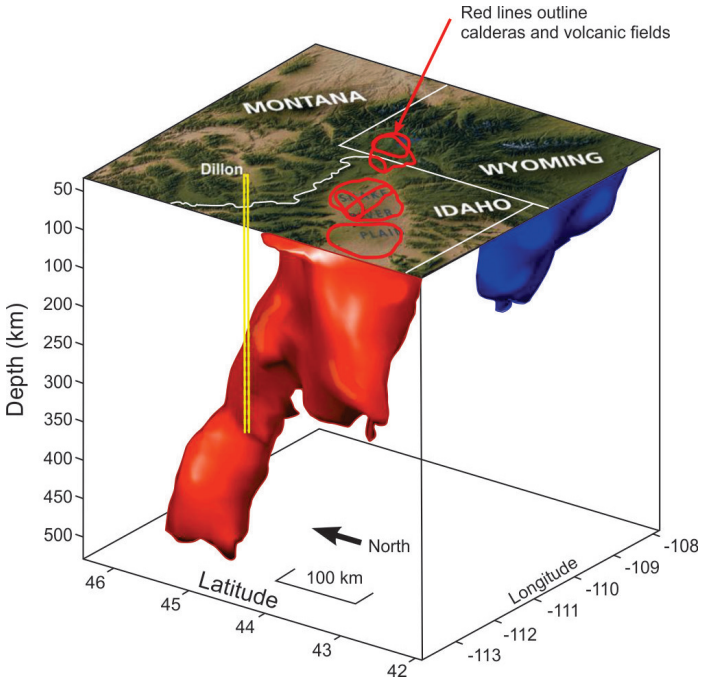

Figure 5. Seismic tomographic image (Yuan and Dueker 2005; Pierce and Morgan 2009) showing inclined conduit of warm mantle, interpreted as a plume that can be tracked northwestward from beneath Yellowstone to a depth of 500 km. Red outlines schematically show the calderas of the Snake River Plain.

old continental margin (Camp and Ross 2004), (iii) slab delamination and consequent asthenospheric upwelling that accompanied the arrival of the Yellowstone plume (Camp and Hanan 2008; Darold and Humphreys 2013), and (iv) a propagating rupture in the Farallon slab (Liu and Stegman 2012). A further explanation may be derived from numerical models which show that when the plume penetrates from the lower into the upper plate via a slab window, plume material becomes complexly distributed and does not follow a simple linear pattern expected for a hot spot track (Betts et al. 2015).

The YSRP is about 700 km in length and is classically interpreted as a northeasterly trending hot spot track (Morgan 1972; Armstrong et al. 1975) characterized by the eruption of voluminous felsic ignimbrite and overlain by a thin succession of basalt, as well as a voluminous mafic sill complex (Shervais et al. 2006). He, Pb, Sr, and Nd isotopic analyses of the mafic rocks are consistent with a mantle plume source (e.g. Craig et al. 1978; Hearn et al. 1990; Vetter and Shervais 1992; Hughes et al. 2002; Hanan et al. 2008; Graham et al. 2009). The rhyolitic volcanic rocks that characterize the YSRP system are diachronous, and their age progression of 4.5 cm/a is viewed as the composite of the migration of the NAP and Basin and Range extension over the same time interval (Shervais and Hanan 2008). The excess topography of the YSRP decreases systematically along its length away from the hot spot and has been modelled to reflect a progressively cooling and contracting lithosphere (Smith and Braile 1994).

Prior to 17 Ma, products within North America related to the Yellowstone plume are controversial. Seligman et al. (2014) provided isotopic and trace element data from 40–30 Ma vol-

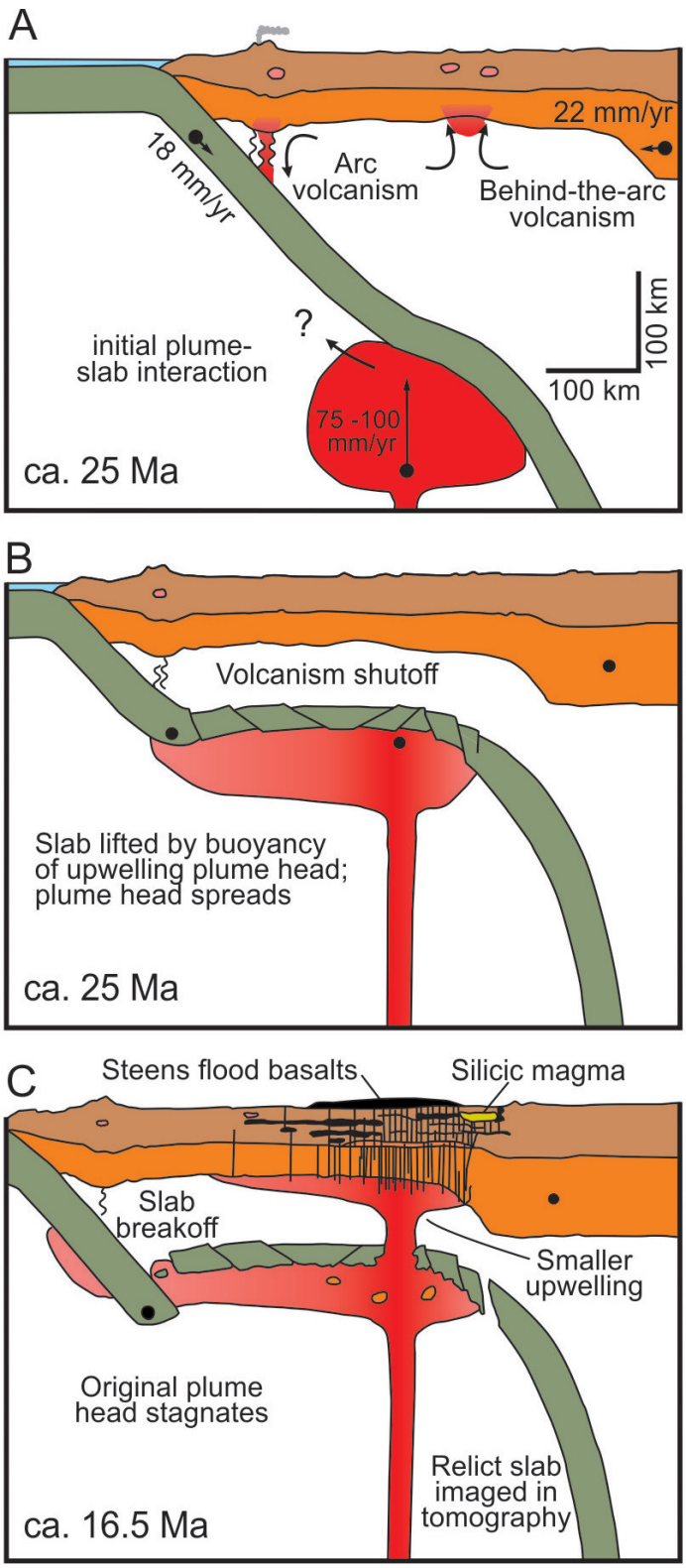

Figure 6. Model for the evolution of Yellowstone plume (after Coble and Mahood 2012) that considers the lifting of the Juan de Fuca slab at 25 Ma (A) to have resulted in volcanic quiescence (B) between ca. 23 and 17 Ma, and the distribution of voluminous bimodal basalts and coeval rhyolites (C) to represent breakthrough of plume material at ca. 17 Ma into the upper plate to form a secondary plume head.

canic centres in Oregon that are located too far east to be directly related to Farallon subduction. Basalt was derived from an enriched subcontinental lithospheric mantle, whereas some felsic complexes (e.g. Crooked River) have $\delta^{18}O$ (zircon) values that require a large heat source, extensive hydrothermal circulation and crustal recycling (Bindeman et al. 2001; Cathey et al. 2011; Watts et al. 2011; Drew et al. 2013; Seligman et al. 2014). Plate reconstructions (Seton et al. 2012; Wells et al. 2014) imply that the Yellowstone plume would have resided beneath Crooked River at that time. Seligman et al. (2014) attributed this magmatism to the earliest eruptions associated with the encroachment of the Yellowstone plume. In their model, the more widespread coeval voluminous felsic magmatism is attributed to 'plume-triggered delamination.' Although Murphy et al. (1998) attributed regional felsic magmatism to the arrival of the plume along the base of the continental lithosphere, Seligman et al. (2014) invoked a model where plume material encroaches through a tear or a gap in the subducting Farallon plate.

ANCESTRAL YELLOWSTONE PLUME

Duncan (1982) proposed that basalt-dominated volcanic complexes accreted to the North American margin in the Eocene originated as oceanic islands above the ancestral Yellowstone hot spot which was located at that time along the Kula–Farallon ridge. This model was underpinned by plate reconstructions which implied that if the Yellowstone plume existed prior to 55–50 Ma, it would have been located beneath oceanic lithosphere.

Since that time, interpretations of the plate configuration in the oceanic realm in the Pacific Northwest have been refined. For example, Haeussler et al. (2003) attributed the migration of Eocene magmatism from Alaska to Oregon to the migration of two triple junctions, requiring the existence of a previously unrecognized oceanic plate, named the Resurrection plate. This plate, if it existed, would have been located to the east of the Kula plate, and would have been subducted, along with its bounding ridges by 50 Ma (see also Madsen et al. 2006). Despite these refinements, the basic relationship of the hypothesized ancestral Yellowstone hot spot with either the Kula–Farallon or Kula–Resurrection oceanic ridges is consistent with more recent reconstructions derived from Gplates (Seton et al. 2012) and the moving hot spot reference frames (Lonsdale 1988; Müller et al. 1993; O'Neill et al. 2005; McCrory and Wilson 2013; Wells et al. 2014).

If correct, manifestations of the Yellowstone plume, including accretion of ocean islands and interaction with oceanic plateaus related to the plume, should be recognized among the tectonic events along the convergent margin of western North America.

Possible Accreted Oceanic Complexes

Mafic complexes hypothesized to have accreted to North America include Siletzia (now fragmented into the Siletz and Crescent terranes) which is exposed in Vancouver Island (Metchosin igneous complex; Massey 1986), Oregon and Washington (Duncan 1982), and the Carmacks Group (Inter-

montane belt) of the Yukon Territory of Canada (Johnston et al. 1996) which oversteps previously amalgamated terranes.

Siletzia is characterized by a 56–49 Ma submarine sequence of tholeiitic–alkalic basalt and associated volcanogenic sedimentary rocks, overlain by a subaerial sequence dominated by alkalic basalt (e.g. Snavely et al. 1968; Wells et al. 1984, 2014; Babcock et al. 1992, 1994) with plume-type geochemistry (Pyle et al. 1997, 2009). The terrane is estimated to be 27 ± 5 km in thickness (Trehu et al. 1994; Graindorge et al. 2003), is exposed over 240,000 km^2, and the volume of its basaltic magmatism is estimated to exceed that of the Columbia River Basalt province by at least one order of magnitude (Duncan 1982; Wells et al. 2014). Post-accretionary magmatism continued until ca. 42 Ma with the emplacement of mafic volcanic and dike complexes in the forearc (Wells et al. 2014).

Paleomagnetic data, although complex, allow the possibility of significant post-depositional episodes of rotation (Simpson and Cox 1977; McCrory and Wilson 2013), but imply a paleolatitude similar to today. Wells et al. (2014) maintained that the oceanic composition, large volume and short duration of magmatism are characteristic of Large Igneous Provinces (LIPs) and they interpreted these rocks to collectively represent an oceanic plateau produced by the ancestral Yellowstone plume. They also showed that, in most hot spot reference frames, plate reconstructions imply these volcanic complexes would have been located close to the Yellowstone hot spot at the time, within 300 km of the continental margin in a near-ridge setting (see also McCrory and Wilson 2013). The southern Vancouver orocline is thought to have formed in response to the accretion of Siletzia to North America (Johnston and Acton 2003).

In northern Siletzia (Crescent terrane), the Metchosin Complex of Vancouver Island consists of a 60–50 Ma sequence of mafic volcanic and interbedded clastic rocks (Massey 1986). This complex is thought to comprise a part of Siletzia that was scraped from a subducting slab which underthrust previously accreted terranes (Hyndman 1995). Tomographic studies (Ramachandran 2001) suggest that the terrane beneath Vancouver Island may be as much as 25 km thick. Paleomagnetic data (Babcock et al. 1992) combined with Mesozoic–Cenozoic plate reconstructions indicate that these basaltic rocks were emplaced in a similar location to the modern Yellowstone hot spot. Murphy et al. (2003) interpreted the shallowing-upward sequence to have formed in a Loihi-type environment and estimated 4.2 km of uplift related to plume activity which yielded a plume buoyancy flux of 1.1 Mg s^{-1}, comparable in vigour to that of the modern Yellowstone hot spot.

The Carmacks Group is a ca. 70 Ma sequence of volcanic rocks that unconformably overlies the previously amalgamated northern Intermontane belt terranes, and possibly the adjacent Omineca belt terranes (e.g. Gladwin and Johnston 2006). The group comprises a thick subaerial succession dominated by alkalic basalt with shoshonitic geochemistry that is comparable with modern plume-related basalt. Paleomagnetic data combined with regional geological data constrain the eruption of the Carmacks Group to a paleolatitude similar to the modern

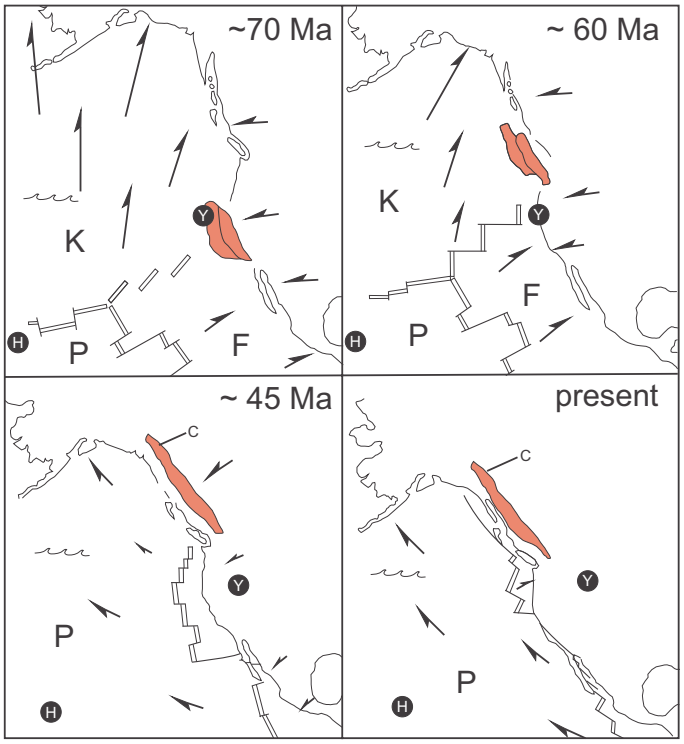

Figure 7. Yellowstone in Yukon model of Johnston et al. (1996) assuming fixed locations of Yellowstone (Y) and Hawaii (H) hot spots. In this model, the Carmacks Group (C; Intermontane belt) is generated by its passage over the Yellowstone hot spot at 70 Ma, and subsequently displaced dextrally along the margin with the North American plate. F – Farallon plate; K – Kula plate; P – Pacific plate.

Yellowstone hot spot implying a 17.2 ± 6.5° (ca. 2000 ± 600 km) northward translation since their eruption (Johnston et al. 1996; Johnston and Thorkelson 2000; Fig. 7).

The interpretation of the Carmacks Group as a representative of the Yellowstone hot spot has important implications for Cordilleran tectonics. As reconstructions place the hot spot to the west of North America at 70 Ma, this would imply the Carmacks Group, as well as the underlying Intermontane belt terranes, lay outboard of continental North America at that time. The obliteration of the oceanic tract between them could explain the lack of preservation of a hot spot track between Siletzia and Carmacks Group. The reconstruction of Hildebrand (2015) provides an explanation of the northward translation of the Carmacks Group, required to move it from an original position along the hot spot track to its modern location in the Yukon. An alternative possibility is that the matching paleolatitudes of Carmacks and Yellowstone are fortuitous, in which case these relationships place no constraints on the relationship of the Intermontane belt terranes and continental North America.

Geophysical Data and Geodynamic Models

Geodynamic models show that plumes have difficulty penetrating oceanic lithosphere (e.g. McNutt and Fischer 1987), let alone lithosphere capped by continental crust (Murphy et al. 1998). The presence of continental crust as well as remnants of the Juan de Fuca–Farallon slab detected by seismic studies

(Xue and Allen 2007; Obrebski et al. 2010) provides additional challenges to the ascent of Yellowstone plume material, suggesting the connection between the plume and corresponding hot spot is likely to be far more complex in continental environments compared to oceanic environments. For example, Geist and Richards (1993) attributed the Columbia Plateau–Snake River Plain to the deflection of the Yellowstone plume. Magmatism far removed from the YSRP track, such as the eastern Oregon Steens–Columbia River Basalt is attributed to delamination of remnant Farallon oceanic lithosphere coincident with the arrival of the Yellowstone plume (Darold and Humphreys 2013). Coble and Mahood (2012) invoked a two-stage process in which the bulk of the plume material stalled beneath the subducted Farallon slab, but some material penetrated the slab creating a secondary 'plume' which impinged on the continental lithosphere at ca. 17 Ma resulting in flood basalt volcanism and coeval silicic magmatism. This secondary plume is purported to explain why the volume of basalt produced is significantly smaller than that of a more typical Large Igneous Province.

The barriers to the ascent of plume material, such as the remnants of the Farallon slab as well as the thick lithosphere that overrides it, suggest that the Yellowstone plume must have originated significantly earlier than its first interaction with North American crust in the middle Miocene and may have been in an 'incubation' phase when it was overridden by a subduction zone (Murphy et al. 1998). According to this model, during this incubation phase plume material would have ponded beneath and progressively assimilated or thermally eroded the overlying Farallon slab following which plume material was transferred from the lower to the upper plate.

However, recent geodynamic models (e.g. Kincaid et al. 2013; Druken et al. 2014) have suggested that mantle downwelling related to subduction in the vicinity of the plume may destroy the plume column (Fig. 8), implying that thermal erosion on its own is not a viable mechanism for transferring plume material from the lower to the upper plate. These results have focused attention on more specialized environments for how the plume may have penetrated to the upper plate. For example, plume material may migrate around the edges of the slab in a bifurcating fashion (Seligman et al. 2014), and/or advect into the upper plate during slab roll-back (Druken et al. 2014). In addition, numerical models (Betts et al. 2012) show that plume material may be transferred to the upper plate via a slab window which is created when the plume buoyancy stalls subduction as it interacts with the convergent margin.

In the conceptual model of Coble and Mahood (2012), plume material migrates into the upper plate via fractures or tears in the slab. A similar model was invoked by Obrebski et al. (2010) who interpreted high resolution tomographic images derived from the USArray deployment to reflect the arrival and emplacement of the ancestral Yellowstone plume beneath the Cascadia subduction zone (Fig. 9) which broke through the Juan de Fuca slab, either by exploiting pre-existing weaknesses or by promoting the tearing of the slab.

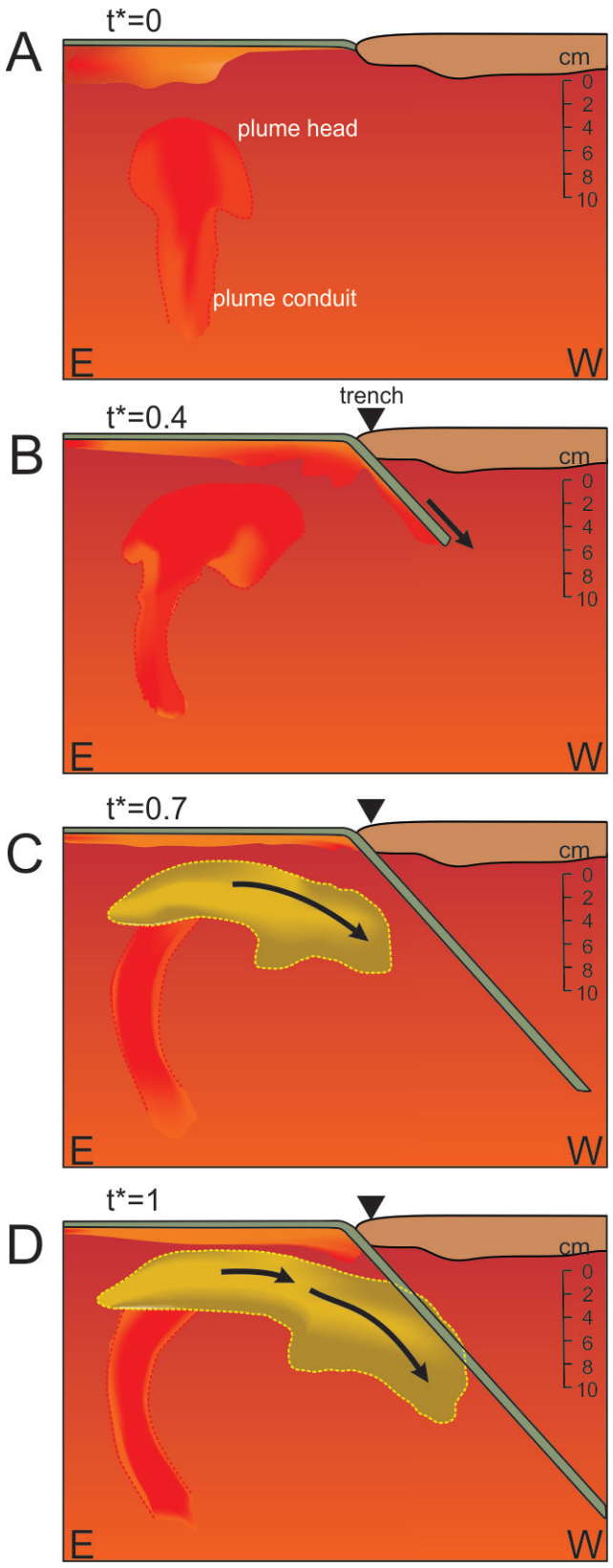

Figure 8. Example of plume-slab interaction (see Druken et al. 2014 for details). (A) Plume structure before subduction initiation. Its head rises vertically at an average rate of 2–3 cm/min. (B) and (C) Subduction induces a downward flow of plume material which is advected back into the mantle (D).

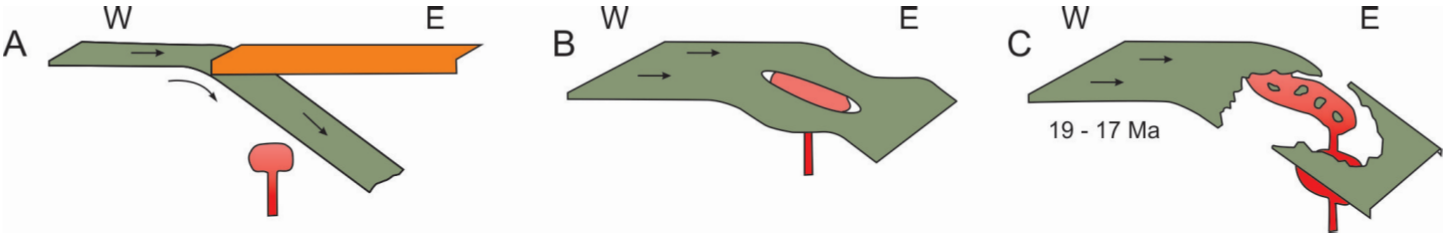

Figure 9. Model for the evolution of the Pacific Northwest after Obrebski et al. (2010). (A) The Yellowstone plume (head in pink, tail in red) penetrates the subducting slab (green) and reaches the base of the continental lithosphere (orange) resulting in slab break-up that was facilitated by pre-existing fractures in the slab (B). Slab break-off results in reduction of slab-pull and consequent decrease in rate of convergence. (C) The plume assimilated fragments of the subduction zone and generated the Columbia River flood basalt.

ANDEAN AND PACIFIC ANALOGUES

The Andean orogenic system is commonly considered to represent a modern analogue for Laramide tectonics of the southwest United States. Seismic imaging reveals that the Andean subducted slab is segmented into flat and steep domains, with the flat segments up to 500 km wide (e.g. Gutscher et al. 2000). These flat slab segments are characterized by a lack of recent magmatism, eastward migration of deformation, and by foreland thick-skinned deformation similar to the Laramide uplifts (Dalziel 1986; Allmendinger et al. 1997). These segments are spatially and temporally correlated with subducting oceanic plateaus (e.g. Pilger 1981; Gutscher et al. 2000; Gutscher 2002; Yáñez et al. 2002; Ramos and McNulty 2002; Fig. 10), implying a genetic relationship between flat slab generation and subduction of relatively thick and buoyant oceanic lithosphere.

Livacarri et al. (1981) proposed that the Laramide orogeny was due to the subduction of an oceanic plateau. According to Cloos (1993), oceanic plateaus with crustal thicknesses in excess of 30 km cause collisional orogenesis during subduction. Liu et al. (2008) reconstructed the subduction record of the Farallon oceanic lithosphere back to 100 million years ago with an inverse mantle convection model that uses stratigraphy to constrain mantle viscosity and buoyancy. Their preferred model predicts an extensive shallow-dipping slab, beginning about 90 Ma, that extended up to 1000 km to the east and north of the flat slab. They attributed the limited width of the flat slab region to the subduction of an oceanic plateau, a scenario supported by recent 3D dynamic models (Betts et al. 2015).

The Hess–Shatsky large igneous province (LIP), located in the northwest Pacific (Fig. 11a), has been suggested as a conjugate for these oceanic plateaus that were subducted in the southwest Cordilleran region in Laramide time (Livacarri et al. 1981; Tarduno et al. 1985; Liu et al. 2010). If correct, these plateaus, which constitute one of Earth's largest LIPs, may provide an indication of the size and age of the oceanic plateau that was subducted in Laramide times. The Shatsky plateau alone has an area of 0.48 million km^2 (comparable in size to California) and a volume of 4.3 million km^3 (Mahoney et al. 2005; Sager 2005). The three volcanic centres have depths of 3200–2000 m, whereas the abyssal ocean floor surrounding the plateau is between 6000–5500 m below sea level (Nakanishi et al. 2015). Adjacent magnetic lineations indicate that the Shatsky plateau originated at about 130 Ma at the Pacific–

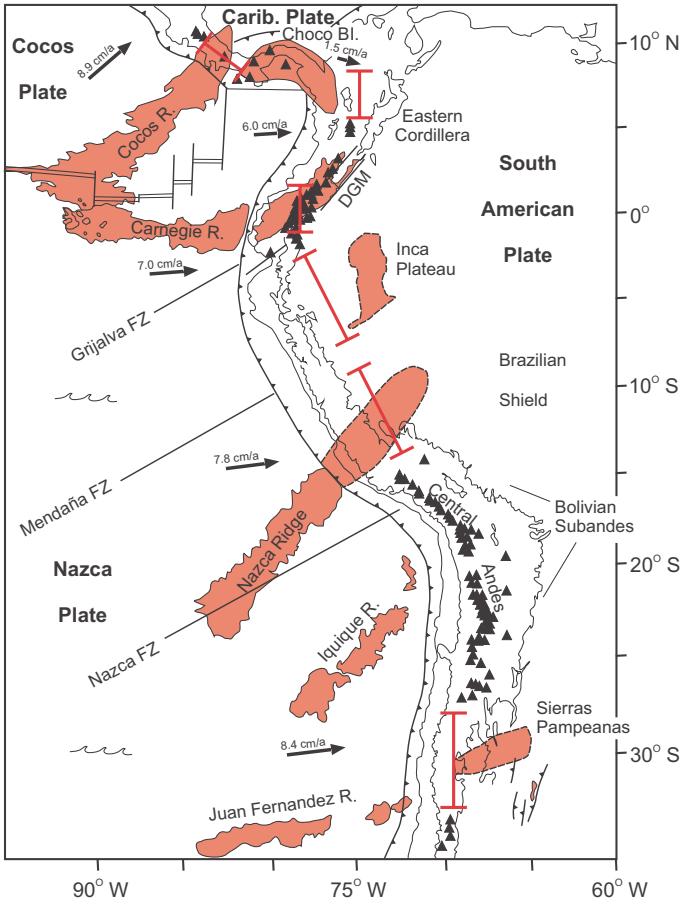

Figure 10. Relationship between flat-slab segments (thick red brackets) and subducted plateau (orange regions) projected beneath the Andean margin (from Gutscher et al. 2000).

Izanagi–Farallon triple junction (Tatsumi et al. 1998) and its Nd and Pb isotopic characteristics are indistinguishable from the East Pacific Rise (Mahoney et al. 2005). The age of the Hess oceanic plateau is not well constrained, but is inferred to represent renewed magmatism about 20 m.y. later (Ito and van Keken 2007). Liu et al. (2010) showed that Laramide deformation tracks the passage of the Shatsky conjugate plateau beneath North America (Fig. 11b), which was then converted to eclogite and foundered into the mantle. They interpreted Laramide uplift as isostatic rebound after this foundering.

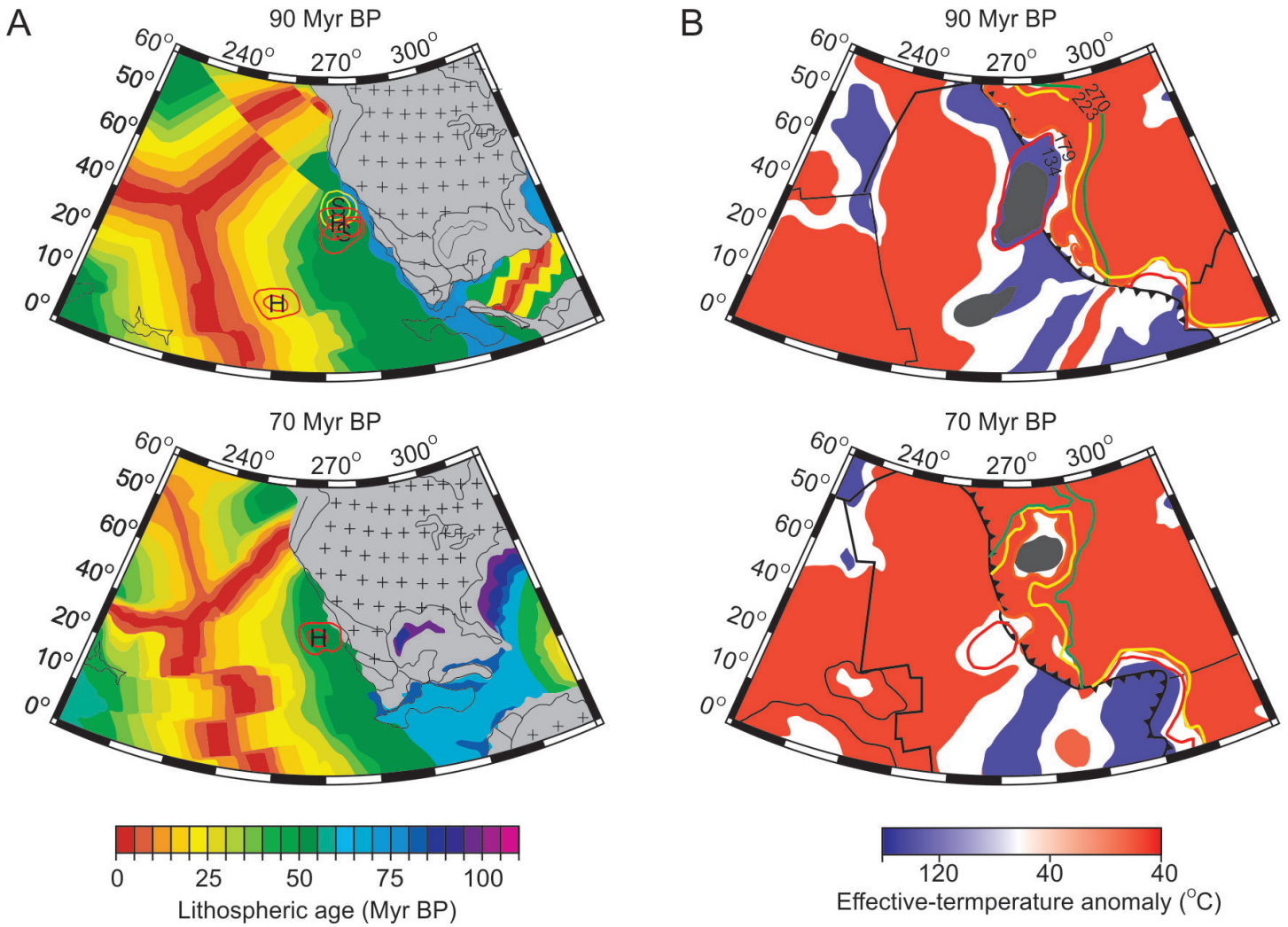

Figure 11. Potential role of the Shatsky (S) and Hess (H) conjugate plateaus in generating the flat-slab environment for the Laramide orogeny (from Liu et al. 2010). Black outlines give current locations of the main plateau. (A) Plate reconstruction of the conjugate plateaus which are inferred to have formed along the Pacific–Farallon and Farallon–Izanagi ridges, respectively. Red contours show their maximum extent, yellow contours their minimum extent. (B) Inverse convection models showing locations of the thickest part of the conjugate lithosphere above 179 km depth. Colour contours show isotherms at different depths (in km). See Liu et al. (2010) for further details.

Murphy et al. (1998, 2003) attributed flat slab subduction in the western United States to overriding of the Yellowstone plume and its associated oceanic plateau/swell by the continental margin. Using the relative motion between the North American and Farallon plates of 120 mm/a (Engebretson et al. 1985), Murphy et al. (1998) estimated that the buoyant swell about 400 km wide (Sleep 1990) would have been elongated up to 2400 km in the direction of Farallon plate motion (i.e. towards the North American trench) in the hot spot reference frame. The plateau would have interacted with the trench about 25–30 m.y. before the plume itself was overridden. Reconstructions that suggest the Yellowstone plume was overridden by the continental margin at ca. 50 Ma imply that the related oceanic plateau and underlying buoyant swell reached the trench at ca. 80–75 Ma, i.e. about the time of commencement of the Laramide orogeny. If the Carmacks Group represents a vestige of the plume, reconstructions imply the existence of an oceanic tract between the Intermontane belt terranes and continental North America at that time.

SUMMARY AND DISCUSSION

The accretion to North America at ca. 50 Ma of large oceanic terranes, such as Siletzia, with plume geochemistry and dimensions suggesting it constitutes the vestiges of a LIP (Wells et al. 2014), is strong evidence that a plume was located in the oceanic realm adjacent to the North American continent, much as envisaged by Duncan (1982). Reconstructions (e.g. McCrory and Wilson 2013; Wells et al. 2014) indicate that the ancestral Yellowstone hot spot, if it existed, would have been located close to the Kula–Farallon ridge or to the Kula–Farallon–Resurrection triple junction at that time and would be a viable source for the Siletzia ocean island basaltic rocks. In northern Siletzia, the calculated buoyancy flux (1.1 Mg s^{-1}) of the plume responsible for the Crescent volcanic rocks (Mur-

phy et al. 2003) is similar to that of the modern Yellowstone plume (Sleep 1990). Taken together, this evidence indicates that at ca. 55–50 Ma, a plume existed in the same location as modern Yellowstone and had comparable vigour.

If so, interaction between the continental margin and the ancestral plume must have been preceded by overriding of the related buoyant swell and oceanic plateau that would have been elongate in the direction of motion of the Farallon plate. In this scenario, the swell and plateau of thick oceanic lithosphere would have been overridden by the North American margin at ca. 75 Ma, i.e. broadly coinciding with the onset of Laramide orogenesis and about 20 m.y. before the ancestral Yellowstone plume was overridden. Although back-of-the-envelope calculations suggest that the swell may supply enough positive buoyancy to counteract the negative buoyancy of 80–50 m.y. old Farallon oceanic lithosphere and hence contribute to the formation of the flat slab (Murphy et al. 1998), this contention has not been evaluated rigorously, and so the relationship between the arrival of the swell at the trench and the onset of flat slab subduction remains enigmatic. However, geodynamic models (e.g. Betts et al. 2012, 2015) show that subduction of oceanic plateaus can generate flat slabs. According to the inverse mantle convection model of Liu et al. (2008, 2010), subduction of an oceanic plateau, corresponding to the conjugate of the Shatsky plateau, beginning at about 90 Ma, could initiate the generation of the flat slab, although they acknowledged that their model yielded an initiation age which is about 10 m.y. older than geological evidence for flat slab inception. As the Shatsky rocks are about 150 Ma, its conjugate plateau could be temporally distinct from the plateau related to the ancestral Yellowstone hot spot. Alternatively, the oldest components of the plateau may not have been sufficiently buoyant to resist subduction. The space–time relationships inferred by Liu et al. (2008, 2010) make the Shatsky conjugate plateau a viable alternative to the plateau associated with the Yellowstone plume in initiating the flat slab. The location of the conjugate to the Hess plateau, for which the age is unconstrained, is intriguingly similar to that inferred for the Yellowstone hot spot. The calculated location for the Hess plateau lies adjacent to the inferred location of the Yellowstone swell. Taken together, these relationships imply the possibility of a very complicated composite plateau geometry with older and younger components being overridden by the NAP between 90 and 70 Ma, followed by the accretion of oceanic islands related to the Yellowstone plume by ca. 50 Ma.

After the plume was overridden by the NAP, its effects become more conjectural as it becomes overlain by continental lithosphere. The models of Betts et al. (2012, 2015) suggest that plume magmatism in the upper plate will be concentrated in regions where rising plume material can exploit weaknesses in the oceanic and continental lithospheres. Forearc magmatism is detected until ca. 42 Ma where the crust overlying the plume is thin and undergoing margin-parallel extension (Wells et al. 2014). More controversially, the next phase of magmatism directly or indirectly related to plume activity may be some of the 40–30 Ma magmatism in Oregon to the east of the Cascadia arc, for which isotopic data suggest a large heat source and extensive hydrothermal circulation, and plate reconstructions imply a subjacent Yellowstone plume (Seligman et al. 2014).

Plume-related magmatism between 17 and 0 Ma associated with the YSRP matches the plate motions of the NAP, much as envisaged by Morgan (1972) and Armstrong et al. (1975). Regionally extensive coeval magmatism that occurs some distance from this track may be due to secondary effects (Betts et al. 2015), such as deflection of plume material as it migrates through the upper plate and/or plume-assisted delamination (e.g. Darold and Humphreys 2013).

Laboratory studies suggesting that plumes may be severely distorted or even destroyed by slab-driven subduction processes (Kincaid et al. 2013; Druken et al. 2014) have drawn attention to the importance of tears or windows in the subducting slab where plume material can be transferred to the upper plate (e.g. Johnston and Thorkelson 1997). Betts et al. (2015) showed that the interaction between an oceanic plateau and a continental margin causes rapid trench advance, accretion of the plateau which is transferred to the upper plate, followed by re-establishment of subduction outboard of the plateau. They also showed that the additional presence of a buoyant plume beneath the plateau results in the formation of a slab window beneath the accreted plateau, where plume material can be transferred from the lower to the upper plate. Such processes provide some theoretical support for the models where plume material is deflected as it exploits weaknesses in the subducted slab (fractures, tears, windows, regions where lithosphere has been delaminated) to enter the upper plate, and explains why the products of these events may not always be located adjacent to the calculated hot spot track. Also, plume material transferred to the upper plate and deflected away from the hot spot track moves with the upper plate, and so is rapidly separated from its heat source.

The synthesis of Fletcher and Wyman (2015) that 29% of mantle plumes have been located within 1000 km of a subduction zone over the past 60 Ma implies that interaction between plumes, their plateaus and buoyant swells with subduction zones should be common in the geologic record. If so, the geologic evolution of the western United States may represent a Late Mesozoic–Cenozoic analogue for a common, but overlooked mode of orogenic activity that has occurred since plate tectonics first operated on Earth. This interaction is very complex in space and time, and a resolution of the rival models (eastward versus westward subduction in the Mesozoic) may be prerequisite to a deeper understanding of this interaction.

ACKNOWLEDGEMENTS

It is with great pleasure that I recognize the role of Andrew Hynes as a professor, supervisor, mentor and friend. The manuscript benefitted considerably from the insightful and constructive reviews of Pete Betts, Bob Hildebrand and Editor Stephen Johnston who do not agree with all the content in this manuscript. I thank Randy Corney for drafting many of the figures and Cindy Murphy for editorial expertise. I take responsibility for any errors in content or interpretation. This research is supported by N.S.E.R.C. Canada.

REFERENCES

Allen, R.M., Xue, M., and Hung, S., 2008, Complex geological interactions in the mantle beneath western USA (Abstract): American Geophysical Union: Fall

Meeting Supplement, v. 89, S31D-02.
Allmendinger, R.W., Jordan, T.E., Kay, S.M., and Isacks, B.L., 1997, The Evolution of the Altiplano-Puna plateau of the Central Andes: Annual Review of Earth and Planetary Sciences, v. 25, p. 139–174, http://dx.doi.org/10.1146/annurev.earth.25.1.139.
Anderson, D.L., 1994, The sublithospheric mantle as the source of continental flood basalts: The case against the continental lithosphere and plume head reservoirs: Earth and Planetary Science Letters, v. 123, p. 269–280.
Armstrong, R.L., Leeman, W.P., and Malde, H.E., 1975, K–Ar dating, Quaternary and Neogene volcanic rocks of the Snake River Plain, Idaho: American Journal of Science, v. 275, p. 225–251, http://dx.doi.org/10.2475/ajs.275.3.225.
Atwater, T., 1970, Implications of plate tectonics for the Cenozoic tectonic evolution of western North America: Geological Society of America Bulletin, v. 81, p. 3513–3536, http://dx.doi.org/10.1130/0016-7606(1970)81[3513:IOPTFT]2.0.CO;2.
Atwater, T., 1989, Plate tectonic history of the northeast Pacific and western North America, *in* Winterer, E.L., Hussong, D.M., and Decker, R.W., *eds.*, The Eastern Pacific Ocean and Hawaii: The Geology of North America, Geological Society of America, Boulder, CO, v. N, p. 21–72, http://dx.doi.org/10.1130/dnag-gna-n.21.
Babcock, R.S., Burmester, R.F., Engebretson, D.C., Warnock, A., and Clark, K.P., 1992, A rifted margin origin for the crescent basalts and related rocks in the northern Coast Range Volcanic Province, Washington and British Columbia: Journal of Geophysical Research, v. 97, p. 6799–6821, http://dx.doi.org/10.1029/91JB02926.
Babcock, R.S., Suczek, C.A., and Engebretson, D.C., 1994, The Crescent "Terrane", Olympic Peninsula and southern Vancouver Island, *in* Lasmanis, R., and Cheney, E.S., *eds.*, Regional Geology of Washington State: Washington Division of Geology and Earth Resources Bulletin, v. 80, p. 141–157.
Barry, T.L., Self, S., Kelley, S.P., Reidel, S., Hooper, P., and Widdowson, M., 2010, New $^{40}Ar/^{39}Ar$ dating of the Grande Ronde lavas, Columbia River Basalts, USA: Implications for duration of flood basalt eruption episodes: Lithos, v. 118, p. 213–222, http://dx.doi.org/10.1016/j.lithos.2010.03.014.
Beck Jr., M.E., 1992, Tectonic significance of paleomagnetic results for the western conterminous United States, *in* Burchfiel, B.C., Lipman, P.W., and Zoback, M.L., *eds.*, The Cordilleran orogen: Conterminous U.S.: Geology of North America, Geological Society of America, Boulder, CO, v. G-3, p. 683–697, http://dx.doi.org/10.1130/dnag-gna-g3.683.
Betts, P.G., Giles, D., Schaefer, B.F., and Mark, G., 2007, 1600–1500 Ma hotspot track in eastern Australia: Implications for Mesoproterozoic continental reconstructions: Terra Nova, v. 19, p. 496–501, http://dx.doi.org/10.1111/j.1365-3121.2007.00778.x.
Betts, P.G., Giles, D., Foden, J., Schaefer, B.F., Mark, G., Pankhurst, M.J., Forbes, C.J., Williams, H.A., Chalmers, N.C., and Hills, Q., 2009, Mesoproterozoic plume-modified orogenesis in eastern Precambrian Australia: Tectonics, v. 28, TC3006, http://dx.doi.org/10.1029/2008TC002325.
Betts, P.G., Mason, W.G., and Moresi, L., 2012, The influence of a mantle plume head on the dynamics of a retreating subduction zone: Geology, v. 40, p. 739–742, http://dx.doi.org/10.1130/G32909.1.
Betts, P.G., Moresi, L., Miller, M.S., and Willis, D., 2015, Geodynamics of oceanic plateau and plume head accretion and their role in Phanerozoic orogenic systems of China: Geoscience Frontiers, v. 6, p. 49–59, http://dx.doi.org/10.1016/j.gsf.2014.07.002.
Bindeman, I.N., Valley, J.W., Wooden, J.L., and Persing, H.M., 2001, Post-caldera volcanism: In situ measurement of U–Pb age and oxygen isotope ratio in Pleistocene zircons from Yellowstone caldera: Earth and Planetary Science Letters, v. 189, p. 197–206, http://dx.doi.org/10.1016/S0012-821X(01)00358-2.
Bird, P., 1988, Formation of the Rocky Mountains, western United States: A continuum computer model: Science, v. 239, p. 1501–1507, http://dx.doi.org/10.1126/science.239.4847.1501.
Bryce, J.G., and DePaolo, D.J., 2004, Pb isotopic heterogeneity in basaltic phenocrysts: Geochimica et Cosmochimica Acta, v. 68, p. 4453–4468, http://dx.doi.org/10.1016/j.gca.2004.01.016.
Burchfiel, B.C., Cowan, D.S., and Davis, G.A., 1992, Tectonic overview of the Cordilleran orogeny in the western United States, *in* Burchfiel, B.C., Lipman, P.W., and Zoback, M.L., *eds.*, The Cordilleran Orogen: Conterminous U.S.: Geology of North America, Geological Society of America, Boulder, CO, v. G-3, p. 407–479, http://dx.doi.org/10.1130/dnag-gna-g3.
Burke, K., Steinberger, B., Torsvik, T.H., and Smethurst, M.A., 2008, Plume generation zones at the margins of large low shear velocity provinces on the core–mantle boundary: Earth and Planetary Science Letters, v. 265, p. 49–60, http://dx.doi.org/10.1016/j.epsl.2007.09.042.
Busby, C., 2004, Continental growth at convergent margins facing large ocean basins: a case study from Mesozoic convergent-margin basins of Baja California, Mexico: Tectonophysics, v. 392, p. 241–277, http://dx.doi.org/10.1016/j.tecto.2004.04.017.
Busby, C., 2012, Extensional and transtensional continental arc basins: Case studies from the southwestern U.S. and Mexico, *in* Busby, C., and Azor, A., *eds.*, Recent Advances in Tectonics of Sedimentary Basins: Wiley-Blackwell, London, p. 382–404.
Camp, V.E., 1995, Mid-Miocene propagation of the Yellowstone mantle plume head beneath the Columbia River basalt source region: Geology, v. 23, p. 435–438, http://dx.doi.org/10.1130/0091-7613(1995)023<0435:MMPOTY>2.3.CO;2.
Camp, V.E., and Hanan, B.B., 2008, A plume-triggered delamination origin for the Columbia River Basalt Group: Geosphere, v. 4, p. 480–495, http://dx.doi.org/10.1130/GES00175.1.
Camp, V.E., and Ross, M.E., 2004, Mantle dynamics and genesis of mafic magmatism in the intermontane Pacific Northwest: Journal of Geophysical Research, v. 109, B08204, http://dx.doi.org/10.1029/2003JB002838.
Carlson, R.W., 1984, Isotopic constraints on Columbia River flood basalt genesis and the nature of the subcontinental mantle: Geochimica et Cosmochimica Acta, v. 48, p. 2357–2372, http://dx.doi.org/10.1016/0016-7037(84)90231-X.
Cathey, H.E., Nash, B.P., Seligman, A.N., Valley, J.W., Kita, N., Allen, C.M., Campbell, I.H., Vazquez, J.A., and Wooden, J.L., 2011, Low $\delta^{18}O$ zircons from the Bruneau-Jarbidge eruptive center: A key to crustal anatexis along the track of the Yellowstone hotspot (Abstract): American Geophysical Union, Fall Meeting 2011, v. 92, V11A-2510.
Christiansen, R.L., Foulger, G.R., and Evans, J.R., 2002, Upper-mantle origin of the Yellowstone hotspot: Geological Society of America Bulletin, v. 114, p. 1245–1256, http://dx.doi.org/10.1130/0016-7606(2002)114<1245:UMOOTY>2.0.CO;2.
Cloos, M., 1993, Lithospheric buoyancy and collisional orogenesis: Subduction of ocean plateaus, continental margins, island arcs, spreading ridges, and seamounts: Geological Society of America Bulletin, v. 105, p. 715–737, http://dx.doi.org/10.1130/0016-7606(1993)105<0715:LBACOS>2.3.CO;2.
Coble, M.A., and Mahood, G.A., 2012, Initial impingement of the Yellowstone plume located by widespread silicic volcanism contemporaneous with Columbia River flood basalts: Geology, v. 40, p. 655–658, http://dx.doi.org/10.1130/G32692.1.
Coney, P.J., 1979, Tertiary evolution of Cordilleran metamorphic core complexes, *in* Armentrout, J.W., Cole, M.R., and TerBest Jr., H., *eds.*, Cenozoic paleogeography of the western United States: Society of Economic Paleontologists and Mineralogists, Pacific Section Symposium 3, p. 15–28.
Coney, P.J., and Reynolds, S.J., 1977, Cordilleran Benioff zones: Nature, v. 270, p. 403–406, http://dx.doi.org/10.1038/270403a0.
Coney, P.J., Jones, D.L., and Monger, J.W.H., 1980, Cordilleran suspect terranes: Nature, v. 288, p. 329–333, http://dx.doi.org/10.1038/288329a0.
Courtillot, V., Davaille, A., Besse, J., and Stock, J., 2003, Three distinct types of hotspots in the Earth's mantle: Earth and Planetary Science Letters, v. 205, p. 295–308, http://dx.doi.org/10.1016/S0012-821X(02)01048-8.
Cowan, D.S., 1994, Alternative hypotheses for the mid-Cretaceous paleogeography of the western Cordillera: GSA Today, v. 4, p. 184–186.
Craig, H., Lupton, J.E., Welhan, J.A., and Poreda, R., 1978, Helium isotope ratios in Yellowstone and Lassen Park volcanic gases: Geophysical Research Letters, v. 5, p. 897–900, http://dx.doi.org/10.1029/GL005i011p00897.
Dalziel, I.W.D., 1986, Collision and Cordilleran orogenesis: an Andean perspective, *in* Coward, M.P., and Ries, A.C., *eds.*, Collision Tectonics: Geological Society, London, Special Publications, v. 19, p. 389–404., http://dx.doi.org/10.1144/GSL.SP.1986.019.01.22.
Dalziel, I.W.D., Lawver, L.A., and Murphy, J.B., 2000, Plumes, orogenesis, and supercontinental fragmentation: Earth and Planetary Science Letters, v. 178, p. 1–11, http://dx.doi.org/10.1016/S0012-821X(00)00061-3.
Darold, A., and Humphreys, E., 2013, Upper mantle seismic structure beneath the Pacific Northwest: A plume-triggered delamination origin for the Columbia River flood basalt eruptions: Earth and Planetary Science Letters, v. 365, p. 232–242, http://dx.doi.org/10.1016/j.epsl.2013.01.024.
Davaille, A., and Vatteville, J., 2005, On the transient nature of mantle plumes: Geophysical Research Letters, v. 32, L14309, http://dx.doi.org/10.1029/2005GL023029.
Davaille, A., Le Bars, M., and Carbonne, C., 2003, Thermal convection in a heterogeneous mantle: Comptes Rendus Geoscience, v. 335, p. 141–156, http://dx.doi.org/10.1016/S1631-0713(03)00003-8.
Davis, G.H., and Coney, P.J., 1979, Geologic development of Cordilleran metamorphic core complexes: Geology, v. 7, p. 120–124, http://dx.doi.org/10.1130/0091-7613(1979)7<120:GDOTCM>2.0.CO;2.
DePaolo, D.J., 1981, A neodymium and strontium isotopic study of the Mesozoic

calc-alkaline granitic batholiths of the Sierra Nevada and Peninsular Ranges, California: Journal of Geophysical Research, v. 86, p. 10470–10488, http://dx.doi.org/10.1029/JB086iB11p10470.

Dewey, J.F., and Bird, J.M., 1970, Mountain belts and the new global tectonics: Journal of Geophysical Research, v. 75, p. 2625–2647, http://dx.doi.org/10.1029/JB075i014p02625.

Dickinson, W.R., 1991, Tectonic setting of faulted Tertiary strata associated with the Catalina core complex in southern Arizona: Geological Society of America Special Papers, v. 264, 106 p., http://dx.doi.org/10.1130/SPE264-p1.

Dickinson, W.R., 2004, Evolution of the North American Cordillera: Annual Review of Earth and Planetary Sciences, v. 32, p. 13–45, http://dx.doi.org/10.1146/annurev.earth.32.101802.120257.

Dickinson, W.R., and Lawton, T.F., 2001, Carboniferous to Cretaceous assembly and fragmentation of Mexico: Geological Society of America Bulletin, v. 113, p. 1142–1160, http://dx.doi.org/10.1130/0016-7606(2001)113<1142:CTCAAF>2.0.CO;2.

Dickinson, W.R., and Snyder, W.S., 1978, Plate tectonics of the Laramide orogeny, *in* Matthews III, V., *ed.*, Laramide folding associated with basement block faulting in the western United States: Geological Society of America Memoirs, v. 151, p. 355–366, http://dx.doi.org/10.1130/MEM151-p355.

Doubrovine, P.V., Steinberger, B., and Torsvik, T.H., 2012, Absolute plate motions in a reference frame defined by moving hot spots in the Pacific, Atlantic, and Indian oceans: Journal of Geophysical Research, v. 117, B09101, http://dx.doi.org/10.1029/2011JB009072.

Draper, D.S., 1991, Late Cenozoic bimodal magmatism in the northern Basin and Range Province in southeastern Oregon: Journal of Volcanology and Geothermal Research, v. 47, p. 299–328, http://dx.doi.org/10.1016/0377-0273(91)90006-L.

Drew, D.L., Bindeman, I.N., Watts, K.E., Schmitt, A.K., Fu, B., and McCurry, M., 2013, Crustal-scale recycling in caldera complexes and rift zones along the Yellowstone hotspot track: O and Hf isotopic evidence in diverse zircons from voluminous rhyolites of the Picabo volcanic field, Idaho: Earth and Planetary Science Letters, v. 381, p. 63–77, http://dx.doi.org/10.1016/j.epsl.2013.08.007.

Druken, K.A., Kincaid, C., Griffiths, R.W., Stegman, D.R., and Hart, S.R., 2014, Plume–slab interaction: The Samoa–Tonga system: Physics of the Earth and Planetary Interiors, v. 232, p. 1–14, http://dx.doi.org/10.1016/j.pepi.2014.03.003.

Duncan, R.A., 1982, A captured island chain in the Coast Range of Oregon and Washington: Journal of Geophysical Research, v. 87, p. 10827–10837, http://dx.doi.org/10.1029/JB087iB13p10827.

Engebretson, D.C., Cox, A., and Gordon, R.G., 1985, Relative motions between the oceanic and continental plates in the Pacific Basin: Geological Society of America Special Papers, v. 206, p. 1–60, http://dx.doi.org/10.1130/spe206-p1.

English, J.M., and Johnston, S.T., 2004, The Laramide Orogeny: What Were the Driving Forces?: International Geology Review, v. 46, p. 833–838, http://dx.doi.org/10.2747/0020-6814.46.9.833.

English, J.M., Johnston, S.T., and Wang, K., 2003, Thermal modelling of the Laramide orogeny: Testing the flat-slab subduction hypothesis: Earth and Planetary Science Letters, v. 214, p. 619–632, http://dx.doi.org/10.1016/S0012-821X(03)00399-6.

Fletcher, M., and Wyman, D.A., 2015, Mantle plume–subduction zone interactions over the past 60 Ma: Lithos, v. 233, p. 162–173, http://dx.doi.org/10.1016/j.lithos.2015.06.026.

Fouch, M.W., 2012, The Yellowstone Hotspot: Plume or Not?: Geology, v. 40, p. 479–480, http://dx.doi.org/10.1130/focus052012.1.

Foulger, G.R., and Natland, J.H., 2003, Is "hotspot" volcanism a consequence of plate tectonics?: Science, v. 300, p. 921–922, http://dx.doi.org/10.1126/science.1083376.

Gans, P.B., Mahood, G.A., and Schermer, E., 1989, Synextensional magmatism in the Basin and Range Province: A case study from the eastern Great Basin: Geological Society of America Special Papers, v. 233, 53 p., http://dx.doi.org 10.1130/SPE233-p1.

Geist, D., and Richards, M., 1993, Origin of the Columbia Plateau and Snake River plain: Deflection of the Yellowstone plume: Geology, v. 21, p. 789–792, http://dx.doi.org/10.1130/0091-7613(1993)021<0789:OOTCPA>2.3.CO;2.

Gladwin, K., and Johnston, S.T., 2006, Mid-Cretaceous pinning of accreted terranes to miogeoclinal assemblages in the northern Cordillera: Irreconcilable with Paleomagnetic data?, *in* Haggert, J., and Enkin, R., *eds.,* Cordilleran Paleogeography: Geological Association of Canada Special Paper 46, p. 299–306.

Glen, J.M.G., and Ponce, D.A., 2002, Large-scale fractures related to inception of the Yellowstone hotspot: Geology, v. 30, p. 647–650, http://dx.doi.org/10.1130/0091-7613(2002)030<0647:LSFRTI>2.0.CO;2.

Graham, D.W., Reid, M.R., Jordan, B.T., Grunder, A.L., Leeman, W.P., and Lupton, J.E., 2009, Mantle source provinces beneath the Northwestern USA delimited by helium isotopes in young basalts: Journal of Volcanology and Geothermal Research, v. 188, p. 128–140, http://dx.doi.org/10.1016/j.jvolgeores.2008.12.004.

Graindorge, D., Spence, G., Charvis, P., Collot, J.Y., Hyndman, R., and Tréhu, A.M., 2003, Crustal structure beneath the Strait of Juan de Fuca and southern Vancouver Island from seismic and gravity analyses: Journal of Geophysical Research, v. 108, 2484, http://dx.doi.org/10.1029/2002JB001823.

Gutscher, M.-A., 2002, Andean subduction styles and their effect on thermal structure and interplate coupling: Journal of South American Earth Sciences, v. 15, p. 3–10, http://dx.doi.org/10.1016/S0895-9811(02)00002-0.

Gutscher, M.-A., Spakman, W., Bijwaard, H., and Engdahl, E.R., 2000, Geodynamics of flat subduction: Seismicity and tomographic constraints from the Andean margin: Tectonics, v. 19, p. 814–833, http://dx.doi.org/10.1029/1999TC001152.

Hadley, D.M., Stewart, G.S., and Ebel, J.E., 1976, Yellowstone: Seismic evidence for a chemical mantle plume: Science, v. 193, p. 1237–1239, http://dx.doi.org/10.1126/science.193.4259.1237.

Haeussler, P.J., Bradley, D.C., Wells, R.E., and Miller, M.L., 2003, Life and death of the Resurrection plate: Evidence for its existence and subduction in the northeastern Pacific in Paleocene–Eocene time: Geological Society of America Bulletin, v. 115, p. 867–880, http://dx.doi.org/10.1130/0016-7606(2003)115<0867:LADOTR>2.0.CO;2.

Hamilton, W.B., 1969, Mesozoic California and the underflow of Pacific mantle: Geological Society of America Bulletin, v. 80, p. 2409–2430, http://dx.doi.org/10.1130/0016-7606(1969)80.

Hanan, B.B., Shervais, J.W., and Vetter, S.V., 2008, Yellowstone plume–continental lithosphere interaction beneath the Snake River Plain: Geology, v. 36, p. 51–54, http://dx.doi.org/10.1130/G23935A.1.

Hassan, R., Flament, N., Gurnis, M., Bower, D.J., and Müller, D., 2015, Provenance of plumes in global convection models: Geochemistry, Geophysics, Geosystems, v. 16. p. 1465–1489, http://dx.doi.org/10.1002/2015GC005751.

Hearn, E.H., Kennedy, B.M., and Truesdell, A.T., 1990, Coupled variations in helium isotopes and fluid chemistry: Shoshone Geyser Basin, Yellowstone National Park: Geochimica et Cosmochimica Acta, v. 54, p. 3103–3113, http://dx.doi.org/10.1016/0016-7037(90)90126-6.

Hildebrand, R.S., 2009, Did westward subduction cause Cretaceous–Tertiary orogeny in the North American Cordillera?: Geological Society of America Special Papers, v. 457, p. 1–71, http://dx.doi.org/10.1130/2009.2457.

Hildebrand, R.S., 2014, Geology, mantle tomography, and inclination corrected paleogeographic trajectories support westward subduction during Cretaceous orogenesis in the North American Cordillera: Geoscience Canada, v. 41, p. 207–224, http://dx.doi.org/10.12789/geocanj.2014.41.032.

Hildebrand, R.S., 2015, Dismemberment and northward migration of the Cordilleran orogen: Baja–BC resolved: GSA Today, v. 25, p. 4–11, http://dx.doi.org/10.1130/GSATG255A.1.

Hildebrand, R.S., and Whalen, J.B., 2014. Arc and slab-failure magmatism in Cordilleran Batholiths II – The Cretaceous Peninsular Ranges Batholith of Southern and Baja California: Geoscience Canada, v. 41, p. 399–458, http://dx.doi.org/10.12789/geocanj.2014.41.059.

Hoffman, P.F., 2013, The Tooth of Time: The North American Cordillera from Tanya Atwater to Karin Sigloch: Geoscience Canada, v. 40, p. 71–93, http://dx.doi.org/10.12789/geocanj.2013.40.009.

Hooper, P.R., and Hawkesworth, C.J., 1993, Isotopic and geochemical constraints on the origin and evolution of the Columbia River Basalt: Journal of Petrology, v. 34, p. 1203–1246, http://dx.doi.org/10.1093/petrology/34.6.1203.

Hooper, P.R., Camp, V.E., Reidel, S.P., and Ross, M.E., 2007, The origin of the Columbia River flood basalt province: Plume versus nonplume models, *in* Foulger, G.R., and Jurdy, D.M., *eds.*, Plates, Plumes, and Planetary Processes: Geological Society of America Special Papers, v. 430, p. 635–668, http://dx.doi.org/10.1130/2007.2430(30).

Hughes, S.S., McCurry, M., and Geist, D.J., 2002, Geochemical correlations and implications for the magmatic evolution of basalt flow groups at the Idaho National Engineering and Environmental Laboratory, *in* Link, P.K., and Mink, L.L. *eds.*, Geology, hydrogeology, and environmental remediation: Idaho National Engineering and Environmental Laboratory, eastern Snake River plain, Idaho: Geological Society of America Special Papers, v. 353, p. 151–173, http://dx.doi.org/10.1130/0-8137-2353-1.151.

Humphreys, E.D., 1995, Post-Laramide removal of the Farallon slab, western United States: Geology, v. 23, p. 987–990, http://dx.doi.org/10.1130/0091-7613(1995)023<0987:PLROTF>2.3.CO;2.

Humphreys, E., Dueker, K., Schutt, D., and Smith, R., 2000, Beneath Yellowstone: Evaluating plume and nonplume models using teleseismic images of the upper

mantle: GSA Today, v. 10, p. 1–7.
Hyndman, R.D., 1995, The Lithoprobe corridor across the Vancouver Island continental margin: the structural and tectonic consequences of subduction: Canadian Journal of Earth Sciences, v. 32, p. 1777–1802, http://dx.doi.org/10.1139/e95-138.
Irving, E., 1985, Tectonics: Whence British Columbia?: Nature, v. 314, p. 673–674, http://dx.doi.org/10.1038/314673a0.
Irving, E., Woodsworth, G.J., Wynne, P.J., and Morrison, J.A., 1985, Paleomagnetic evidence for displacement from the south of the Coast Plutonic Complex, British Columbia: Canadian Journal of Earth Sciences, v. 22, p. 584–598, http://dx.doi.org/10.1139/e85-058.
Irving, E., Thorkelson, D.J., Wheadon, P.M., and Enkin, R.J., 1995, Paleomagmatism of the Spences Bridge Group and northward displacement of the Intermontane Belt, British Columbia: A second look: Journal of Geophysical Research, v. 100, p. 6057–6071, http://dx.doi.org/10.1029/94JB03012.
Irving, E., Wynne, P.J., Thorkelson, D.J., and Schiarizza, P., 1996, Large (1000 to 4000 km) northward movements of tectonic domains in the northern Cordillera, 83 to 45 Ma: Journal of Geophysical Research, v. 101, p. 17901–17916, http://dx.doi.org/10.1029/96JB01181.
Ito, G., and van Keken, P.E., 2007, Hotspots and melting anomalies, *in* Bercovi, D., *ed.*, Mantle Dynamics: Treatise on Geophysics, v. 7, p. 371–435, http://dx.doi.org/10.1016/B978-044452748-6/00123-1.
Johnston, S.T., 2001, The Great Alaskan Terrane Wreck: reconciliation of paleomagnetic and geologic data in the northern Cordillera: Earth and Planetary Science Letters, v. 193, p. 259–272, http://dx.doi.org/10.1016/S0012-821X(01)00516-7.
Johnston, S.T., 2008, The Cordilleran Ribbon Continent of North America: Annual Review of Earth and Planetary Sciences, v. 36, p. 495–530, http://dx.doi.org/10.1146/annurev.earth.36.031207.124331.
Johnston, S.T., and Acton, S., 2003, The Eocene southern Vancouver Island orocline — a response to seamount accretion and the cause of fold-and-thrust belt and extensional basin formation: Tectonophysics, v. 365, p.165–183, http://dx.doi.org/10.1016/S0040-1951(03)00021-0.
Johnston, S.T., and Borel, G.D., 2007, The odyssey of the Cache Creek terrane, Canadian Cordillera: Implications for accretionary orogens, tectonic setting of Panthalassa, the Pacific superswell, and break-up of Pangea: Earth and Planetary Science Letters, v. 253, p. 415–428, http://dx.doi.org/10.1016/j.epsl.2006.11.002.
Johnston, S.T., and Thorkelson, D.J., 1997, Cocos–Nazca slab window beneath Central America: Earth and Planetary Science Letters, v. 146, p. 465–474, http://dx.doi.org/10.1016/S0012-821X(96)00242-7.
Johnston, S.T., and Thorkelson, D.J., 2000, Continental flood basalts: episodic magmatism above long-lived hotspots: Earth Planetary Science Letters, v. 175, p. 247–256, http://dx.doi.org/10.1016/S0012-821X(99)00293-9.
Johnston, S.T., Wynne, P.J., Francis, D., Hart, C.J.R., Enkin, R.J., and Engebretson, D.C., 1996, Yellowstone in Yukon: The Late Cretaceous Carmacks Group: Geology, v. 24, p. 997–1000, http://dx.doi.org/10.1130/0091-7613(1996)024<0997:YIYTLC>2.3.CO;2.
Kelbert, A., Egbert, G.D., and deGroot-Hedlin, C., 2012, Crust and upper mantle electrical conductivity beneath the Yellowstone Hotspot Track: Geology, v. 40, p. 447–450, http://dx.doi.org/10.1130/G32655.1.
Kelley, K.P., and Engebretson, D.C., 1994, Updated relative motions and terrane trajectories for North America and oceanic plates: Cretaceous to present (Abstract): Geological Society of America Abstracts with Programs, v. 26, p. A459.
Kent, D.V., and Irving, E., 2010, Influence of inclination error in sedimentary rocks on the Triassic and Jurassic apparent pole wander path for North America and implications for Cordilleran tectonics: Journal of Geophysical Research, v. 115, B10103, http://dx.doi.org/10.1029/2009JB007205.
Kincaid, C., Druken, K.A., Griffiths, R.W., and Stegman, D.R., 2013, Bifurcation of the Yellowstone plume driven by subduction-induced mantle flow: Nature Geoscience, v. 6, p. 395–399, http://dx.doi.org/10.1038/ngeo1774.
King, S.D., 2007, Hotspots and edge-driven convection: Geology, v. 35, p. 223–226, http://dx.doi.org/10.1130/G23291A.1.
King, S.D., and Anderson, D.L., 1998, Edge-driven convection: Earth and Planetary Science Letters, v. 160, p. 289–296, http://dx.doi.org/10.1016/S0012-821X(98)00089-2.
Kistler, R.W., and Peterman, Z.E., 1973, Variations in Sr, Rb, K, Na, and initial Sr^{87}/Sr^{86} in Mesozoic granitic rocks and intruded wall rocks in central California: Geological Society of America Bulletin, v. 84, p. 3489–3512, http://dx.doi.org/10.1130/0016-7606(1973)84<3489:VISRKN>2.0.CO;2.
Kistler, R.W., and Peterman, Z.E., 1978, Reconstruction of crustal rocks of California on the basis of initial strontium isotopic compositions of Mesozoic granitic rocks: U.S. Geological Survey Professional Paper 1071, 17 p.
Lipman, P.W., Protska, H.J., and Christiansen, R.L., 1972, Cenozoic volcanism and plate tectonic evolution of the western United States: 1. Early and Middle Cenozoic: Royal Society of London Philosophical Transactions, Series A 271, p. 217–248, http://dx.doi.org/10.1098/rsta.1972.0008.
Liu, L., and Stegman, D.R., 2012, Origin of Columbia River flood basalt controlled by propagating rupture of the Farallon slab: Nature, v. 482, p. 386–389, http://dx.doi.org/10.1038/nature10749.
Liu, L., Spasojević, S., and Gurnis, M., 2008, Reconstructing Farallon Plate subduction beneath North America back to the Late Cretaceous: Science, v. 322, p. 934–938, http://dx.doi.org/10.1126/science.1162921.
Liu, L., Gurnis, M., Seton, M., Saleeby, J., Müller, R.D., and Jackson, J.M., 2010, The role of oceanic plateau subduction in the Laramide orogeny: Nature Geoscience, v. 3, p. 353–357, http://dx.doi.org/10.1038/ngeo829.
Livaccari, R.F., Burke, K., and Şengör, A.M.C., 1981, Was the Laramide orogeny related to subduction of an oceanic plateau?: Nature, v. 289, p. 276–278, http://dx.doi.org/10.1038/289276a0.
Lonsdale, P.F., 1988, Geography and history of the Louisville Hotspot Chain in the southwest Pacific: Journal of Geophysical Research, v. 93, p. 3078–3104, http://dx.doi.org/10.1029/JB093iB04p03078.
Madsen, J.K., Thorkelson, D.J., Friedman, R.M., and Marshall, D.D., 2006, Cenozoic to Recent plate configurations in the Pacific Basin: Ridge subduction and slab window magmatism in western North America: Geosphere, v. 2, p. 11–34, http://dx.doi.org/10.1130/GES00020.1.
Mahoney, J.J., Duncan, R.A., Tejada, M.L.G., Sager, W.W., and Bralower, T.J., 2005, Jurassic–Cretaceous boundary age and mid-oceanic-ridge-type mantle source for Shatsky Rise: Geology, v. 33, p. 185–188, http://dx.doi.org/10.1130/G21378.1.
Massey, N.W.D., 1986, Metchosin Igneous Complex, southern Vancouver Island: Ophiolite stratigraphy developed in an emergent island setting: Geology, v. 14, p. 602–605, http://dx.doi.org/10.1130/0091-7613(1986)14<602:MICSVI>2.0.CO;2.
Maxson, J., and Tikoff, B., 1996, Hit-and-run collision model for the Laramide orogeny, western United States: Geology, v. 24, p. 968–972, http://dx.doi.org/10.1130/0091-7613(1996)024<0968:HARCMF>2.3.CO;2.
McCrory, P.A., and Wilson, D.S., 2013, A kinematic model for the formation of the Siletz-Crescent forearc terrane by capture of coherent fragments of the Farallon and Resurrection plates: Tectonics, v. 32, p. 718–736, http://dx.doi.org/10.1002/tect.20045.
McKenzie, D.P., 1983, The Earth's mantle, *in* Siever, R., *ed.,* The Dynamic Earth, Freeman, New York, p. 25–78.
McNutt, M.K., and Fischer, K.M., 1987, The South Pacific superswell, seamounts, islands and atolls: American Geophysical Union Geophysical Monographs, v. 43, p. 25–34.
Monger, J.W.H., 2014, Seeking the suture: The Coast–Cascade conundrum: Geoscience Canada, v. 41, p. 379–398, http://dx.doi.org/10.12789/geocanj.2014.41.058.
Monger, J.W.H., van der Heyden, P., Journeay, J.M., Evenchick, C.A., and Mahoney, J.B., 1994, Jurassic–Cretaceous basins along the Canadian Coast Belt: Their bearing on pre–mid-Cretaceous sinistral displacements: Geology, v. 22, p. 175–178, http://dx.doi.org/10.1130/0091-7613(1994)022<0175:JCBATC>2.3.CO;2.
Montelli, R., Nolet, G., Dahlen, F.A., and Masters, G., 2006, A catalogue of deep mantle plumes: New results from finite-frequency tomography: Geochemistry, Geophysics, Geosystems, v. 7, Q11007, http://dx.doi.org/10.1029/2006GC001248.
Morgan, W.J., 1971, Convection plumes in the lower mantle: Nature, v. 230, p. 42–43, http://dx.doi.org/10.1038/230042a0.
Morgan, W.J., 1972, Plate motions and deep mantle convection, *in* Shagam, R., Hargraves, R.B., Morgan, W.J., Van Houten, F.B., Burk, C.A., Holland, H.D., and Hollister, L.C., *eds.*, Studies in Earth and Space Sciences: Geological Society of America Memoirs, v. 132, p. 7–22, http://dx.doi.org/10.1130/MEM132-p7.
Müller, R.D., Royer, J.-Y., and Lawver, L.A., 1993, Revised plate motions relative to the hotspots from combined Atlantic and Indian Ocean hotspot tracks: Geology, v. 21, p. 275–278, http://dx.doi.org/10.1130/0091-7613(1993)021<0275:RPMRTT>2.3.CO;2.
Murphy, J.B., Oppliger, G.L., Brimhall Jr., G.H., and Hynes, A., 1998, Plume-modified orogeny: An example from the western United States: Geology, v. 26, p. 731–734, http://dx.doi.org/10.1130/0091-7613(1998)026<0731:PMOAEF>2.3.CO;2.
Murphy, J.B., Hynes, A.J., Johnston, S.T., and Keppie, J.D., 2003, Reconstructing the ancestral Yellowstone plume from accreted seamounts and its relationship to flat-slab subduction: Tectonophysics, v. 365, p. 185–194, http://dx.doi.org/

10.1016/S0040-1951(03)00022-2.

Nakanishi, M., Sager, W.W., and Korenaga, J., 2015, Reorganization of the Pacific-Izanagi-Farallon triple junction in the Late Jurassic: Tectonic events before the formation of the Shatsky Rise, *in* Erba, E., Neal, C., Sager, W.W., and Sano, T., *eds.,*The Origin, Evolution, and Environmental Evolution of Oceanic Large Igneous Provinces: Geological Society of America Special Papers, v. 511, p. 85–101, http://dx.doi.org/10.1130/2015.2511(05).

Obrebski, M., Allen, R.M., Xue, M., and Hung, S.-H., 2010, Slab-plume interaction beneath the Pacific Northwest: Geophysical Research Letters, v. 37, L14305, http://dx.doi.org/10.1029/2010GL043489.

Oldow, J.S., Bally, A.W., Avé Lallemant, H.G., and Leeman, W.P., 1989, Phanerozoic evolution of the North American Cordillera; United States and Canada, *in* Bally, A.W., and Palmer, A.R., *eds.*, The geology of North America—An overview: Geological Society of America, Boulder, CO, p. 139–232.

O'Neill, C., Müller, D., and Steinberger, B., 2005, On the uncertainties in hot spot reconstructions and the significance of moving hot spot reference frames: Geochemistry, Geophysics, Geosystems, v. 6, Q04003, http://dx.doi.org/10.1029/2004GC000784.

Oppliger, G.L., Murphy, J.B., and Brimhall Jr., G.H., 1997, Is the ancestral Yellowstone hotspot responsible for the Tertiary "Carlin" mineralization in the Great Basin of Nevada?: Geology, v. 25, p. 627–630, http://dx.doi.org/10.1130/0091-7613(1997)025<0627:ITAYHR>2.3.CO;2.

Pierce, K.L., and Morgan, L.A., 2009, Is the track of the Yellowstone hotspot driven by a deep mantle plume? —Review of volcanism, faulting, and uplift in light of new data: Journal of Volcanology and Geothermal Research, v. 188, p. 1–25, http://dx.doi.org/10.1016/j.jvolgeores.2009.07.009.

Pilger Jr., R.H., 1981, Plate reconstruction, aseismic ridges, and low-angle subduction beneath the Andes: Geological Society of America Bulletin, v. 92, p. 448–456, http://dx.doi.org/10.1130/0016-7606(1981)92<448:PRARAL>2.0.CO;2.

Porritt, R.W., Allen, R.M., and Pollitz, F.F., 2014, Seismic imaging east of the Rocky Mountains with USArray: Earth and Planetary Science Letters, v. 402, p. 16–25, http://dx.doi.org/10.1016/j.epsl.2013.10.034.

Price, R.A., and Carmichael, D.M., 1986, Geometric test for Late Cretaceous–Paleogene intracontinental transform faulting in the Canadian Cordillera: Geology, v. 14, p. 468–471, http://dx.doi.org/10.1130/0091-7613(1986)14<468:GTFLCI>2.0.CO;2.

Pyle, D., Duncan, R., Wells, R.E., Graham, D.W., Harrison, B., and Hanan, B., 2009, Siletzia: An oceanic large igneous province in the Pacific Northwest (Abstract): Geological Society of America Abstracts with Programs, v. 41, p. 369.

Pyle, D.G., Hanan, B.B., Graham, D.W., and Duncan, R.A., 1997, Siletzia; geochemistry and geochronology of Yellowstone hot spot volcanism in a suboceanic setting (Abstract): Geological Society of America Abstracts with Programs, v. 29, p. 298.

Ramachandran, K., 2001, Velocity Structure of SW British Columbia and NW Washington, from 3-D non-linear seismic tomography: Unpublished PhD thesis, University of Victoria, Victoria, BC, 198 p.

Ramos, V.A., and McNulty, B. (*editors*), 2002, Flat-slab subduction in the Andes: Journal of South American Earth Sciences, Special Issue, v. 15, p. 1–155.

Ribe, N.M., and Christensen, U.R., 1994, Three-dimensional modeling of plume-lithosphere interaction: Journal of Geophysical Research, v. 99, p. 669–682, http://dx.doi.org/10.1029/93JB02386.

Richards, M.A., Hager, B.H., and Sleep, N.H., 1988, Dynamically supported geoid highs over hotspots: Observation and theory: Journal of Geophysical Research, v. 93, p. 7690–7708, http://dx.doi.org/10.1029/JB093iB07p07690.

Sager, W.W., 2005, What built Shatsky Rise, a mantle plume or ridge tectonics?, *in* Foulger, G.R., Natland, J.H., Presnall, D.C., and Anderson, D.L., *eds.*, Plumes, Plates, and Paradigms: Geological Society of America Special Papers, v. 388, p. 721–733, http://dx.doi.org/10.1130/0-8137-2388-4.721.

Saleeby, J., 2003, Segmentation of the Laramide slab—evidence from the southern Sierra Nevada region: Geological Society of America Bulletin, v. 115, p. 655–668, http://dx.doi.org/10.1130/0016-7606(2003)115<0655:SOTLSF>2.0.CO;2.

Schmandt, B., and Humphreys, E., 2010, Complex subduction and small-scale convection revealed by body-wave tomography of the western United States upper mantle: Earth and Planetary Science Letters, v. 297, p. 435–445, http://dx.doi.org/10.1016/j.epsl.2010.06.047.

Schmandt, B., Dueker, K., Humphreys, E., and Hansen, S., 2012, Hot mantle upwelling across the 660 beneath Yellowstone: Earth and Planetary Science Letters, v. 331–332, p. 224–236, http://dx.doi.org/10.1016/j.epsl.2012.03.025.

Schutt, D.L., and Humphreys, E.D., 2004, *P* and *S* wave velocity and V_P/V_S in the wake of the Yellowstone hot spot: Journal of Geophysical Research, v. 109, B01305, http://dx.doi.org/10.1029/2003JB002442.

Seligman, A.N., Bindeman, I.N., McClaughry, J., Stern, R.A., and Fisher, C., 2014, The earliest low and high $\delta^{18}O$ caldera-forming eruptions of the Yellowstone plume: implications for the 30–40 Ma Oregon calderas and speculations on plume-triggered delaminations: Frontiers in Earth Science, v. 2, Article 34, http://dx.doi.org/10.3389/feart.2014.00034.

Seton, M., Müller, R.D., Zahirovic, S., Gaina, C., Torsvik, T., Shephard, G., Talsma, A., Gurnis, M., Turner, M., Maus, S., and Chandler, M., 2012, Global continental and ocean basin reconstructions since 200 Ma: Earth-Science Reviews, v. 113, p. 212–270, http://dx.doi.org/10.1016/j.earscirev.2012.03.002.

Severinghaus, J., and Atwater, T., 1990, Cenozoic geometry and thermal state of the subducting slabs beneath North America, *in* Wernicke, B.P., *ed.*, Basin and Range extensional tectonics near the latitude of Las Vegas, Nevada: Geological Society of America Memoirs, v. 176, p. 1–22, http://dx.doi.org/10.1130/MEM176-p1.

Shervais, J.W., and Hanan, B.B., 2008, Lithospheric topography, tilted plumes, and the track of the Snake River–Yellowstone hot spot: Tectonics, v. 27, TC5004, http://dx.doi.org/10.1029/2007TC002181.

Shervais, J.W., Vetter, S.K., and Hanan, B.B., 2006, A layered mafic sill complex beneath the eastern Snake River Plain: Evidence from cyclic geochemical variations in basalt: Geology, v. 34, p. 365–368, http://dx.doi.org/10.1130/G22226.1.

Sigloch, K., 2011, Mantle provinces under North America from multifrequency *P* wave tomography: Geochemistry, Geophysics, Geosystems, v. 12, Q02W08, http://dx.doi.org/10.1029/2010GC003421.

Sigloch, K., and Mihalynuk, M.G., 2013, Intra-oceanic subduction shaped the assembly of Cordilleran North America: Nature, v. 496, p. 50–56, http://dx.doi.org/10.1038/nature12019.

Simpson, R.W., and Cox, A., 1977, Paleomagnetic evidence for tectonic rotation of the Oregon Coast Range: Geology, v. 5, p. 585–589, http://dx.doi.org/10.1130/0091-7613(1977)5<585:PEFTRO>2.0.CO;2.

Sleep, N.H., 1990, Hotspots and mantle plumes: Some phenomenology: Journal of Geophysical Research, v. 95, p. 6715–6736, http://dx.doi.org/10.1029/JB095iB05p06715.

Smith, R.B., and Braile, L.W., 1994, The Yellowstone hotspot: Journal of Volcanology and Geothermal Research, v. 61, p. 121–129, 135–187, http://dx.doi.org/10.1016/0377-0273(94)90002-7.

Smith, R.B., Jordan, M., Steinberger, B., Puskas, C.M., Farrell, J., Waite, G.P., Husen, S., Chang, W.-L., and O'Connell, R., 2009, Geodynamics of the Yellowstone hotspot and mantle plume: Seismic and GPS imaging, kinematics, and mantle flow: Journal of Volcanology and Geothermal Research, v. 188, p. 26–56, http://dx.doi.org/10.1016/j.jvolgeores.2009.08.020.

Snavely, P.D., MacLeod, N.S., and Wagner, H.C., 1968, Tholeiitic and alkalic basalts of the Eocene Siletz River Volcanics, Oregon Coast Range: American Journal of Science, v. 266, p. 454–481, http://dx.doi.org/10.2475/ajs.266.6.454.

Steinberger, B., and O'Connell, R.J., 1998, Advection of plumes in mantle flow: Implications for hotspot motion, mantle viscosity and plume distribution: Geophysical Journal International, v. 132, p. 412–434, http://dx.doi.org/10.1046/j.1365-246x.1998.00447.x.

Steinberger, B., and O'Connell, R.J., 2000, Effects of mantle flow on hotspot motion, *in* Richards, M.A., Gordon, R.G., and Van Der Hilst, R.D., *eds.*, The History and Dynamics of Global Motions: American Geophysical Union, Washington, DC, p. 377–398, http://dx.doi.org/10.1029/gm121p0377.

Steinberger, B., Sutherland, R., and O'Connell, R.J., 2004, Prediction of Emperor-Hawaii seamount locations from a revised model of global plate motion and mantle flow: Nature, v. 430, p. 167–173, http://dx.doi.org/10.1038/nature02660.

Tan, E., Leng, W., Zhong, S., and Gurnis, M., 2011, On the location of plumes and lateral movement of thermochemical structures with high bulk modulus in the 3-D compressible mantle: Geochemistry, Geophysics, Geosystems, v. 12, Q07005, http://dx.doi.org/10.1029/2011GC003665.

Tarduno, J.A., McWilliams, M., Debiche, M.G., Sliter, W.V., and Blake Jr., M.C., 1985, Franciscan Complex Calera limestones: accreted remnants of Farallon Plate oceanic plateaus: Nature, v. 317, p. 345–347, http://dx.doi.org/10.1038/317345a0.

Tatsumi, Y., Shinjoe, H., Ishizuka, H., Sager, W.W., and Klaus, A., 1998, Geochemical evidence for a mid-Cretaceous superplume: Geology, v. 26, p. 151–154, http://dx.doi.org/10.1130/0091-7613(1998)026<0151:GEFAMC>2.3.CO;2.

Torsvik, T.H., Smethurst, M.A., Burke, K., and Steinberger, B., 2006, Large igneous provinces generated from the margins of the large low velocity provinces in the deep mantle: Geophysical Journal International, v. 167, p. 1447–1460, http://dx.doi.org/10.1111/j.1365-246X.2006.03158.x.

Trehu, A.M., Asudeh, I., Brocher, T.M., Luetgert, J.H., Mooney, W.D., Nabelek, J.L., and Nakamura, Y., 1994, Crustal architecture of the Cascadia forearc: Science, v. 266, p. 237–243, http://dx.doi.org/10.1126/science.266.5183.237.

Usui, T., Nakamura, E., Kobayashi, K., Maruyama, S., and Helmstaedt, H., 2003, Fate of the subducted Farallon plate inferred from eclogite xenoliths in the Colorado Plateau: Geology, v. 31, p. 589–592, http://dx.doi.org/10.1130/0091-7613(2003)031<0589:FOTSFP>2.0.CO;2.

Vetter, S.K., and Shervais, J.W., 1992, Continental basalts of the Boise River Group near Smith Prairie, Idaho: Journal of Geophysical Research, v. 97, p. 9043–9061, http://dx.doi.org/10.1029/92JB00209.

Waite, G.P., Smith, R.B., and Allen, R.M., 2006, V_P and V_S structure of the Yellowstone hot spot from teleseismic tomography: Evidence for an upper mantle plume: Journal of Geophysical Research, v. 111, B04303, http://dx.doi.org/10.1029/2005JB003867.

Watts, K.E., Bindeman, I.N., and Schmitt, A.K., 2011, Large-volume rhyolite genesis in caldera complexes of the Snake River Plain: Insights from the Kilgore Tuff of the Heise Volcanic Field, Idaho, with comparison to Yellowstone and Bruneau–Jarbidge rhyolites: Journal of Petrology, v. 52, p. 857–890, http://dx.doi.org/10.1093/petrology/egr005.

Wells, R., Bukry, D., Friedman, R., Pyle, D., Duncan, R., Haeussler, P., and Wooden, J., 2014, Geologic history of Siletzia, a large igneous province in the Oregon and Washington Coast Range: Correlation to the geomagnetic polarity time scale and implications for a long-lived Yellowstone hotspot: Geosphere, v. 10, p. 692–719, http://dx.doi.org/10.1130/GES01018.1.

Wells, R.E., Engebretson, D.C., Snavely Jr., P.D., and Coe, R.S., 1984, Cenozoic plate motions and the volcano-tectonic evolution of western Oregon and Washington: Tectonics, v. 3, p. 275–294, http://dx.doi.org/10.1029/TC003i002p00275.

Williams, Q., Revenaugh, J., and Garnero, E., 1996, Hotspots are correlated with ultra-low basal velocities in the mantle (Abstract): American Geophysical Union, v. 77, p. 710.

Wynne, P.J., Irving, E., Maxson, J.A., and Kleinspehn, K.L., 1995, Paleomagnetism of the Upper Cretaceous strata of Mount Tatlow: Evidence for 3000 km of northward displacement of the eastern Coast Belt, British Columbia: Journal of Geophysical Research, v. 100, p. 6073–6091, http://dx.doi.org/10.1029/94JB02643.

Xue, M., and Allen, R.M., 2007, The fate of the Juan de Fuca plate: Implications for a Yellowstone plume head: Earth and Planetary Science Letters, v. 264, p. 266–276, http://dx.doi.org/10.1016/j.epsl.2007.09.047.

Yáñez, G., Cembrano, J., Pardo, M., Ranero, C., and Selles, D., 2002, The Challenger–Juan Fernández–Maipo major tectonic transition of the Nazca–Andean subduction system at 33–34°S: geodynamic evidence and implications: Journal of South American Earth Sciences, v. 15, p. 23– 38, http://dx.doi.org/10.1016/S0895-9811(02)00004-4.

Yuan, H., and Dueker, K., 2005, Teleseismic *P*-wave tomogram of the Yellowstone plume: Geophysical Research Letters, v. 32, L07304, http://dx.doi.org/10.1029/2004GL022056.

Zhao, D., 2007, Seismic images under 60 hotspots: Search for mantle plumes: Gondwana Research, v. 12, p. 335–355, http://dx.doi.org/10.1016/j.gr.2007.03.001.

Zhdanov, M.S., Smith, R.B., Gribenko, A., Cuma, M., and Green, M., 2011, Three dimensional inversion of large scale EarthScope magnetotelluric data based on the integral equation method: Geoelectrical imaging of the Yellowstone conductive mantle plume: Geophysical Research Letters, v. 38, L08307, http://dx.doi.org/10.1029/2011GL046953.

Received May 2016
Accepted as revised September 2016
First published on the web October 2016

SERIES

Igneous Rock Associations 21. The Early Permian Panjal Traps of the Western Himalaya

J. Gregory Shellnutt

Department of Earth Sciences,
National Taiwan Normal University,
88 Tingzhou Road Section 4,
Taipei 11677, Taiwan
E-mail: jgshelln@ntnu.edu.tw

SUMMARY

The Early Permian (290 Ma) Panjal Traps are the largest contiguous outcropping of volcanic rocks associated with the Himalayan Magmatic Province (HMP). The eruptions of HMP-related lava were contemporaneous with the initial break-up of Pangea. The Panjal Traps are primarily basalt but volumetrically minor intermediate and felsic volcanic rocks also occur. The basaltic rocks range in composition from continental tholeiite to ocean-floor basalt and nearly all have experienced, to varying extent, crustal contamination. Uncontaminated basaltic rocks have Sr–Nd isotopes similar to a chondritic source (ISr = 0.7043 to 0.7073; $\varepsilon_{Nd}(t) = 0 \pm 1$), whereas the remaining basaltic rocks have a wide range of Nd ($\varepsilon_{Nd}(t) = -6.1$ to $+4.3$) and Sr (ISr = 0.7051 to 0.7185) isotopic values. The calculated primary melt compositions of basalt are picritic and their mantle potential temperatures ($T_P \leq 1450$°C) are similar to ambient mantle rather than anomalously hot mantle. The silicic volcanic rocks were likely derived by partial melting of the crust whereas the andesitic rocks were derived by mixing between crustal and mantle melts. The Traps erupted within a continental rift setting that developed into a shallow sea. Sustained rifting created a nascent ocean basin that led to seafloor spreading and the rifting of microcontinents from Gondwana to form the ribbon-like continent Cimmeria and the Neotethys Ocean.

RÉSUMÉ

Les Panjal Traps du début Permien (290 Ma) constituent le plus grand affleurement contigu de roches volcaniques associées à la province magmatique de himalayienne (HMP). Les éruptions de lave de type HMP étaient contemporaines de la rupture initiale de la Pangée. Les Panjal Traps sont essentiellement des basaltes, mais on y trouve aussi des roches volcaniques intermédiaires et felsiques en quantités mineures. La composition de ces roches basaltiques varie de tholéiite continentale à basalte de plancher océanique, et presque toutes ont subi, à des degrés divers, une contamination de matériaux crustaux. Les roches basaltiques non contaminées ont des contenus isotopiques Sr–Nd similaires à une source chondritique (Isr = 0,7043 à 0,7073; $\varepsilon_{Nd}(t) = 0 \pm 1$), alors que les roches basaltiques autres montrent une large gamme de valeurs isotopiques en Nd ($\varepsilon_{Nd}(t) = -6,1$ à $+4,3$) et Sr (Isr = de 0,7051 à 0,7185). Les compositions de fusion primaire calculées des basaltes sont picritiques et leurs températures potentielles mantelliques (T_P de ≤ 1450°C) sont similaires à la température ambiante du manteau plutôt que celle d'un manteau anormalement chaud. Les roches volcaniques siliciques dérivent probablement de la fusion partielle de la croûte alors que les roches andésitiques proviennent du mélange entre des matériaux de fusion crustaux et mantelliques. Les Traps ont fait irruption dans un contexte de rift continental qui s'est développé dans une mer peu profonde. Un rifting soutenu a créé un début de bassin océanique lequel conduit à une expansion du fond océanique et au rifting de microcontinents tirés du Gondwana pour former le continent rubané de Cimméria et l'océan Néotéthys.

Traduit par le Traducteur

INTRODUCTION

The Late Paleozoic (ca. 300 Ma to ca. 252 Ma) was a time of large polar glaciations, the zenith of Pangea and two mass extinctions (Martin 1981; Bond and Wignall 2014). Moreover, at least five major mafic continental large igneous provinces

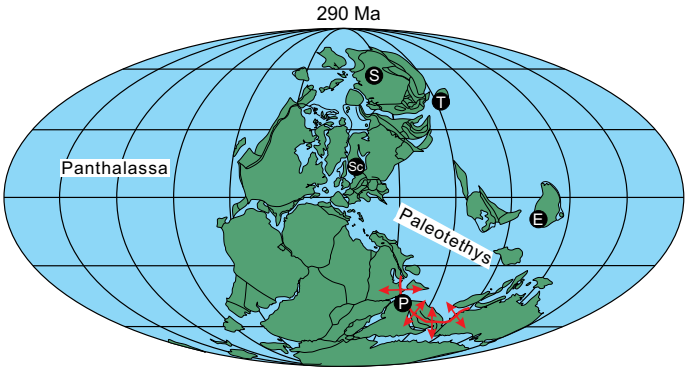

Figure 1. Paleogeographic reconstructions of Pangea at ca. 290 million years showing the location of the Panjal Traps (P) and possible rift propagation and the locations of the five major mafic continental large igneous provinces of the Late Paleozoic. The reconstruction is based on Torsvik et al. (2014). E = Emeishan large igneous province (ca. 260 Ma); S = Siberian Traps (ca. 250 Ma); Sc = Skagerrak-Centred large igneous province (ca. 300 Ma); T = Tarim large igneous province (ca. 280–270 Ma).

(LIP) were emplaced (Fig. 1). The Skagerrak-centred large igneous province (ca. 300 Ma) in central Laurasia, the Himalayan magmatic province (ca. 290–270 Ma) along the Tethyan margin of Gondwana, the Tarim large igneous province (ca. 290–270 Ma) on the Tethyan margin of Laurasia, the Emeishan large igneous province (ca. 260 Ma) of the South China Block and the Siberian Traps (ca. 251 Ma) of northeastern Laurasia cover a combined area >7 x 10^6 km^2 (Ernst and Buchan 2001; Torsvik et al. 2008; Saunders and Reichow 2009; Zhu et al. 2010; Shellnutt et al. 2014; Shellnutt 2014; Ernst 2014; Wang et al. 2014; Xu et al. 2014). The Late Paleozoic mafic continental LIPs, unlike their Mesozoic and Cenozoic counterparts, are exclusively unrelated to plate separation with the exception of the ill-defined, poorly constrained Himalayan magmatic province (HMP).

The HMP is an assortment of volcanic and plutonic rocks and mafic dykes throughout the Himalaya that were contemporaneous with the rifting of microcontinental terranes from the Tethyan margin of Gondwana (Bhat et al. 1981; Bhat 1984; Garzanti et al. 1999; Ernst and Buchan 2001; Yan et al. 2005; Zhu et al. 2010; Shellnutt et al. 2014, 2015; Ali et al. 2012; Zhai et al. 2013; Wang et al. 2014; Xu et al. 2016). The rifting of 'Cimmerian' terranes and accompanying magmatism are thought to have been related to a regional-scale mantle plume but the petrogenetic and precise temporal relationships between the magmatic rocks of the HMP remains uncertain (Lapierre et al. 2004; Zhai et al. 2013; Shellnutt et al. 2015; Xu et al. 2016). The Panjal Traps, located in the western Himalaya, provide the largest spatially contiguous exposure of HMP-related rocks (Bhat et al. 1981; Honegger et al. 1982; Papritz and Rey 1989; Chauvet et al. 2008; Shellnutt et al. 2014, 2015). In comparison with other Phanerozoic flood basalt provinces, the Panjal Traps are not well studied as they are located in relatively remote regions of the Himalaya.

Understanding the formation of the Panjal Traps can help to unravel the pre-India–Eurasia collision tectonics of Gondwana and can elucidate first order geological problems such as the geodynamic and tectonomagmatic evolution of LIPs with specific relevance to the differences between the passive (i.e. 'plate hypothesis') and active (i.e. 'mantle plume theory') extensional Late Paleozoic LIPs. This paper presents a current 'state of knowledge' on the Panjal Traps. The paper is subdivided into topic-specific sections that include: 1) the geological background, 2) the age and duration of volcanism, 3) geochemical characteristics of the volcanic rocks, 4) tectonomagmatic evolution vis-à-vis active vs. passive extension, and 5) a regional comparison of HMP-related rocks. The final section brings together all of the available information in an attempt to offer a working hypothesis on the formation of the Panjal Traps and their relationship to the formation of the Neotethys Ocean and Cimmeria.

GEOLOGICAL BACKGROUND

The Tethyan domain of the western Indian Himalaya comprises Precambrian to Late Paleozoic rocks that form part of the Higher Himalaya. The Precambrian Central Crystalline complex consists of augen granite-gneiss, nebulitic migmatite, grey, and dark paragneiss and is the basement to Tethyan passive margin sedimentary sequences. Overlying the basement is a series of Cambrian to Lower Carboniferous sedimentary formations that consist mainly of sandstone, shale, siltstone, arkose, carbonate, and evaporite rocks (Gaetani et al. 1986; Fuchs 1987; Garzanti et al. 1992, 1994, 1996a, b; Myrow et al. 2006; Brookfield et al. 2013).

Above the Lower Carboniferous units is the Middle to Upper Carboniferous fossiliferous (*Spirifer varuna*- and *Camarophoria*-bearing) Fenestella shale followed by agglomeratic slate, a mixture of siliciclastic and volcaniclastic material, which may represent the first eruptive unit of the Panjal Traps. The Upper Permian siliciclastic Nishatbagh beds are deposited on the agglomeratic slate, and are followed by the main eruptive sequence of the Panjal Traps (Nakazawa et al. 1975; Garzanti et al. 1998; Wopfner and Jin 2009). The reported total thickness of the volcanic rocks is ca. 3000 m in the Pir Panjal Range (western Kashmir) and ≤ 300 m in the Zanskar Range (eastern Kashmir) with individual flows around 30 m thick (Middlemiss 1910; Wadia 1934, 1961; Nakazawa et al. 1975; Chauvet et al. 2008). The deposition of the flora- and fauna-rich Gangamopteris beds (siliceous shale and novaculite) on top of the Panjal Traps constrains the basalt eruption age to the Upper Permian. The Gangamopteris beds are followed by the Zewan Formation (sandstone and carbonate) and the uppermost Permian–Lower Triassic Khunamuh Formation (shale) (Nakazawa et al. 1975; Wopfner and Jin 2009; Brookfield et al. 2013). The Late Paleozoic sedimentary rocks were deposited as a response to differential uplift of the Indian margin during rifting (Vannay and Spring 1993; Garzanti et al. 1999).

The Panjal Traps underlie an area of ca. 10,000 km^2 exposed primarily around the Kashmir Valley along the Pir Panjal and Zanskar Ranges and were first documented in the 19th century by Lydekker (1883) (Fig. 2). The Traps are mostly basalt but there are minor volumes of basaltic andesite, andesite, rhyolite and dacite (Ganju 1944; Nakazawa and Kapoor 1973; Shellnutt et al. 2012, 2014). The Traps show evi-

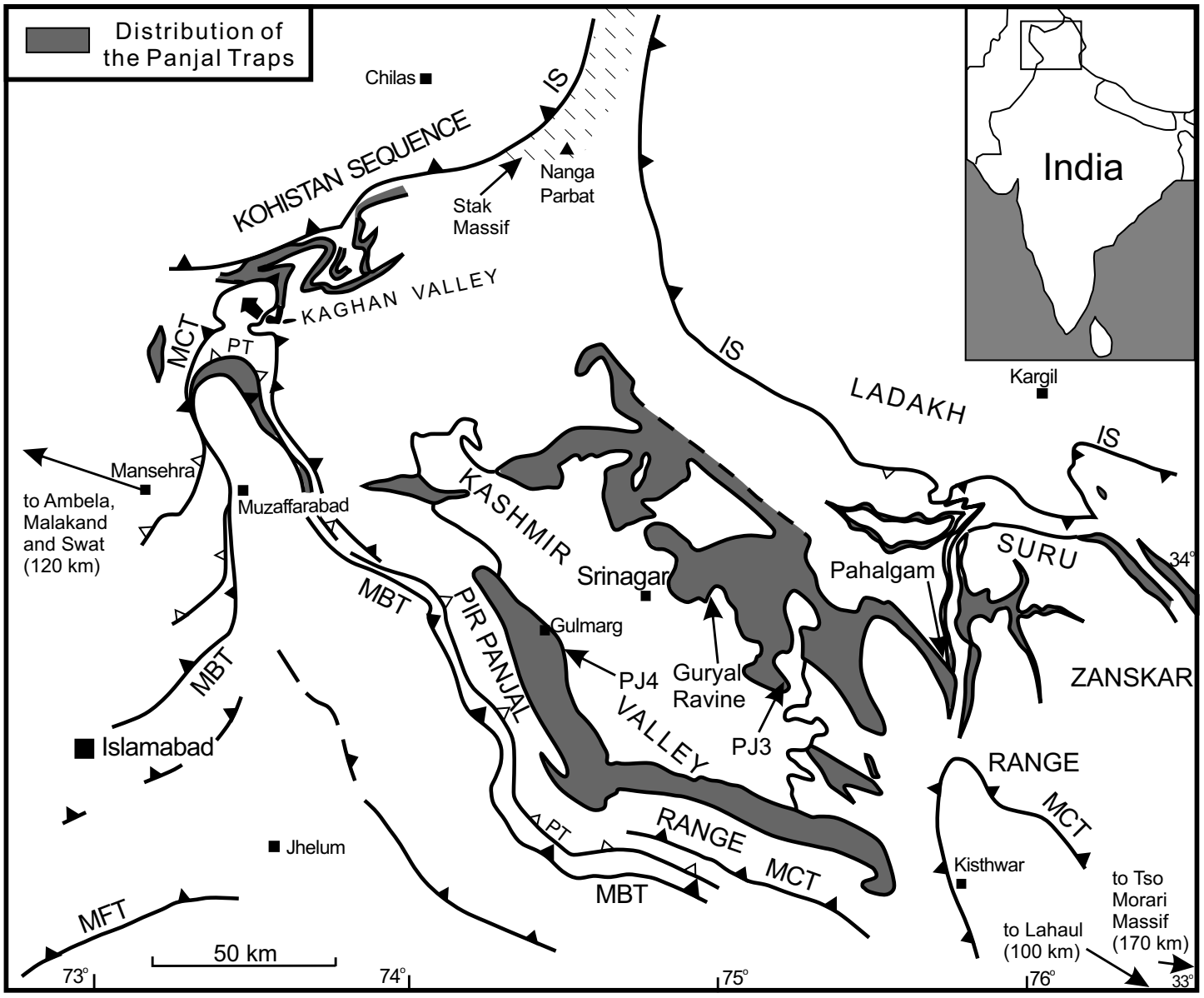

Figure 2. Distribution of the Panjal Traps, major faults of the western Himalaya and the sampling localities at Guryal Ravine, Pahalgam, PJ3 and PJ4 (based on Papritz and Rey 1989). IS = Indus suture; MBT = main boundary thrust; MCT = main central thrust; MFT = Salt Range main frontal thrust; PT = Panjal thrust.

dence of both subaerial (e.g. columnar joints and intertrappean sedimentary deposits) and subaqueous (i.e. pillow structures) eruptive environments that Nakazawa and Kapoor (1973) interpreted as indicative of a near-shore, transgressive shallow marine environment. Intertrappean limestone, shale and slate are reported near Gulmarg and Srinagar suggesting there were local intermittent pauses during volcanism.

AGE AND DURATION OF VOLCANISM

The precise age and duration of the Panjal Traps was, until recently, only inferred based on the stratigraphic record. The Traps were initially considered to be Lower Paleozoic but Middlemiss (1910), based on the presence of ammonites from the genus *Ophiceras* in overlying sedimentary rocks, interpreted their age as Upper Paleozoic. Subsequent studies revealed the Traps erupted during the Late Paleozoic to Early Mesozoic (i.e. Late Carboniferous to Early Triassic), but detailed structural and sedimentological studies by Nakazawa et al. (1975) showed that the rocks erupted after the deposition of the Middle to Upper Carboniferous Fenestella shale and before the deposition of the Upper Permian Gangamopteris beds (Mamal Beds) which contain lower Gondwana flora. The first isotopic ages of the Panjal Traps were determined from zircon collected from the silicic Traps near Srinagar and yielded a mean $^{206}Pb/^{238}U$ age of 289 ± 3 Ma (Shellnutt et al. 2011).

Presently, very few definitive statements can be made regarding the duration of Panjal magmatism but it is clear that magmatism was underway by the Early Permian. The initial volcanic rocks are thought to be agglomeratic slate which is interpreted to be an 'explosive volcanic' unit and consists of

ash and possibly volcanic bombs, although non-volcanic fossiliferous material appears to dominate (Nakazawa and Kapoor 1973; Nakazawa et al. 1975). Gaetani et al. (1990) suggested the eruption duration was 2 to 3 m.y. based on faunal markers from NW Lahul–SE Zanskar, but the volcanic sequences are thinner than those around the Kashmir Valley and may be incomplete. The basalts at Guryal Ravine are capped by marine sedimentary rocks that are Early Permian (Artinskian) in age but that does not preclude the possibility that magmatism continued after the rift transitioned from a continental setting to an oceanic setting (Nakazawa et al. 1975; Wopfner and Jin 2009; Tewari et al. 2015; Shellnutt et al. 2015).

MAFIC PANJAL TRAPS

Chemical Characterization

The mafic Panjal Traps are tholeiitic to mildly alkalic basalt (Fig. 3) (Nakazawa and Kapoor 1973; Bhat et al. 1981; Honegger et al. 1982; Papritz and Rey 1989; Chauvet et al. 2008; Shellnutt et al. 2014). Bhat et al. (1981) demonstrated that the Panjal Traps have chemical affinity to basalt related to a within-plate tectonic setting. A slightly more nuanced view, using the tectonic classification scheme of Pearce et al. (1977), shows the Panjal Traps fall within the fields of 'continental basalt' and 'ocean ridge basalt' (Fig. 4).

The volcanic sequences around the Kashmir Valley have chemostratigraphic variations, specifically the TiO_2 concentration, as there appears to be high-Ti and low-Ti basalt. The variability within specific sequences is real but if all basalt data are considered, then it is less clear that there are two types but rather a spectrum of compositions (Fig. 3e). In broad terms, the Mg# ($[Mg^{2+}/(Mg^{2+}+Fe^{2+})]*100$) can better distinguish groupings of basalt as there appear to be three groups (Fig. 3f): 1) high Mg# group (> 57), 2) middle Mg# group (50 to 57), and 3) low Mg# group (< 50). Furthermore, the rocks with the highest Mg# likely represent more 'primitive' lavas as they tend to have higher Ni (> 100 ppm) content than the rocks with lower Mg# values (Ni < 100 ppm).

To date only a few studies have reported the Sr–Nd isotopes of the Panjal Traps (Chauvet et al. 2008; Shellnutt et al. 2014, 2015). The Sr isotopes are quite variable (ISr = 0.7043 to 0.7185) which may be due to Rb or Sr mobility during greenschist-facies metamorphism (Fig. 5). Basalt with lower ISr values (ISr = 0.7043–0.7073) is probably indicative of source composition, whereas the higher values (ISr > 0.7100) are probably related to element mobility associated with greenschist-facies metamorphism and/or crustal contamination. The Nd isotopes are also variable ($\varepsilon_{Nd}(t)$ = –6.1 to +4.3) but Sm and Nd are less susceptible to mobility and likely indicative of their 'unaltered' compositions. Some samples may be representative of the initial, uncontaminated basaltic magmas as they have $\varepsilon_{Nd}(t)$ values between –1.4 and +1.3, ISr values between 0.7043 and 0.7073 and low Th/Nb_{PM} ($\leq$ 1) ratios (PM = normalized to primitive mantle values of Sun and McDonough 1989) and high Nb/U ($\geq$ 49) ratios, but generally most samples appear to have been affected by crustal contamination.

Magma Differentiation and Crustal Contamination

Most of the mafic Panjal Traps have experienced to varying degrees either crystal fractionation or crustal contamination or both. Shellnutt et al. (2014, 2015) suggested that the 'high-Ti' rocks from Pahalgam and some rocks (i.e. 'low-Ti') from the Pir Panjal Range experienced crystal fractionation where the 'high-Ti' rocks experienced olivine and plagioclase fractionation and the 'low-Ti' rocks experienced clinopyroxene and olivine fractionation. However, many rocks do not show clear evidence of mineral fractionation.

The range of trace element ratios (e.g. Nb/La, Th/Yb, Ta/Yb and Nb/U) sensitive to crustal contamination and the initial Nd isotopes suggests much of the basalt experienced crustal contamination (Campbell 2002; Rudnick and Gao 2003). The Nb/La values of the Panjal Traps are generally < 1.0 although a few samples have higher values, whereas the Nb/U (6 to 102) and Th/Nb_{PM} (0.5 to 6.9) ratios have a wide range of values (Fig. 6). Some of the Nd isotope signatures (e.g. $\varepsilon_{Nd}(t) < -4$) are likely due to contamination by crustal melts. Isotopic modelling indicates that the amount of crustal contamination is probably between 5% and 10% for most basaltic rocks but there are some exceptions and larger amounts (> 20%) of contamination likely occurred (Shellnutt et al. 2014, 2015).

Mantle Source

Trace element modelling suggests that low and moderate degrees of partial melting of a spinel lherzolite source, assuming a primitive mantle starting composition, can reproduce the range of the chondrite-normalized rare-earth element (REE) patterns seen in the Panjal rocks (Fig. 7). Basalt from Guryal Ravine and Pahalgam that does not show clear evidence for crustal assimilation can be modelled by 3% to 7% batch melting using a spinel lherzolite (olivine = 57%, orthopyroxene = 26%, clinopyroxene = 15%, spinel = 2%) source composition (Shellnutt et al. 2014, 2015). Rocks that have high Mg# (> 57), high Ni (> 100 ppm), flat REE patterns and fall within the ocean floor field of tectonomagmatic discrimination diagrams can be model by ca. 10% partial melting or more. Although it is not possible to completely rule out the presence of garnet in the source (typically Sm/Yb_N < 2.7), it would have to be a very minor (< 1%) constituent.

It is likely that the Panjal Traps were derived from two isotopically distinct mantle sources, one similar to chondritic mantle (i.e. $\varepsilon_{Nd}(t) = 0 \pm 1$) and another similar to asthenospheric mantle (Chauvet et al. 2008; Shellnutt et al. 2014, 2015). Figure 8 shows three regression lines (Guryal Ravine line, Pahalgam line and PJ4 line) of the Panjal Traps using $\varepsilon_{Nd}(t)$ and the Th/Nb_{PM} ratio. The Th/Nb_{PM} ratio is an indicator for crustal contamination where upper crust (UC) has a value of 7.3, depleted MORB mantle (DMM) has a value of 0.45 and primitive mantle (PM) is 1.1. Therefore, the 'uncontaminated' Traps should be closer to either the DMM or PM values and the contaminated rocks should be between either DMM or PM and UC. It is clear that only a small cluster of samples has chondritic $\varepsilon_{Nd}(t)$ values with low Th/Nb_{PM} values (0.5 to 1.0). The

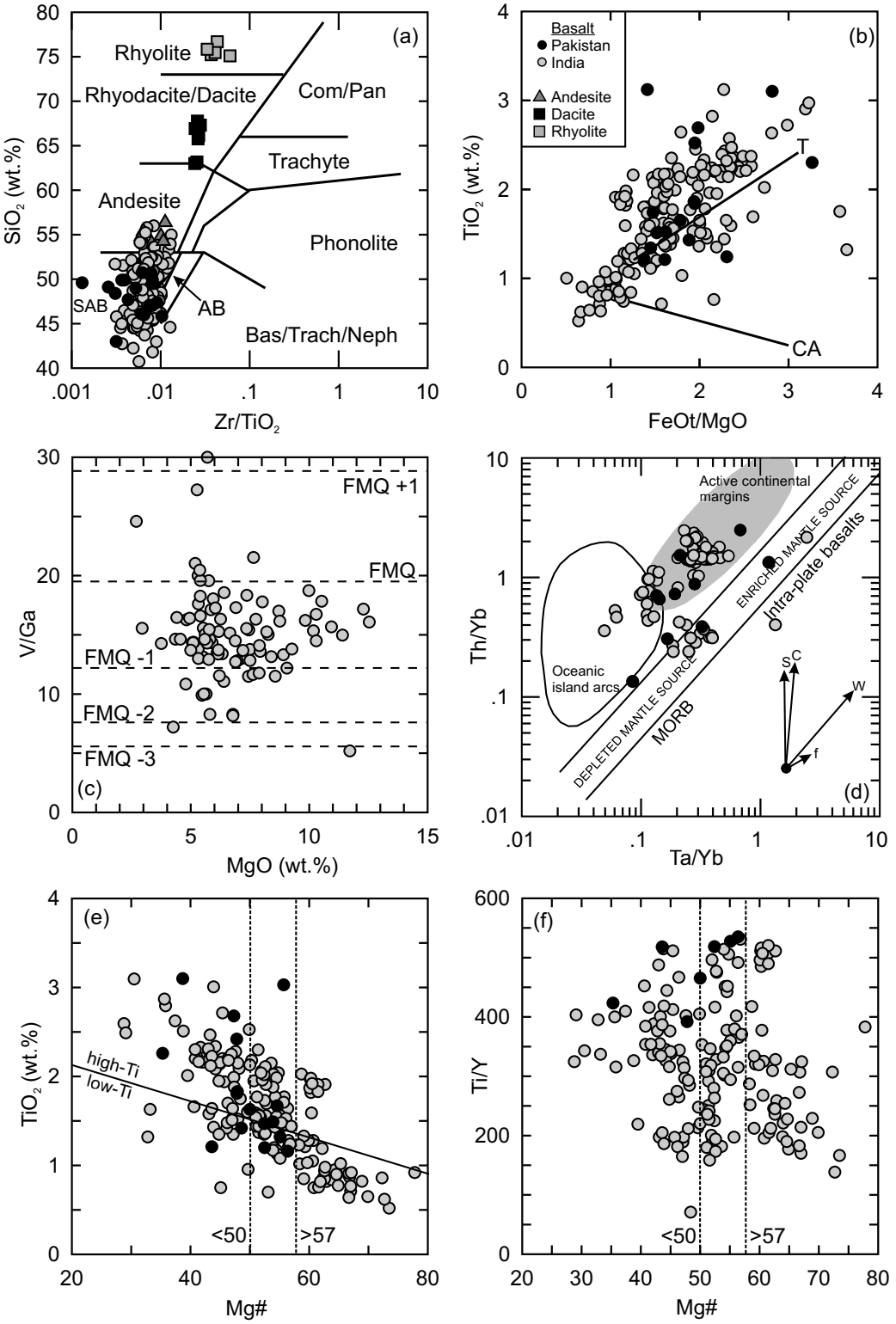

Figure 3. (a) Rock classification of the Panjal Traps using immobile elements (Winchester and Floyd 1977). SAB = sub-alkaline basalts; AB = alkaline basalt; Com/Pan = Comendite/Pantellerite; Bas/Trach/Neph = basanite, trachybasanite, nephelinite. (b) Discrimination of tholeiitic (T) basaltic rocks from calc-alkaline (CA) basaltic rocks (Miyashiro 1974). (c) Binary diagram showing the use of bulk-rock V/Ga to indicate the redox condition of the mafic Panjal Traps. Reference lines at various fO_2 are after Mallmann and O'Neill (2009). (d) Th/Yb vs. Ta/Yb basalt discrimination diagram of Wilson (1989) showing the differences between subduction and oceanic basalt derived from depleted and enriched sources. Vectors show influences of each component, S = subduction component; C = crustal component; W = within-plate enrichment; f = fractional crystallization. Ti-classification of the Panjal Traps showing (e) TiO_2 (wt.%) vs. Mg# and (f) Mg# vs. Ti/Y. Data from Pareek (1976), Bhat and Zainuddin (1978, 1979), Bhat et al. (1981), Honegger et al. (1982), Papritz and Rey (1989), Pogue et al. (1992), Vannay and Spring (1993), Rao and Rai (2007), Chauvet et al. (2008) and Shellnutt et al. (2012, 2014, 2015).

http://www.dx.doi.org/10.12789/geocanj.2016.43.104

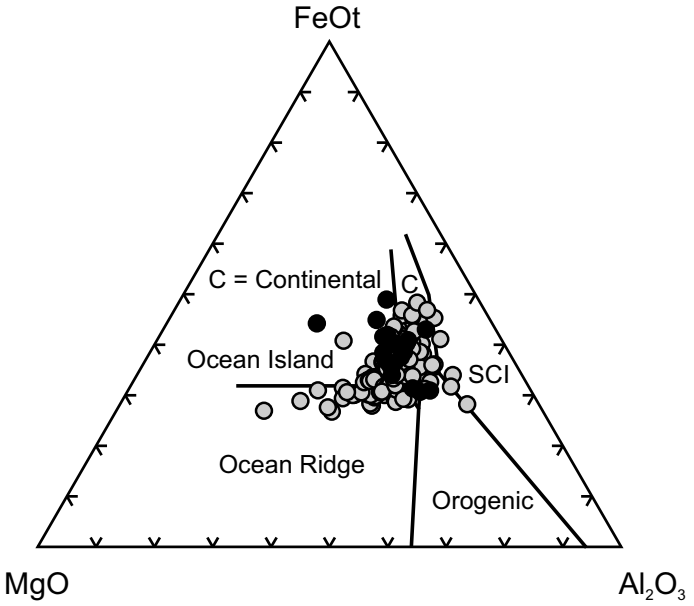

Figure 4. Basalt tectonomagmatic discrimination diagram of Pearce et al. (1977) for the mafic Panjal Traps. C = continental basalt; SCI = spreading centre island basalt. Symbols as in Figure 2. Data from Pareek (1976), Bhat and Zainuddin (1978, 1979), Bhat et al. (1981), Honegger et al. (1982), Papritz and Rey (1989), Pogue et al. (1992), Vannay and Spring (1993), Rao and Rai (2007), Chauvet et al. (2008) and Shellnutt et al. (2012, 2014, 2015).

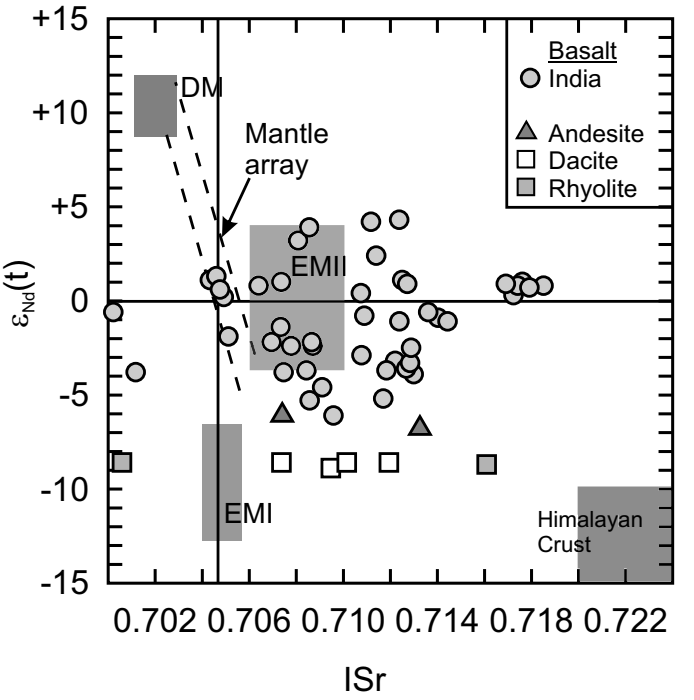

Figure 5. Sr–Nd plot showing the mafic and silicic Panjal traps from the Kashmir Valley region. DM = deplete mantle; EMI = enriched mantle I; EMII = enriched mantle II (Zindler and Hart 1986; Workman et al. 2004; Workman and Hart 2005). Isotopic range of the Himalayan crust from Spencer et al. (1995). Data from Chauvet et al. (2008) and Shellnutt et al. (2012, 2014, 2015).

uncontaminated chondritic samples show two separate mixing lines, one with basalt from Guryal Ravine whereas the other is with basalt from Pahalgam. When the mixing lines are extend-

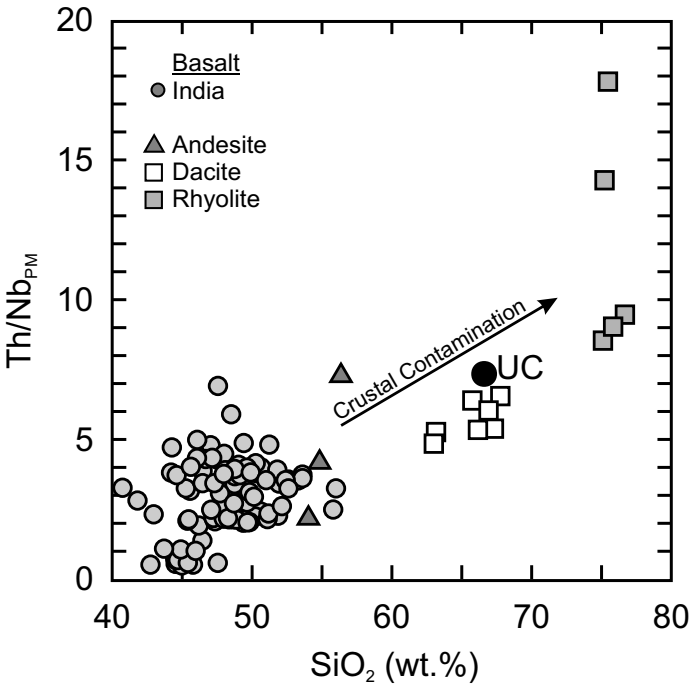

Figure 6. Th/Nb_{PM} vs. SiO_2 (wt.%) of the Panjal mafic, intermediate and silicic rocks. The trend toward higher Th/Nb_{PM} and SiO_2 within the basaltic rocks is likely due to crustal contamination. UC = upper crust values from Rudnick and Gao (2003). Data from Spring et al. (1993), Chauvet et al. (2008) and Shellnutt et al. (2012, 2014, 2015).

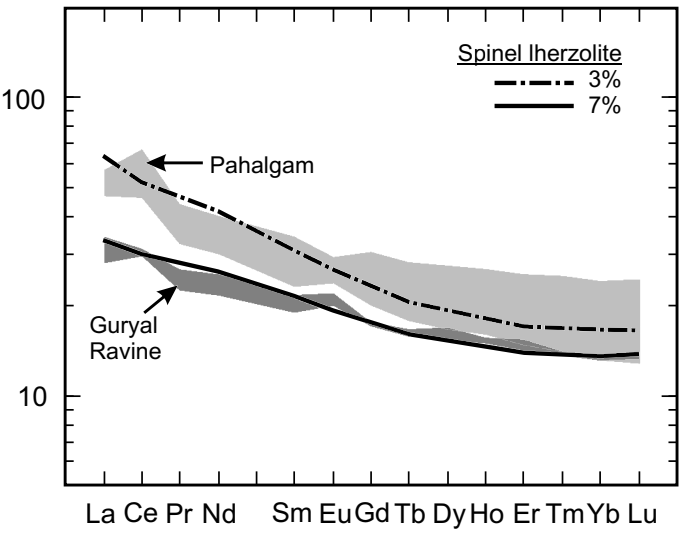

Figure 7. Results of rare earth element modelling with respect to the least contaminated Panjal Traps from Guryal Ravine and Pahalgam. The models assume a primitive mantle starting composition (Sun and McDonough 1989). The composition of the spinel lherzolite is: olivine = 57%, orthopyroxene = 26%, clinopyroxene = 15%, spinel = 2%. Elements are normalized to chondrite values of Sun and McDonough (1989).

ed to higher Th/Nb_{PM} values they passed through or very close to either the Panjal dacite (Guryal Ravine line) or the Panjal rhyolite (Pahalgam line) suggesting specific silicic volcanic rocks may have acted as the enriched end-members for mixing with specific basaltic sections (Fig. 8). A third mixing line (PJ4

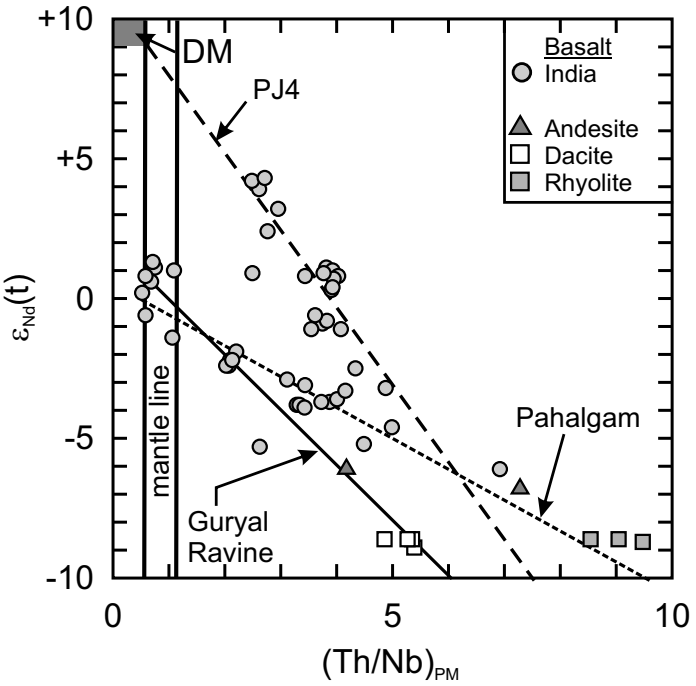

Figure 8. $\varepsilon_{Nd}(t)$ vs. Th/Nb_{PM} showing three mixing lines of the Panjal basaltic rocks and silicic rocks calculated by Shellnutt et al. (2015). Total mafic Panjal Traps data are superimposed on the calculated mixing lines. The mantle line is based on the depleted MORB mantle of Workman and Hart (2005). The calculated regression lines for the basalt data are extended to the x-axis and the mantle line. Th/Nb_{PM} is normalized to primitive mantle values of Sun and McDonough (1989). DM = depleted mantle of Workman and Hart (2005). Data from Chauvet et al. (2008) and Shellnutt et al. (2012, 2014, 2015).

line) is observed involving rocks collected from the Pir Panjal Range near Gulmarg. The PJ4 line, when extended to higher Th/Nb_{PM} values, passes through the values for basalt collected from the Zanskar Valley and crosses between the dacite and rhyolite. If the PJ4 regression line is extended to intercept either the DMM or the PM line then the corresponding $\varepsilon_{Nd}(t)$ value is between +8 and +9 and similar to depleted mantle. The samples that fall along the upper trend-line appear to favour a contaminant similar to or something in between the Panjal silicic rocks. Based on the T_{DM} (1240 Ma to 2170 Ma) model ages of uncontaminated chondritic basalt, it is possible that the original mantle source was the sub-continental lithospheric mantle (SCLM), whereas basaltic rocks with higher $\varepsilon_{Nd}(t)$ values were derived from a source that had a larger proportion of asthenospheric mantle.

Primary Melt Composition and Thermal Regime

Most flood basalt rocks do not represent primary magma compositions but rather derivative liquids that have experienced crystal fractionation or contamination (Herzberg et al. 2007; Herzberg and Asimow 2015). Deducing the temperature and primary melt composition of ultramafic and mafic volcanic rocks can reveal important information regarding the possible thermal conditions of flood basalt provinces. For example, the identification of anomalously hot mantle potential temperatures may be evidence for a hotspot (Herzberg and Gazel 2009; Ali et al. 2010; Hole 2015). The eruptive temperatures (T) and mantle potential temperatures (T_P) of the Panjal Traps are estimated to be ≤ 1340°C and ≤ 1450°C, respectively (Table 1). The calculations suggest the primary magmas were picritic (Le Bas et al. 2000) and experienced ca. 10–20% olivine loss. The T_P estimates are closer to ambient mantle (1300°C to 1400°C) thermal conditions rather than anomalously hot conditions (Ali et al. 2010; Hole 2015).

SILICIC PANJAL TRAPS

The Panjal Traps have a volumetrically minor but petrologically significant portion of silicic volcanic rocks that appear to be restricted to the eastern part of the Kashmir Valley (Ganju 1944; Pareek 1976; Shellnutt et al. 2012). The volcanic rocks are classified as dacite and rhyolite and are quartz porphyry with cryptocrystalline to microcrystalline textures. The primary petrographic difference between the dacite and rhyolite is the amount of quartz phenocrysts. Thus far silicic volcanic rocks have not been reported outside the Kashmir Valley. Early investigations suggested they were derived by differentiation of mafic Panjal magmas but more recent studies indicate they were derived by partial melting of the crust (Wadia 1961; Nakazawa and Kapoor 1973; Nakazawa et al. 1975; Shellnutt et al. 2012). The whole rock chemistry shows the rocks are peraluminous, calcic to calc-alkalic and have isotopic compositions ($\varepsilon_{Nd}(t)$ = –8.6 to –8.9) that are more similar to average Himalayan crust ($\varepsilon_{Nd}(t)$.= –10 to –14) than to the mafic Panjal rocks (Figs. 5 and 9). Furthermore, the silicic rocks have very low Nb/U (< 10) and high Th/Nb_{PM} (> 3) values that are typical of crust-derived igneous rocks (Fig. 6). Geochemical modelling by Shellnutt et al. (2012) indicated that rhyolite and dacite can each be derived by partial melting of the middle crust (from different lithologies) but it is also possible that rhyolite could be derived by fractional crystallization of a dacitic parental magma. Regardless of the relationship between the rhyolite and dacite it is very likely that the injection of mafic Panjal magmas caused the crust to melt and produced at least the dacitic melts.

ANDESITIC PANJAL TRAPS

The basaltic sequences around the Kashmir Valley have horizons of andesitic rocks. Panjal andesitic rocks have been reported from Guryal Ravine, Pir Panjal and the Lidder Valley near Pahalgam (Bhat and Zainuddin 1978; Shellnutt et al. 2014, 2015). The compositions are typically basaltic andesite as they have SiO_2 contents between 54 and 56 wt.%.

The Panjal andesitic rocks are compositionally transitional between the mafic and silicic rocks and are probably derived by mixing of mafic magmas and crustal melts. The whole rock Sr-Nd isotopes ($\varepsilon_{Nd}(t)$ = –6.8 to –6.1) are more enriched than the basalt but less than in the silicic rocks (Fig. 5). Moreover, Th/Nb_{PM} (2.0 to 6.8) values and Nb/U (5.2 to 22.1) values also lie between the silicic and basaltic rocks (Fig. 6). The silicic rocks have $\varepsilon_{Nd}(t)$ values ($\varepsilon_{Nd}(t)$ = –8.6 to –8.9) that are broadly similar to the $\varepsilon_{Nd}(t)$ values ($\varepsilon_{Nd}(t)$ = –10 to –15) of Himalayan crust but the SiO_2 and TiO_2 content are very different (dacite: SiO_2 = ca. 65 wt.%, TiO_2 = ca. 1.1 wt.%, rhyolite: SiO_2 = ca. 75 wt.%, TiO_2 = ca. 0.4 wt.%). Isotope and trace element

Table 1. Primary melt compositions and mantle potential temperatures of the Panjal Traps.

Sample Region	PJ2-003 Pahalgam	AFM	AFM	PJ4-006 Pir Panjal	AFM	AFM
SiO_2 (wt.%)	51.23	50.62	50.90	52.14	51.97	52.33
TiO_2	0.76	0.64	0.66	0.98	0.87	0.90
Al_2O_3	14.70	12.30	12.63	12.37	10.90	11.25
Fe_2O_3	9.04	0.32	0.65	8.69	0.43	0.89
FeO		9.01	8.62		8.19	7.67
FeOt	8.35			7.82		
MnO	0.15	0.16	0.16	0.15	0.16	0.16
MgO	7.50	15.44	14.55	7.37	13.65	12.54
CaO	12.24	10.28	10.56	11.90	10.52	10.86
Na_2O	1.33	1.11	1.14	3.25	2.86	2.95
K_2O	0.07	0.06	0.06	0.43	0.38	0.39
P_2O_5	0.08	0.07	0.07	0.07	0.06	0.06
Pressure (bars)		1	1		1	1
FeO (source)		8.54	8.53		8.47	8.43
MgO (source)		38.12	38.12		38.12	38.12
Fe_2O_3/TiO_2		0.5	1.0		0.5	1.0
% ol addition		21.8	19.0		16.4	13.1
Melt Fraction		0.30	0.29		0.28	0.27
Temperature (°C)		1340	1320		1330	1300
T_P (°C)		1450	1420		1400	1370

FeOt = Fe_2O_3t * 0.8998. AFM = accumulated fractional melting composition. Two models are presented for each sample and reflect differences in relative oxidation state (oxidized mantle source is Fe_2O_3/TiO_2 = 1; reduced mantle source is Fe_2O_3/TiO_2 = 0.5). The model compositions are normalized to 100% for the PRIMELT3 calculation. Data from Shellnutt et al. (2014, 2015).

modelling suggests that between 20% and 30% mixing of dacite or rhyolite and basalt can produce the compositions similar to the andesitic rocks. It seems that in some cases a specific contaminant (rhyolite or dacite) can be identified within the volcanic sequences (Fig. 8). Although it is difficult to confirm, it is possible that the andesitic rocks throughout the Kashmir Valley represent a marker horizon of a very specific eruptive episode that involved significant mixing between crustal melts and mafic magmas.

ACTIVE OR PASSIVE EXTENSION ORIGIN?

There is a tremendous debate regarding the existence of mantle plumes let alone the association between LIPs and plumes (cf. King and Anderson 1995; Ernst and Buchan 2003; Ernst et al. 2005; Campbell 2007; Bryan and Ernst 2008; Foulger 2007, 2010; Ernst 2014). The mantle plume model advocates that a hot diapiric upwelling of mantle material, originating from the lower mantle, impinges at the base of the lithosphere and is followed by the injection of high temperature mafic to ultramafic magmas into the crust. Some of the magmas form dyke networks, plutonic bodies and may induce crustal melting, whereas the magmas that reach the surface erupt and form spectacular trap structures (Richards et al. 1989; Campbell and Griffiths 1990; Campbell 2005, 2007). The spatial association between some LIPs and volcanic rifted margins suggests that mantle plumes may exploit thermal and structural heterogeneities in the lithosphere which assist in continental breakup, but some LIPs are unrelated to plate separation and thus the regional plate stress regime likely plays an important role (Courtillot et al. 1999; Ernst 2014). In contrast, passive rifting and thermal convection models, known as the 'plate' model, have also been put forth as an explanation of some LIPs (White and McKenzie 1989; Foulger 2007, 2010). The premise of the 'plate' model is that "causative processes of melting anomalies of the Earth's top thermal boundary layer" are a consequence of the lithosphere under tensional stress (Foulger 2010). It is possible that the debate is contentious because of the focus on a singular or restricted group of LIPs and that a 'one-size fits all' model is inappropriate for all LIPs given their inherent chemical and tectonic differences, e.g. plate separation vs. non-plate separation. In other words, the mantle plume model may be applicable for some but not all LIPs.

Assessing the involvement of a mantle plume within an ancient LIP is based on a number of criteria. In addition to large volumes of magma (> 100,000 km^3), a mantle plume-derived LIP may exhibit: 1) short duration of magmatism (e.g. ≤ 1 m.y.), 2) high thermal regime (presence of ultramafic volcanic rocks) and 3) evidence of pre-volcanic uplift of the crust (Campbell 2007). In the best of circumstances the criteria are difficult to assess but even more so if the LIP is dismembered or tectonized. The total magmatic duration of many mafic continental LIPs commonly exceeds 10 million years for the main effusive period and may be preceded and followed by sporadic eruptions or intrusions. Consequently, the evaluation of rapid emplacement usually emphasizes peak effusion rates that represent a substantial (e.g. ≥ 70%) portion of the vol-

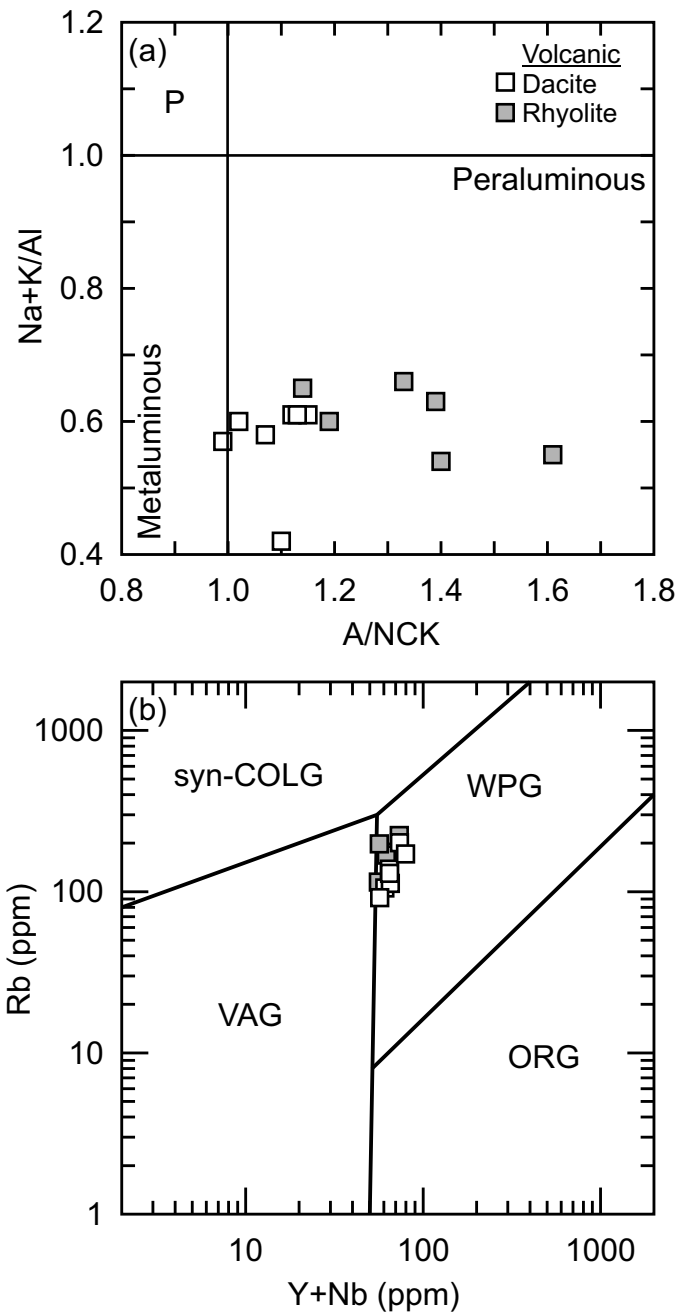

Figure 9. (a) Alkali index (Na+K/Al) vs. aluminum saturation index (ASI; A/NCK = Al/Ca+Na+K). P = peralkaline. (b) Rb (ppm) vs. Y+Nb (ppm) tectonomagmatic classification of granitic rocks of Pearce et al. (1984). Data of the silicic rocks from Shellnutt et al. (2012).

canic system (Campbell 2007; Bryan and Ernst 2008). Identifying evidence for a high thermal regime is largely based on the presence of non-cumulate ultramafic volcanic rocks but assessing evidence for pre-volcanic uplift can be difficult (cf. He et al. 2003; Ukstins Peate and Bryan 2008).

Evidence in support of a mantle plume for the genesis of the Panjal Traps is limited (Lapierre et al. 2004; Zhai et al. 2013). First, the total duration of volcanism is uncertain. Although Nakazawa and Kapoor (1973), Nakazawa et al. (1975), Gaetani et al. (1990) and Stojanovic et al. (2016) suggested volcanism was likely short-lived (< 5 Ma), there is a dearth of high-precision isotopic ages. It is possible that the initial continental portion of the Panjal Traps erupted within a few million years but that volcanism was continuous for tens of millions of years as the continental rift transitioned into sea-floor spreading (Shellnutt et al. 2015). Consequently, the only preserved remnants of the Panjal Traps erupted within a continental setting whereas the transitional to oceanic portions were likely subducted or highly deformed. Second, there are no definitively associated non-cumulate ultramafic rocks within the Panjal Traps and the calculated mantle potential temperatures of the primary magmas are typical of ambient mantle temperatures (Herzberg et al. 2007; Ali et al. 2010). Third, evidence of pre- and syn-volcanic uplift is documented by the progression from older marine sedimentation to younger continental sedimentation throughout the Kashmir and Zanskar Valleys but the transition is attributed to rifting rather than thermal uplift (Gaetani et al. 1990; Garzanti et al. 1996a, b).

At the moment, it appears that the Panjal Traps were not derived from an active rift system but rather a passive rift system controlled by the prevailing plate stress (north-directed subduction of the Paleotethys Ocean) and possibly the isostatic effects of deglaciation (Yeh and Shellnutt 2016). The low estimated mantle potential temperatures and the changing nature of the Nd isotopes from chondritic to more depleted is likely due to the transition from a continental rifting setting to a nascent ocean basin (Shellnutt et al. 2015).

PERMIAN MAFIC ROCKS OF THE HIMALAYA AND THEIR ASSOCIATION WITH THE PANJAL TRAPS

There are many occurrences of Permian rift-related volcanic rocks within the Tethyan domains of Oman, Pakistan, India and China (Bhat et al. 1981; Bhat 1984; Papritz and Rey 1989; Garzanti et al. 1999; Ernst and Buchan 2001; Lapierre et al. 2004; Zhu et al. 2010; Ali et al. 2012, 2013; Zhai et al. 2013; Shellnutt et al. 2014, 2015; Wang et al. 2014; Xu et al. 2016). The Panjal, Abor, Nar-Tsum, Bhote Kosi, Selong, Mojiang volcanic groups, Qiangtang mafic dykes and the Garze Ophiolite are among the many Early to Mid-Permian basaltic rocks that are attributed to rifting and formation of the Neotethys Ocean (Fig. 10). The rocks of east-central Himalaya (i.e. Abor and Nar-Tsum) are not as well studied as there are only a few published geochemical studies, none of which present the isotopic systematics, and consequently it is difficult to link all of the Permian rocks petrogenetically. In comparison to the Panjal Traps, the Jilong and Selong basalt units of Tibet are younger (< 280 Ma), have moderate TiO_2 (1.8–2.0 wt.%), high MgO (> 10 wt.%), high Mg# (> 60), high ISr (0.7160–0.7185) and high chondritic $\varepsilon_{Nd}(t)$ values (+0.7 to +1.2). The mafic dykes of the Qiangtang terrane range in age from 270 to 290 Ma and generally have higher $\varepsilon_{Nd}(t)$ (+2.3 to +7.6) values (Zhai et al. 2013; Xu et al. 2016). The Wusu basalt of the Mojiang volcanic group is dated at ca. 288 Ma and has high $\varepsilon_{Nd}(t)$ values (+4.0 to +5.5) but lower ISr values (0.70376–0.70420) than the Panjal Traps (Fig. 11).

Some suggestions indicate that the Panjal Traps represent a continuation of flood basalts from a mantle plume centred

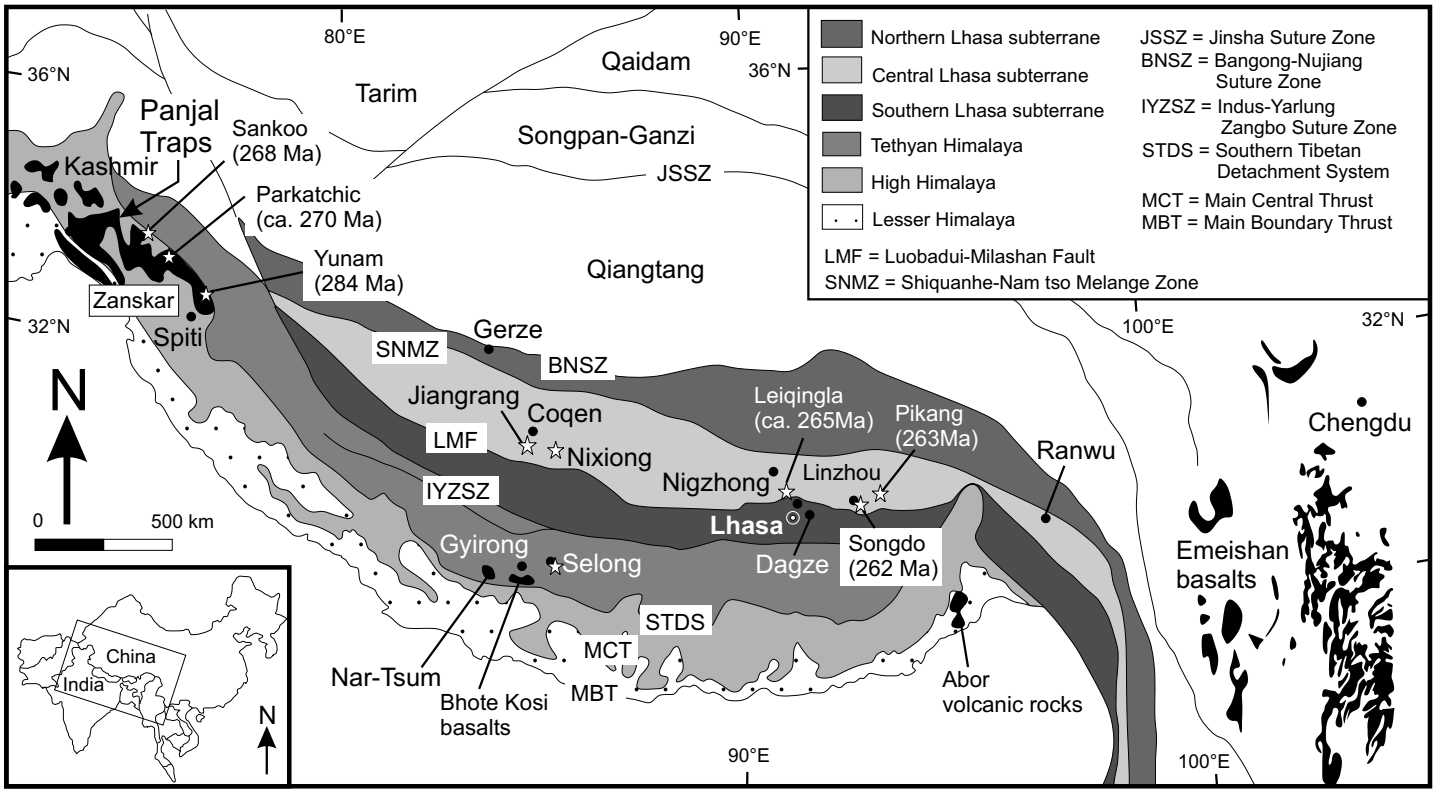

Figure 10. Distribution of Permian Himalayan Magmatic Province volcanic rocks (based on Zhu et al. 2010).

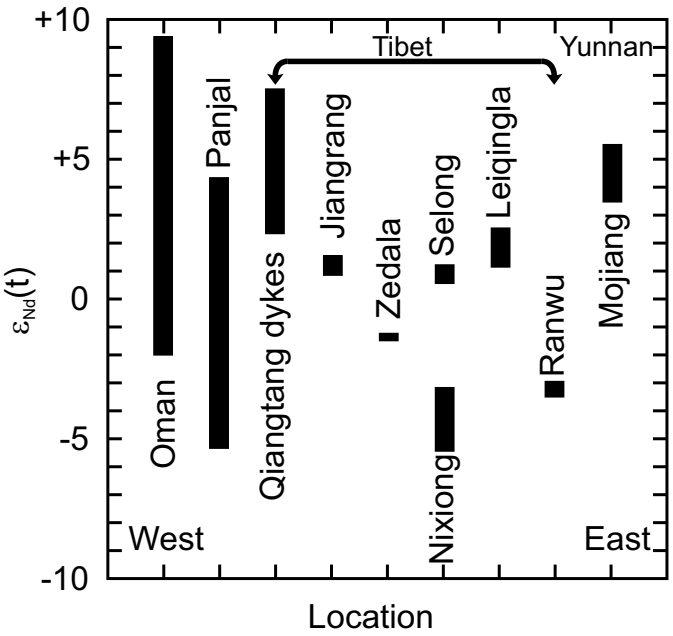

Figure 11. The variability of $\varepsilon_{Nd}(t)$ of Early to Mid-Permian mafic volcanic rocks from west to east across the Himalaya including the Permian volcanic rocks from Oman (Lapierre et al. 2004; Fan et al. 2010; Zhu et al. 2010; Zhai et al. 2013; Shellnutt et al. 2014, 2015; Xu et al. 2016).

within either the Qiangtang block (East) or the Arabian plate (West). However, the Panjal Traps are the thickest and most continuous outcrops of basalt in the Himalaya, suggesting they may represent a central volcanic eruption location (Lapierre et al. 2004; Zhai et al. 2013; Shellnutt et al. 2014, 2015). Nakazawa et al. (1975) and Nakazawa and Kapoor (1973) suggested that volcanism was most intense within the Kashmir Valley and migrated to the south and southeast. Although there is some chemical overlap between the different Permian Himalayan–Arabian basaltic groups there are significant differences in the reported ages (> 10 Ma) and Nd isotopes (Fig. 11). It is likely that the Permian magmatic rocks in the Himalaya and Arabia are members of the same disjointed regional scale rifting that led to the formation of the Neotethys but that they represent separate magmatic systems derived from 'local' mantle sources. The precise reason (exploitation of a structural heterogeneity) or mechanism (mantle plume vs. lithospheric extension) of the formation and propagation of the rift is not constrained but it could be that different regions of the rift had unique tectonic features.

SYNTHESIS OF THE PANJAL TRAPS

Neoproterozoic to Late Carboniferous continental to marine sedimentary rocks were deposited on the passive margin of Tethyan Gondwana at mid-southern latitudes (Stojanovic et al. 2016). The large Gondwanan ice sheet began to melt and the deposition of Middle Carboniferous fossiliferous (bryozoans, brachiopods and crinoids) Fenestella shale was followed by the lower diamictite unit of the Upper Carboniferous agglomeratic slate. The middle units of the agglomeratic slate appear to contain more tuffaceous material, possibly marking the first volcanic unit of the Panjal Traps, followed by the deposition of

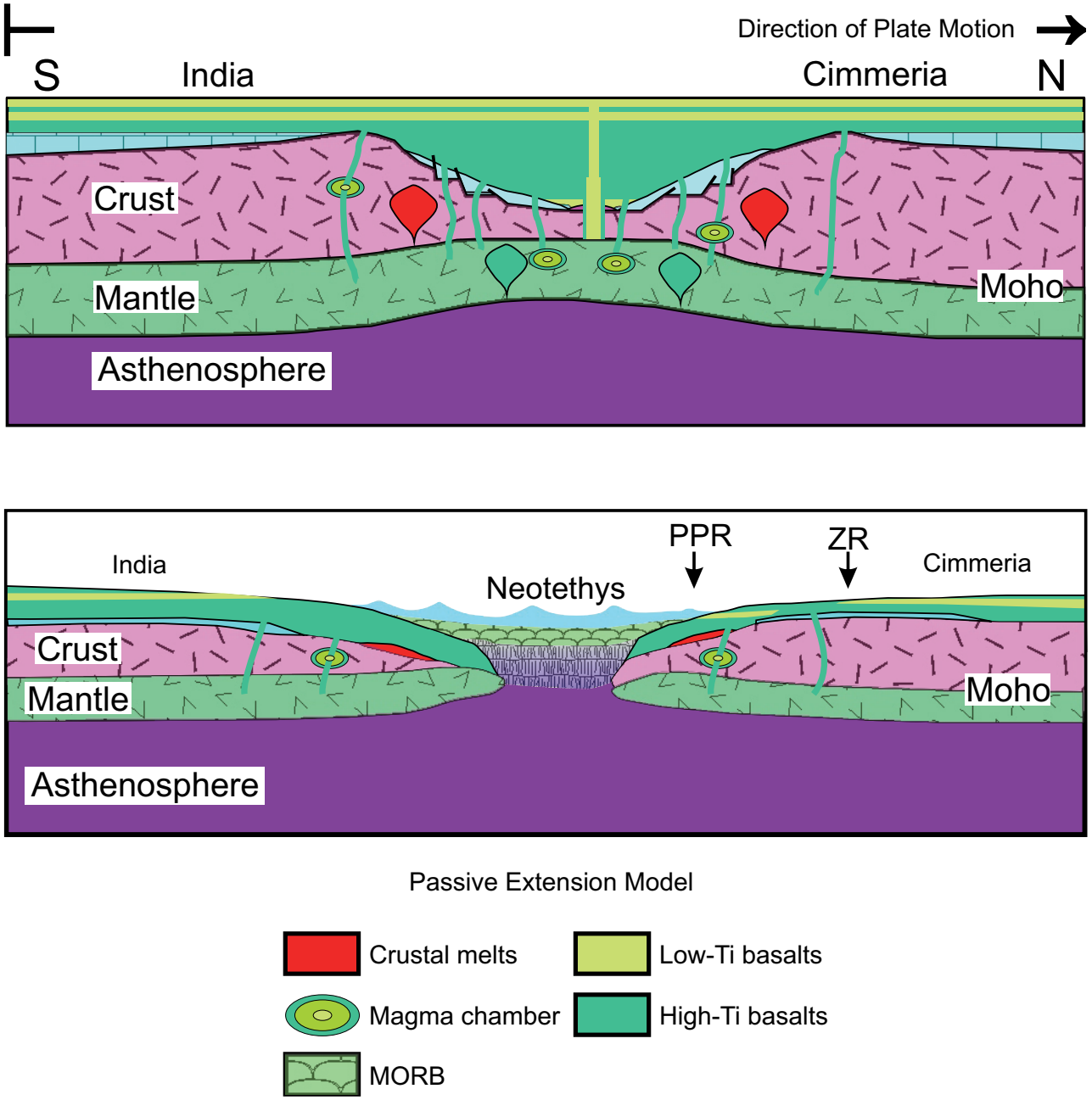

Figure 12. Tectonic synthesis of the Panjal Traps. (a) The initial subaerial eruption followed by the (b) subaqueous eruptions and eventual opening of the Neotethys Ocean. The possible pre-India–Eurasia collision locations of the Pir Panjal (PPR) and Zanskar Range (ZR) basaltic units are shown.

fossiliferous marine units marking eustatic sea-level rise following deglaciation (Wopfner and Jin 2009). Pyroclastic flows appeared within the freshwater, plant-bearing siliciclastic Nishatbagh Beds and were followed by the main effusive sequence of the Panjal Traps.

The least contaminated lower basaltic flows have compositions similar to 'low-Ti' continental tholeiite and chondritic Sr–Nd isotope compositions. The injection of mafic magmas into the crust likely induced melting that led to the formation of the silicic volcanic rocks (Fig. 12a). Some of the mafic magmas mixed with crustal melts to produce the andesitic rocks that erupted at distinct horizons, whereas other basaltic units experienced smaller amounts of contamination. The younger flows appear to have erupted within a shallow marine or lagoonal basin and developed pillow structures (Fig. 12b). Basalt from the Pir Panjal Range has Nd isotopic compositions and characteristics of E-MORB. The geochemical change is likely related to the tectonic setting transitioning from a predominantly continental setting to a predominantly oceanic setting. It is possible that during the continental–oceanic transition volcanogenic massive sulphide (VMS) deposits formed.

The final continental Traps are capped by marine sedimentary rocks, whereas regions farther from the volcanic centre were likely still under extension as sea-floor spreading began

and the first microcontinental blocks of Cimmeria drifted away from Gondwana. The Neotethys Ocean was born and the initial rift completely transitioned from a continental setting into a mid-ocean ridge setting. Cimmerian blocks drifted northward until they accreted to the southern margin of Eurasia during the mid-Mesozoic (Metcalfe 2013; Torsvik et al. 2014). It is likely that only the continental portion and the earliest subaqueous Traps were preserved within the accreted Cimmerian blocks, whereas the younger oceanic equivalents were subducted during closure of the Neotethys Ocean. It is possible that some of the subducted Panjal Traps were taken to a depth of 2–3 GPa and brought back to the surface as the Stak Valley, Kaghan and Tso Morari eclogite units (Spencer et al. 1995; Luais et al. 2001; Kouketsu et al. 2015; Rehman et al. 2016).

ACKNOWLEDGEMENTS

I am grateful to Loÿc Vanderkuysen and Richard Ernst for their comments that helped to improve this manuscript. I am very appreciative of the stimulating discussions with Ghulam M. Bhat, Ghulam-ud-Din Bhat, G.M. Zaki, Kuo-Lung Wang, Bor-Ming Jahn, Sun-Lin Chung, Mike Brookfield, Mary Yeh, Jaroslav Dostal and Kwan-Nang Pang on a variety of petrological and structural matters related to the Panjal Traps.

REFERENCES

Ali, J.R., Fitton, J.G., and Herzberg, C., 2010, Emeishan large igneous province (SW China) and the mantle-plume up-doming hypothesis: Journal of the Geological Society, v. 167, p. 953–959, http://dx.doi.org/10.1144/0016-76492009-129.

Ali, J.R., Aitchison, J.C., Chik, S.Y.S., Baxter, A.T., and Bryan, S.E., 2012, Paleomagnetic data support Early Permian age for the Abor volcanics in the lower Siang Valley, NE India: Significance for Gondwana-related break-up models: Journal of Asian Earth Sciences, v. 50, p. 105–115, http://dx.doi.org/10.1016/j.jseaes.2012.01.007.

Ali, J.R., Cheung, H.M.C., Aitchison, J.C., and Sun, Y., 2013, Palaeomagnetic reinvestigation of Early Permian rift basalts from the Baoshan Block, SW China: constraints on the site-of-origin of the Gondwana-derived eastern Cimmerian terranes: Geophysical Journal International, v. 193, p. 650–663, http://dx.doi.org/10.1093/gji/ggt012.

Bhat, M.I., 1984, Abor Volcanics: further evidence for the birth of the Tethys Ocean in the Himalayan segment: Journal of the Geological Society, v. 141, p. 763–775, http://dx.doi.org/10.1144/gsjgs.141.4.0763.

Bhat, M.I., and Zainuddin, S.M., 1978, Environment of eruption of the Panjal Traps: Himalayan Geology, v. 8, p. 727–738.

Bhat, M.I., and Zainuddin, S.M., 1979, Origin and evolution of the Panjal volcanics: Himalayan Geology, v. 9, p. 421–461.

Bhat, M.I., Zainuddin, S.M., and Rais, A., 1981, Panjal Trap chemistry and the birth of Tethys: Geological Magazine, v. 118, p. 367–375, http://dx.doi.org/10.1017/S0016756800032234.

Bond, D.P.G., and Wignall, P.B., 2014, Large igneous provinces and mass extinctions: An update, *in* Keller, G., and Kerr, A.C., *eds.,* Volcanism, Impacts, and Mass Extinctions: Causes and Effects: Geological Society of America Special Papers, v. 505, p. 29–55, http://dx.doi.org/10.1130/2014.2505(02).

Brookfield, M.E., Algeo, T.J., Hannigan, R., Williams, J., and Bhat, G.M., 2013, Shaken and stirred: seismites and tsunamites at the Permian–Triassic boundary, Guryal Ravine, Kashmir, India: Palaios, v. 28, p. 568–582, http://dx.doi.org/10.2110/palo.2012.p12-070r.

Bryan, S.E., and Ernst, R.E., 2008, Revised definition of large igneous provinces (LIPs): Earth-Science Reviews, v. 86, p. 175–202, http://dx.doi.org/10.1016/j.earscirev.2007.08.008.

Campbell, I.H., 2002, Implication of Nb/U, Th/U and Sm/Nd in plume magmas for the relationship between continental and oceanic crust formation and the development of the depleted mantle: Geochimica et Cosmochimica Acta, v. 66, p. 1651–1661, http://dx.doi.org/10.1016/S0016-7037(01)00856-0.

Campbell, I.H., 2005, Large igneous provinces and the mantle plume hypothesis: Elements, v. 1, p. 265–269, http://dx.doi.org/10.2113/gselements.1.5.265.

Campbell, I.H., 2007, Testing the plume theory: Chemical Geology, v. 241, p. 153–176, http://dx.doi.org/10.1016/j.chemgeo.2007.01.024.

Campbell, I.H., and Griffiths, R.W., 1990, Implications of mantle plume structure for the evolution of flood basalts: Earth and Planetary Science Letters, v. 99, p. 79–93, http://dx.doi.org/10.1016/0012-821X(90)90072-6.

Chauvet, F., Lapierre, K., Bosch, D., Guillot, S., Mascle, G., Vannay, J.-C., Cotton, J., Brunet, P., and Keller Z., 2008, Geochemistry of the Panjal Traps basalts (NW Himalaya): records of the Pangea Permian break-up: Bulletin de la Société Géologique de France, v. 179, p. 383–395, http://dx.doi.org/10.2113/ gssgfbull.179.4.383.

Courtillot, V., Jaupart, C., Manighetti, I., Tapponier, P., and Besse, J., 1999, On causal links between flood basalts and continental breakup: Earth and Planetary Science Letters, v. 166, p. 177–195, http://dx.doi.org/10.1016/S0012-821X(98)00282-9.

Ernst, R.E., 2014, Large igneous provinces: Cambridge University Press, Cambridge, 653 p., http://dx.doi.org/10.1017/CBO9781139025300.

Ernst, R.E., and Buchan, K.L., 2001, Large mafic magmatic events through time and links to mantle-plume heads, *in* Ernst, R.E., and Buchan, K.L., *eds.,* Mantle Plumes: Their Identification Through Time; Geological Society of America Special Papers, v. 352, p. 483–575, http://dx.doi.org/10.1130/0-8137-2352-3.483.

Ernst, R.E., and Buchan, K.L., 2003, Recognizing mantle plumes in the geological record: Annual Reviews of Earth and Planetary Sciences, v. 31, p. 469–523, http://dx.doi.org/10.1146/annurev.earth.31.100901.145500.

Ernst, R.E., Buchan, K.L., and Campbell, I.H., 2005, Frontiers in large igneous province research: Lithos, v. 79, p. 271–297, http://dx.doi.org/10.1016/j.lithos.2004.09.004.

Fan W., Wang Y., Zhang A., Zhang F., and Zhang Y., 2010, Permian arc–back-arc basin development along the Ailaoshan tectonic zone: Geochemical, isotopic and geochronological evidence from the Mojiang volcanic rocks, Southwest China: Lithos, v. 119, p. 553–568, http://dx.doi.org/10.1016/j.lithos.2010.08.010.

Foulger, G.R., 2007, The "plate" model for the genesis of melting anomalies, *in* Foulger, G.R., and Jurdy, D.M., *eds.,* Plates, Plumes and Planetary Processes: Geological Society of America Special Papers, v. 430, p. 1–28, http://dx.doi.org/10.1130/2007.2430(01).

Foulger, G.R., 2010, Plates vs. Plumes: A Geological Controversy: John Wiley and Sons, Chichester, UK, 328 p., http://dx.doi.org/10.1002/9781444324860.

Fuchs, G., 1987, The geology of Southern Zanskar (Ladakh) – evidence for the autochthony of the Tethys zone of the Himalaya: Jahrbuch der Geologischen Bundesanstalt, v. 130, p. 465–491.

Gaetani, M., Casnedi, R., Fois, E., Garzanti, E., Jadoul, F., Nicora, A., and Tintori, A., 1986, Stratigraphy of the Tethys Himalaya in Zanskar, Ladakh initial report: Rivisita Italiana di Paleontologia e Stratigrafia, v. 91, p. 443–478.

Gaetani, M., Garzanti, E., and Tintori, A., 1990, Permo–Carboniferous stratigraphy in SE Zanskar and NW Lahul (NW Himalaya, India): Eclogae Geologicae Helvetiae, v. 83, p. 143–161.

Ganju, P.N., 1944, The Panjal Traps: acid and basic volcanic rocks: Proceedings of the Indian Academy of Sciences, v. 18, p. 125–131.

Garzanti, E., Nicora, A., and Tintori, A., 1992, Late Paleozoic to Early Mesozoic stratigraphy and sedimentary evolution of central Dolpo (Nepal Himalaya): Rivisita Italiana di Paleontologia e Stratigrafia, v. 98, p. 271–298.

Garzanti, E., Nicora, A., Tintori, T., Sciunnach, D., and Angiolini, L., 1994, Late Paleozoic stratigraphy and petrography of the Thini Chu Group (Manang, Central Nepal): sedimentary record of Gondwana glaciation and rifting of Neotethys: Rivisita Italiana di Paleontologia e Stratigrafia, v. 100, p. 155–194.

Garzanti, E., Angiolini, L., and Sciunnach, D., 1996a, The mid-Carboniferous to lowermost Permian succession of Spiti (Po Group and Ganmachidam Formations; Tethys Himalaya, northern India): Gondwana glaciation and rifting of Neo-Tethys: Geodinamica Acta, v. 9, p. 78–100, http://dx.doi.org/10.1080/09853111.1996.11105279.

Garzanti, E., Angiolini, L., and Sciunnach, D., 1996b, The Permian Kulung Group (Spiti, Lahaul and Zanskar; NW Himalaya): sedimentary evolution during rift/drift transition and initial opening of Neo-Tethys: Rivisita Italiana di Paleontologia e Stratigrafia, v. 102, p. 175–200.

Garzanti, E., Angiolini, L., Brunton, H., Sciunnach, D., and Balini, M., 1998, The Bashkirian "Fenestella Shales" and the Moscovian "Chaetetid Shales" of the Tethys Himalaya (South Tibet, Nepal and India): Journal of Asian Earth Sciences, v. 16, p. 119–141, http://dx.doi.org/10.1016/S0743-9547(98)00006-3.

Garzanti, E., Le Fort, P., and Sciunnach, D., 1999, First report of Lower Permian basalts in south Tibet: tholeiitic magmatism during break-up and incipient opening of Neotethys: Journal of Asian Earth Sciences, v. 17, p. 533–546, http://dx.doi.org/10.1016/S1367-9120(99)00008-5.

He Bin, Xu Yi-Gang, Chung Sun-Ling, Xiao Long, and Wang Yamei, 2003, Sedimentary evidence for a rapid, kilometer-scale crustal doming prior to the eruption of the Emeishan flood basalts: Earth and Planetary Science Letters, v. 213,

p. 391–405, http://dx.doi.org/10.1016/S0012-821X(03)00323-6.
Herzberg, C., and Asimow, P.D., 2015, PRIMELT3 MEGA.XLSM software for primary magma calculation: Peridotite primary magma MgO contents from the liquidus to the solidus: Geochemistry, Geophysics, Geosystems, v. 16, p. 563–578, http://dx.doi.org/10.1002/2014GC005631.
Herzberg, C., and Gazel, E., 2009, Petrological evidence for secular cooling in mantle plumes: Nature, v. 458, p. 619–622, http://dx.doi.org/10.1038/nature07857.
Herzberg, C., Asimow, P.D., Arndt, N., Niu, Y., Lesher, C.M., Fitton, J.G., Cheadle, M.J., and Saunders, A.D., 2007, Temperatures in ambient mantle and plumes: Constraints from basalts, picrites, and komatiites: Geochemistry, Geophysics, Geosystems, v. 8, Q02006, http://dx.doi.org/10.1029/2006GC001390.
Hole, M.J., 2015, The generation of continental flood basalts by decompressional melting of internally heated mantle: Geology, v. 43, p. 311–314, http://dx.doi.org/10.1130/G36442.1.
Honegger, K., Dietrich, V., Frank, W., Gansser, A., Thöni, M., and Trommsdorff, V., 1982, Magmatism and metamorphism in the Ladakh Himalayas (the Indus–Tsangpo suture zone): Earth and Planetary Science Letters, v. 60, p. 253–292, http://dx.doi.org/10.1016/0012-821X(82)90007-3.
King, S.D., and Anderson, D.L., 1995, An alternative mechanism of flood basalt formation: Earth and Planetary Science Letters, v. 136, p. 269–279, http://dx.doi.org/10.1016/0012-821X(95)00205-Q.
Kouketsu, Y., Hattori, K., and Guillot, S., 2015, Protolith of the Stak eclogite in the northwestern Himalaya: Italian Journal of Geosciences, v. 134, f.0, http://dx.doi.org/10.3301/IJG.2015.41.
Lapierre, H., Samper, A., Bosch, D., Maury, R.C., Béchennec, F., Cotten, J., Demant, A., Brunet, P., Keller, F., and Marcoux, J., 2004, The Tethyan plume: geochemical diversity of Middle Permian basalts from the Oman rifted margin: Lithos, v. 74, p. 167–198, http://dx.doi.org/10.1016/j.lithos.2004.02.006.
Le Bas, M.J., 2000, IUGS Reclassification of the high-Mg and picritic volcanic rocks: Journal of Petrology, v. 41, p. 1467–1470, http://dx.doi.org/10.1093/petrology/41.10.1467.
Luais, B., Duchêne, S., and de Sigoyer, J., 2001, Sm–Nd disequilibrium in high-pressure, low-temperature Himalayan and Alpine rocks: Tectonophysics, v. 342, p. 1–22, http://dx.doi.org/10.1016/S0040-1951(01)00154-8.
Lydekker, R., 1883, Geology of Kashmir and Chamba territories and the British district of Khagan: Memoirs of the Geological Society of India, v. 22, p. 211–224.
Mallmann, G., and O'Neill, H.St.C., 2009, The crystal/melt partitioning of V during mantle melting as a function of oxygen fugacity compared with some other elements (Al, P, Ca, Sc, Ti, Cr, Fe, Ga, Y, Zr and Nb): Journal of Petrology, v. 50, p. 1765–1794, http://dx.doi.org/10.1093/petrology/egp053.
Martin, H., 1981, The late Paleozoic Gondwana glaciation: Geologische Rundschau, v. 70, p. 480–496, http://dx.doi.org/10.1007/BF01822128.
Metcalfe, I., 2013, Gondwana dispersion and Asian accretion: Tectonic and palaeogeographic evolution of eastern Tethys: Journal of Asian Earth Sciences, v. 66, p. 1–33, http://dx.doi.org/10.1016/j.jseaes.2012.12.020.
Middlemiss, C.S., 1910, A Revision of Silurian–Trias Sequence in Kashmir: Records of the Geological Survey of India, v. 40, p. 206–260.
Miyashiro, A., 1974, Volcanic rock series in island arcs and active continental margins: American Journal of Science, v. 274, p. 321–355, http://dx.doi.org/10.2475/ajs.274.4.321.
Myrow, P.M., Snell, K.E., Hughes, N.C., Paulsen, T.S., Heim, N.A., and Parcha, S.K., 2006, Cambrian depositional history of the Zanskar Valley region of the Indian Himalaya: tectonic implications: Journal of Sedimentary Research, v. 76, p. 364–381, http://dx.doi.org/10.2110/jsr.2006.020.
Nakazawa, K., and Kapoor, H.M., 1973, Spilitic pillow lava in Panjal Trap of Kashmir, India: Memoirs of the Faculty of Science, Kyoto University, Series of Geology and Mineralogy, v. 39, p. 83–98.
Nakazawa, K., Kapoor, H.M., Ishii, K.-I., Bando, Y., Okimura, Y., Tokuoka, T., Murata, M., Nakamura, K., Nogami, Y. Sakagami, S., and Shimizu, D., 1975, The upper Permian and the lower Triassic in Kashmir, India: Memoirs of the Faculty of Science, Kyoto University, Series of Geology and Mineralogy, v. 42, p. 1–106.
Papritz, K., and Rey, R., 1989, Evidence for the occurrence of Permian Panjal Trap basalts in the lesser- and higher Himalayas of the western syntaxis area, NE Pakistan: Eclogae Geologicae Helvetiae, v. 82, p. 603–627.
Pareek, H.S., 1976, On studies of the agglomerate slate and Panjal Trap in the Jhelum, Liddar, and Sind Valleys, Kashmir: Records of the Geological Survey of India, v. 107, p. 12–37.
Pearce, J.A., Harris, N.B.W., and Tindle, A.G., 1984, Trace element discrimination diagrams for the tectonic interpretation of granitic rocks: Journal of Petrology, v. 25, p. 956–983, http://dx.doi.org/10.1093/petrology/25.4.956.
Pearce, T.H., Gorman, B.E., and Birkett, T.C., 1977, The relationship between major element chemistry and tectonic environment of basic and intermediate volcanic rocks: Earth and Planetary Science Letters, v. 36, p. 121–132, http://dx.doi.org/10.1016/0012-821X(77)90193-5.
Pogue, K.R., DiPeitro, J.A., Khan, S.R., Hughes, S.S., Dilles, J.H., and Lawrence, R.D., 1992, Late Paleozoic rifting in northern Pakistan: Tectonics, v. 11, p. 871–883, http:/,/dx.doi.org/10.1029/92TC00335.
Rao, D.R., and Rai, H., 2007, Permian komatiites and associated basalts from the marine sediments of Chhongtash Formation, southeast Karakoram, Ladakh, India: Mineralogy and Petrology, v. 91, p. 171–189, http://dx.doi.org/10.1007/s00710-007-0206-4.
Rehman, H.U., Lee, H.-Y., Chung, S.-L., Khan, T., O'Brien, P.J., and Yamamoto, H., 2016, Source and mode of the Permian Panjal Trap magmatism: Evidence from zircon U–Pb and Hf isotopes and trace element data from the Himalayan ultra-high-pressure rocks: Lithos, v. 260, p. 286–299, http://dx.doi.org/10.1016/j.lithos.2016.06.001.
Richards, M.A., Duncan, R.A., and Courtillot, V.E., 1989, Flood basalts and hot-spot tracks: Plume heads and tails: Science, v. 246, p. 103–107, http://dx.doi.org/10.1126/science.246.4926.103.
Rudnick, R.L., and Gao, S., 2003, Composition of the continental crust, *in* Rudnick, R.L., *ed.,* The Crust: Treatise on Geochemistry, v. 3, p. 1–64, http://dx.doi.org/10.1016/b0-08-043751-6/03016-4.
Saunders, A., and Reichow, M., 2009, The Siberian Traps and the end-Permian mass extinction: a critical review: Chinese Science Bulletin, v. 54, p. 20–37, http://dx.doi.org/10.1007/s11434-008-0543-7.
Shellnutt, J.G., 2014, The Emeishan large igneous province: A synthesis: Geoscience Frontiers, v. 5, p. 369–394, http://dx.doi.org/10.1016/j.gsf.2013.07.003.
Shellnutt, J.G., Bhat, G.M., Brookfield, M.E., and Jahn, B.-M., 2011, No link between the Panjal Traps (Kashmir) and the Late Permian mass extinctions: Geophysical Research Letters, v. 38, L19308, http://dx.doi.org/10.1029/2011GL049032.
Shellnutt, J.G., Bhat, G.M., Wang, K.-L., Brookfield, M.E., Dostal, J., and Jahn, B.-M., 2012, Origin of the silicic volcanic rocks of the Early Permian Panjal Traps, Kashmir, India: Chemical Geology, v. 334, p. 154–170, http://dx.doi.org/10.1016/j.chemgeo.2012.10.022.
Shellnutt, J.G., Bhat, G.M., Wang, K.-L., Brookfield, M.E., Jahn, B.-M., and Dostal, J., 2014, Petrogenesis of the flood basalts from the Early Permian Panjal Traps, Kashmir, India: Geochemical evidence for shallow melting of the mantle: Lithos, v. 204, p. 159–171, http://dx.doi.org/10.1016/j.lithos.2014.01.008.
Shellnutt, J.G., Bhat, G.M., Wang, K.-L., Yeh, M.-W., Brookfield, M.E., and Jahn, B.-M., 2015, Multiple mantle sources of the Early Permian Panjal Traps, Kashmir, India: American Journal of Science, v. 315, p. 589–619, http://dx.doi.org/10.2475/07.2015.01.
Spencer, D.A., Tonarini, S., and Pognante, U., 1995, Geochemical and Sr–Nd isotopic characterisation of Higher Himalayan eclogites (and associated metabasites): European Journal of Mineralogy, v. 7, p. 89–102, http://dx.doi.org/10.1127/ejm/7/1/0089.
Spring, L., Bussy, F., Vannay, J.-C., Huon, S., and Cosca, M.A., 1993, Early Permian granitic dykes of alkaline affinity in the Indian High Himalaya of Upper Lahul and SE Zanskar: geochemical characterization and geotectonic implications, *in* Treloar, P.J., and Searle, M.P., *eds.,* Himalayan Tectonics: Geological Society, London, Special Publications, v. 74, p. 251–264, http://dx.doi.org/10.1144/gsl.sp.1993.074.01.18.
Stojanovic, D., Aitchison, J.C., Ali, J.R., Ahmad, T., and Dar, R.A., 2016, Paleomagnetic investigation of the Early Permian Panjal Traps of NW India: regional tectonic implications: Journal of Asian Earth Sciences, v. 115, p. 114–123, http://dx.doi.org/10.1016/j.jseaes.2015.09.028.
Sun, S.-s., and McDonough, W.F., 1989, Chemical and isotopic systematics of oceanic basalts: implications for mantle composition and processes, *in* Saunders, A.D., and Norry, M.J., *eds.,* Magmatism in the Ocean Basins: Geological Society, London, Special Publications, v. 42, p. 313–345, http://dx.doi.org/10.1144/gsl.sp.1989.042.01.19.
Tewari, R., Awatar, R., Pandita, S.K., McLoughlin, S., Agnihotri, D., Pillai, S.S.K., Singh, V., Kumar, K., and Bhat, G.D., 2015, The Permian–Triassic palynological transition in the Guryul Ravine section, Kashmir, India: implications for Tethyan–Gondwanan correlations: Earth-Science Reviews, v. 149, p. 53–66, http://dx.doi.org/10.1016/j.earscirev.2014.08.018.
Torsvik, T.H., Smethurst, M.A., Burke, K., and Steinberger, B., 2008, Long term stability in deep mantle structure: Evidence from the ~300 Ma Skagerrak-Centered large igneous province (the SCLIP): Earth and Planetary Science Letters, v. 267, p. 444–452, http://dx.doi.org/10.1016/j.epsl.2007.12.004.
Torsvik, T.H., van der Voo, R., Doubrovine, P.V., Burke, K., Steinberger, B., Ashwal, L.D., Trønnes, R.G., Webb, S.J., and Bull, A.L., 2014, Deep mantle structure as a reference frame for movements in and on the Earth: Proceedings of the National Academy of Sciences, v. 111, p. 8735–8740, http://dx.doi.org/10.1073/pnas.1318135111.

Ukstins Peate, I., and Bryan, S.E., 2008, Re-evaluating plume-induced uplift in the Emeishan large igneous province: Nature Geosciences, v. 1, p. 625–629, http://dx.doi.org/10.1038/ngeo281.

Vannay, J.C., and Spring, L., 1993, Geochemistry of the continental basalts within the Tethyan Himalaya of Lahul-Spiti and SE Zanskar, northwest India, *in* Treloar, P.J., and Searle, M.P., *eds.,* Himalayan Tectonics: Geological Society, London, Special Publications, v. 74, p. 237–249, http://dx.doi.org/10.1144/gsl.sp.1993.074.01.17.

Wadia, D.N., 1934, The Cambrian-Trias sequence of North-Western Kashmir (Parts of Muzaffarabad and Baramular districts): Records of the Geological Survey of India, v. 68, p. 121–176.

Wadia, D.N., 1961, Geology of India: McMillan and Company, London, 536 p.

Wang Ming, Li Cai, Wu Yan-Wang, and Xie Chao-Ming, 2014, Geochronology, geochemistry, Hf isotopic compositions and formation mechanism of radial mafic dikes in northern Tibet: International Geology Review, v. 56, p. 187–205, http://dx.doi.org/10.1080/00206814.2013.825076.

White, R., and McKenzie, D., 1989, Magmatism at rift zones: The generation of volcanic continental margins and flood basalts: Journal of Geophysical Research, v. 94, p. 7685–7729, http://dx.doi.org/10.1029/JB094iB06p07685.

Wilson, M., *editor,* 1989, Igneous Petrogenesis. A Global Tectonic Approach: Springer Netherlands, 466 p., http://dx.doi.org/10.1007/978-1-4020-6788-4.

Winchester, J.A., and Floyd, P.A., 1977, Geochemical discrimination of different magma series and their differentiation products using immobile elements: Chemical Geology, v. 20, p. 325–343, http://dx.doi.org/10.1016/0009-2541(77)90057-2.

Wopfner, H., and Jin, X.C., 2009, Pangea megasequences of Tethyan Gondwana-margin reflect global changes of climate and tectonism in Late Palaeozoic and Early Triassic times – A review: Palaeoworld, v. 18, p. 169–192, http://dx.doi.org/10.1016/j.palwor.2009.04.007.

Workman, R.K., and Hart, S.R., 2005, Major and trace element composition of the depleted MORB mantle (DMM): Earth and Planetary Science Letters, v. 231, p. 53–72, http://dx.doi.org/10.1016/j.epsl.2004.12.005.

Workman, R.K., Hart, S.R., Jackson, M., Regelous, M., Farley, K.A., Blusztajn, J., Kurz, M., and Staudigel, H., 2004, Recycled metasomatized lithosphere as the origin of the enriched mantle II (EM2) end-member: evidence from the Samoan volcanic chain: Geochemistry, Geophysics, Geosystems, v. 5, Q04008, http://dx.doi.org/10.1029/2003GC000623.

Xu Wang, Dong Yongsheng, Zhang Xiuzheng, Deng Mingrong, and Zhang Le, 2016, Petrogenesis of high-Ti mafic dykes from Southern Qiangtang, Tibet: Implications for a ca. 290 Ma large igneous province related to the early Permian rifting of Gondwana: Gondwana Research, v. 36, p. 410–422, http://dx.doi.org/10.1016/j.gr.2015.07.016.

Xu Yi-Gang, Wei Xun, Luo Zhen-Yu, Liu Hai-Quan, and Cao Jun, 2014, The Early Permian Tarim large igneous province: Main characteristics and a plume incubation model: Lithos, v. 204, p. 20–35, http://dx.doi.org/10.1016/j.lithos.2014.02.015.

Yan Quanren, Wang Zongqi, Liu Shuwen, Li Quigen, Zhang Hongyuan, Wang Tao, Liu Dunyi, Shi Yuruo, Jian Ping, Wang Jianguo, Zhang Dehui, and Zhao Jian, 2005, Opening of the Tethys in southwest China and its significance to the breakup of East Gondwanaland in the late Paleozoic: evidence from SHRIMP U–Pb zircon analyses for the Garzê ophiolite block: Chinese Science Bulletin, v. 50, p. 256–264, http://dx.doi.org/10.1007/BF02897536.

Yeh Meng-Wan, and Shellnutt, J.G., 2016, The initial break-up of Pangæa elicited by Late Palæozoic deglaciation: Scientific Reports, v. 6, 31442, http://dx.doi.org/10.1038/srep31442.

Zhai Qing-guo, Jahn Bor-ming, Su Li, Ernst, R.E., Wang Kuo-lung, Zhang Ru-yuan, Wang Jun, and Tang Suohan, 2013, SHRIMP zircon U–Pb geochronology, geochemistry and Sr–Nd–Hf isotopic compositions of a mafic dyke swarm in the Qiangtang terrane, northern Tibet and geodynamic implications: Lithos, v. 174, p. 28–43, http://dx.doi.org/10.1016/j.lithos.2012.10.018.

Zhu Di-Cheng, Mo Xuan-Xue, Zhao Zhi-Dan, Niu Yaoling, Wang Li-Quan, Chu Qiu-Hong, Pan Gui-Tang, Xu Ji-Feng, and Zhou Chang-Yong, 2010, Presence of Permian extension- and arc-type magmatism in southern Tibet: Paleogeographic implications: Geological Society of America Bulletin, v. 122, p. 979–993, http://dx.doi.org/10.1130/B30062.1.

Zindler, A., and Hart, S., 1986, Chemical geodynamics: Annual Review of Earth and Planetary Sciences, v. 14, p. 493–571, http://dx.doi.org/10.1146/annurev.ea.14.050186.002425.

Received March 2016
Accepted as revised July 2016
First published on the web August 2016

SERIES

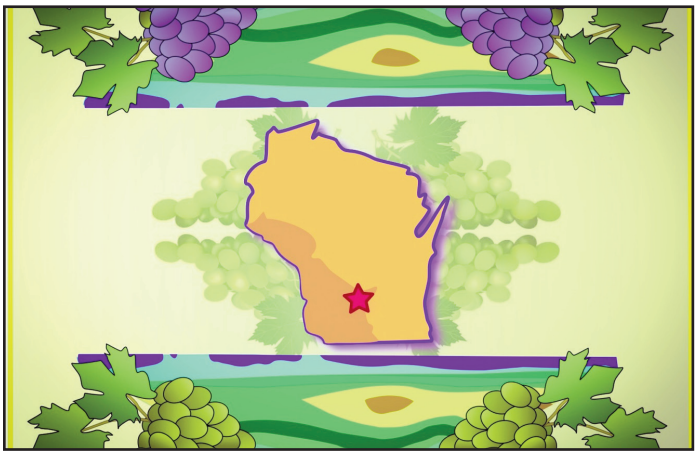

Geology and Wine 14. Terroir of Historic Wollersheim Winery, Lake Wisconsin American Viticultural Area

Snejana Karakis, Barry Cameron, and William Kean

Department of Geosciences
University of Wisconsin-Milwaukee
PO Box 413, Milwaukee, Wisconsin, 53201 USA
Email: karakis@uwm.edu

SUMMARY

The viticultural history of Wisconsin started in the 1840s, with the very first vine plantings by Hungarian Agoston Haraszthy on the Wollersheim Winery property located in the Lake Wisconsin American Viticultural Area (AVA). This study examines the terroir of historic Wollersheim Winery, the only winery within the confines of the Lake Wisconsin AVA, to understand the interplay of environmental factors influencing the character and quality as well as the variability of Wollersheim wines. Soil texture, chemistry, and mineralogy in conjunction with precision viticulture tools such as electromagnetic induction and electrical resistivity tomography surveys, are utilized in the Wollersheim Winery terroir characterization and observation of spatially variable terroir at the vineyard scale. Establishing and comparing areas of variability at the plot level for two specific vineyard plots (Domaine Reserve and Lot 19) at Wollersheim Winery provides insight into the effects of soil properties and land characteristics on grape and wine production using precision viticulture tools.

The viticultural future of Wisconsin looks quite favourable, as the number of wineries keeps rising to meet the demand for Wisconsin wine and local consumption. As climate change continues to affect the grape varieties cultivated across the world's wine regions, more opportunities arise for Wisconsin to cultivate cool-climate European varieties, in addition to the American and French-American hybrid varieties currently dominating grape production in this glacially influenced wine region.

RÉSUMÉ

L'histoire viticole du Wisconsin a commencé dans les années 1840, avec les premières plantations de vigne par le Hongrois Agoston Haraszthy sur la propriété du vignoble Wollersheim situé dans la région de l'American Viticultural Area (AVA) du lac Wisconsin. Cette étude porte sur le terroir historique du vignoble Wollersheim, le seul à l'intérieur de l'AVA du lac Wisconsin, qui soit soumis à l'interaction des facteurs environnementaux qui influencent le caractère, la qualité et la variabilité des vins Wollersheim. La caractérisation et l'observation des variations spatiales du terroir à l'échelle du vignoble Wollersheim se font par l'étude de la texture du sol, sa chimie et sa minéralogie en conjonction avec des outils de viticulture de précision comme l'induction électromagnétique et la tomographie par résistivité électrique. En définissant des zones de variabilité au niveau de la parcelle et en les comparant pour deux parcelles de vignobles spécifiques (domaine Reserve et lot 19) du vignoble Wollersheim on peut mieux comprendre les effets des propriétés du sol et des caractéristiques du paysage sur la production de raisin et de vin.

Le nombre de vignoble augmentant pour répondre à la demande de vin du Wisconsin et à la demande locale, l'avenir viticole du Wisconsin semble assez prometteur. Comme le changement climatique continue d'influer sur la variétés des cépages cultivés dans les régions viticoles du monde, c'est l'occasion pour le Wisconsin de cultiver des variétés européennes de climat frais, en plus des variétés hybrides américaines et franco–américaines qui dominent actuellement la production de raisin dans ce vin glaciaire région.

Traduit par le Traducteur

INTRODUCTION

The state of Wisconsin is perhaps best known for cheese and beer, invoking placid images of lush pastureland, clear lakes, and the north woods, but in the last decade, there has been a significant increase in the number of wineries established

across this Midwestern state. Although Wisconsin has a long winemaking history, the Wisconsin grape growing and wine industry has experienced rapid growth in recent years. The viticultural history of the state of Wisconsin extends back to the 1840s, when the illustrious nobleman Agoston Haraszthy, a Hungarian-born immigrant who subsequently became a pioneer in California's grape and wine industry, first settled in south-central Wisconsin. Haraszthy planted the first vines in 1847 and 1848 and built a 40-foot cellar on the prairie bordering the Wisconsin River − the current location of Wollersheim Winery, which has become a National Historic Site. The traditional European vines planted by Haraszthy did not survive the harsh Wisconsin winters. At the end of 1848 he followed the gold rush to California, where he founded some of the first productive vineyards (including Buena Vista Winery in Sonoma), introduced over 300 varieties of imported European vines, and ultimately became known as the founder of the California wine industry (Pinney 1989). Agoston Haraszthy's vine planting and cellar digging efforts on the hill of Wollersheim Winery in Prairie du Sac, Wisconsin, mark the humble beginning of the state's viticultural history.

Wine production in Wisconsin has always been minimal due to its climate, which is susceptible to extremes of temperature (the record low of –48.3°C, or –55°F, was reported in February 1996), making Wisconsin's mesoclimates incompatible with the cultivation of most Vitis Vinifera varieties. Overall, average annual minimum temperatures in the state of Wisconsin range between –2°C and 3°C, and average annual maximum temperatures vary from 10°C to 14°C. Data from the Wisconsin State Climatology Office show that Wisconsin's continental climate, moderated by Lake Michigan and Lake Superior, is characterized by a short growing season of 140 to 150 days in the east-central Lake Michigan coast and southwestern valleys and even shorter in the central portion of the state, as a result of inward cold air drainage. These cool-climate conditions commonly limit yield and quality of grapes because of occasional spring freezes, which can occur from early May in southern counties and Lake Michigan coastal areas to early June in northern counties, and fall frosts, which can occur from late August/early September in northern and central lowlands to mid-October along the Lake Michigan coastline. Based on a long-term climatological temperature average (calculated using the 1981−2010 U.S. Climate Normals), a total of 2264 Growing Degree Days (GDD, base 50°F) were calculated for Wisconsin from April 1st to October 31st, which puts Wisconsin in Winkler's Region I (2500 or less GDD). The Winkler scale, which is a method of classifying climate of grape growing regions based on heat summations (one degree day per degree Fahrenheit over 50°F), includes five climate regions: Region I (≤2500 GDD); Region II (2501–3000 GDD); Region III (3001–3500 GDD); Region IV (3501–4000 GDD); and Region V (>4000 GDD). Because Vinifera vines typically cannot survive the cold Wisconsin winters, mostly cold-resistant native American and French-American hybrid varieties, such as Marechal Foch, Leon Millot, Edelweiss, La Crosse, Frontenac, St. Peppin, Seyval Blanc, Marquette, and many other resilient varieties, are cultivated in Wisconsin. Many Wisconsin winemakers procure grapes from other areas of the USA (California, Washington, New York), and also make wine from other types of fruit, including cherries, strawberries, blueberries, raspberries, cranberries, peaches, apples, and pears. Most Wisconsin wineries make a combination of grape and fruit wines, and increasingly more producers make wine from locally grown cold-climate grapes.

In spite of the Midwestern USA climatic challenges, the Wisconsin grape industry has expanded exponentially in the last decade, as most vineyards were planted between 2005 and 2010. The number of Wisconsin wineries keeps climbing, with over 100 wineries to date (2016) across the state, according to the Wisconsin Winery Association. As global temperatures continue to increase, the current areal extent of grape growing regions will shift accordingly, allowing new varieties to be cultivated in certain regions, as well as limiting the production and affecting the quality of established cultivars in other regions. As climate change continues to affect the selection of grape varieties that can be cultivated in Wisconsin, some grape growers are starting to experiment with Vitis Vinifera varieties; cool-climate Riesling is the frontrunner.

In 2012, Wisconsin grape growers and winery owners were surveyed regarding grape-growing practices, winery operating practices, and sales and production performance in order to establish industry baselines and quantify economic contribution. The survey was conducted by Tuck and Gartner (2014) as part of the United States Department of Agriculture (USDA)-funded Northern Grapes Project. Based on the survey results, approximately 708 acres of vines were planted and approximately 1400 tons of grapes harvested in 2011. Of the 71,699 planted vines in the state, the majority (58,300) are cold-hardy vines, comprising 34,400 red cultivars and 24,000 white cultivars. The top three red cultivars are Marquette, Frontenac, and Marechal Foch, constituting 42%, 26%, and 9%, respectively, of the total planted cold-hardy red varieties. The top three white cultivars are Frontenac Gris, Brianna, and La Crescent, representing 27%, 19%, and 15%, respectively, of the total planted cold-hardy white varieties (Tuck and Gartner 2014). As evidenced by these survey results, Wisconsin is a very small grape producer. For comparison, the top 13 United States grape producers are listed in Table 1, based on data from the Crop Production Report (ISSN: 1936-3737) released on August 12, 2015, by the National Agricultural Statistics Service (NASS), Agricultural Statistics Board, USDA. California leads the way with 6,822,000 tons (89%), followed by Washington with 512,000 tons (5%), and New York with 188,000 tons (2%) of total production in 2014.

The state of Wisconsin is divided into five distinctive wine regions: the Northwoods Region, Fox Valley Region, Glacial Hills Region, Door County Region, and Driftless Region, and within these five wine regions, there are three established American Viticultural Areas (AVAs), including the Lake Wisconsin AVA, the Upper Mississippi River Valley (UMRV) AVA, and the Wisconsin Ledge AVA (Fig. 1). The Lake Wisconsin AVA, established on February 4, 1994, is situated in the south-central part of the state and encompasses approximately 130 square kilometres (km^2) in two counties. It includes within its

Table 1. Summary of 2014 US grape production showing the top 13 United States grape producers.*

State	Total Grape Production (tons)
California	6,822,000
Washington	512,000
New York	188,000
Pennsylvania	91,000
Michigan	63,300
Oregon	58,000
Texas	9,400
Virginia	8,800
North Carolina	6,000
Missouri	4,030
Georgia	4,000
Ohio	3,810
Arkansas	1,490

*Source: Crop production report (ISSN: 1936–3737) released August 12, 2015, by the National Agricultural Statistics Service, Agricultural Statistics Board, United States Department of Agriculture.

boundaries the location of the historic Wollersheim Winery. The UMRV AVA, established on June 22, 2009, is the largest designated appellation in the world, stretching approximately 78,000 km² across southeastern Minnesota, southwest Wisconsin, northwest Illinois, and northeast Iowa, and it includes within its boundaries the Lake Wisconsin AVA. The Wisconsin Ledge AVA, established on March 22, 2012, is located in the northeastern part of the state, covering approximately 9800 km² in 11 counties, and is part of the Niagara escarpment corridor, stretching along the Lake Michigan shores.

This research study examines the terroir of historic Wollersheim Winery, the only winery within the confines of the Lake Wisconsin AVA, to understand the interplay of environmental factors influencing the character, quality, and variability of Wollersheim wines.

OVERVIEW OF THE TERROIR OF LAKE WISCONSIN AVA

Lake Wisconsin AVA is situated in south-central Wisconsin, approximately 70% in Columbia County and 30% in Dane County. The AVA is bordered to the west and north by the Wisconsin River and Lake Wisconsin, respectively, to the east by Spring Creek and State Highway 113, and to the south by Mack Road and State Highway Y (Fig. 2); its boundaries are defined by federal regulations (GPO Electronic Code of Federal Regulations 2015). The climate within the Lake Wisconsin AVA displays minor variability. The Wisconsin River and Lake Wisconsin moderate the temperatures, and average annual precipitation ranges from approximately 762 to 813 mm, which is lower than most of the state. The number of frost-free days ranges from 125 to 170 across the AVA and represents the number of days in the interval between the last spring day and the first autumn day with freezing temperatures. Based on a 30-year climatological temperature average using data from Columbia and Dane counties weather stations, Lake Wisconsin AVA falls in the low range of the Winkler Region II (2501−3000 GDD), with an average of 2555 GDD. The geology of the Lake Wisconsin AVA comprises Precambrian bedrock units consisting of crystalline igneous and metamorphic rocks, overlain by lower Paleozoic (Cambrian and Ordovician) sedimentary rocks. Specifically, Cambrian sandstone interbedded with secondary dolostone and shale constitute the Elk Mound, Tunnel City, and Trempealeau groups, whereas Ordovician dolostone with secondary sandstone and shale is assigned to the Prairie du Chien Group (Oneota and Shakopee formations).

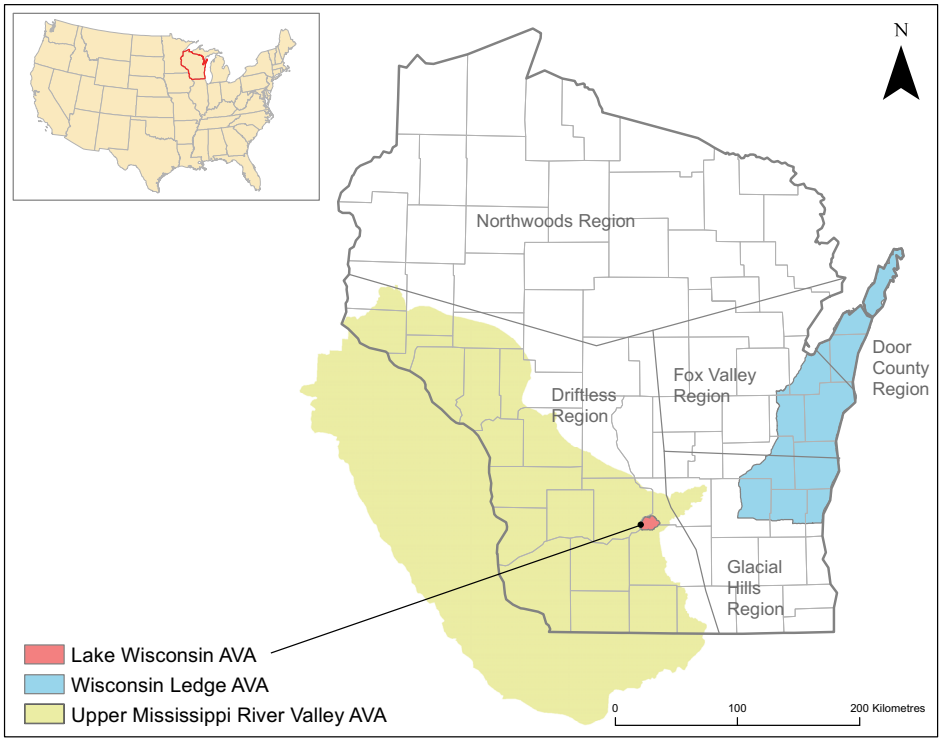

Figure 1. Map showing the five Wisconsin Wine Regions (Northwoods, Fox Valley, Glacial Hills, Door County, and Driftless) and the three American Viticultural Areas (AVA; Lake Wisconsin, the Upper Mississippi River Valley, and the Wisconsin Ledge).

The Lake Wisconsin AVA extends along the eastern margin of the Driftless Area or Paleozoic Plateau, which remained unglaciated during the last glacial advance. The USA upper Midwest region was covered by ice during four glacial stages: the Nebraskan, Kansan, Illinoisan, and Wisconsinan. The most recent major glacial advance of the North American Laurentide Ice Sheet was the Wisconsinan, which lasted from approximately 25,000 to 15,000 years ago (Attig et al. 2011). The glacial lobes of the Laurentide Ice Sheet extended down into the northern and eastern parts of the state, covering its terrain

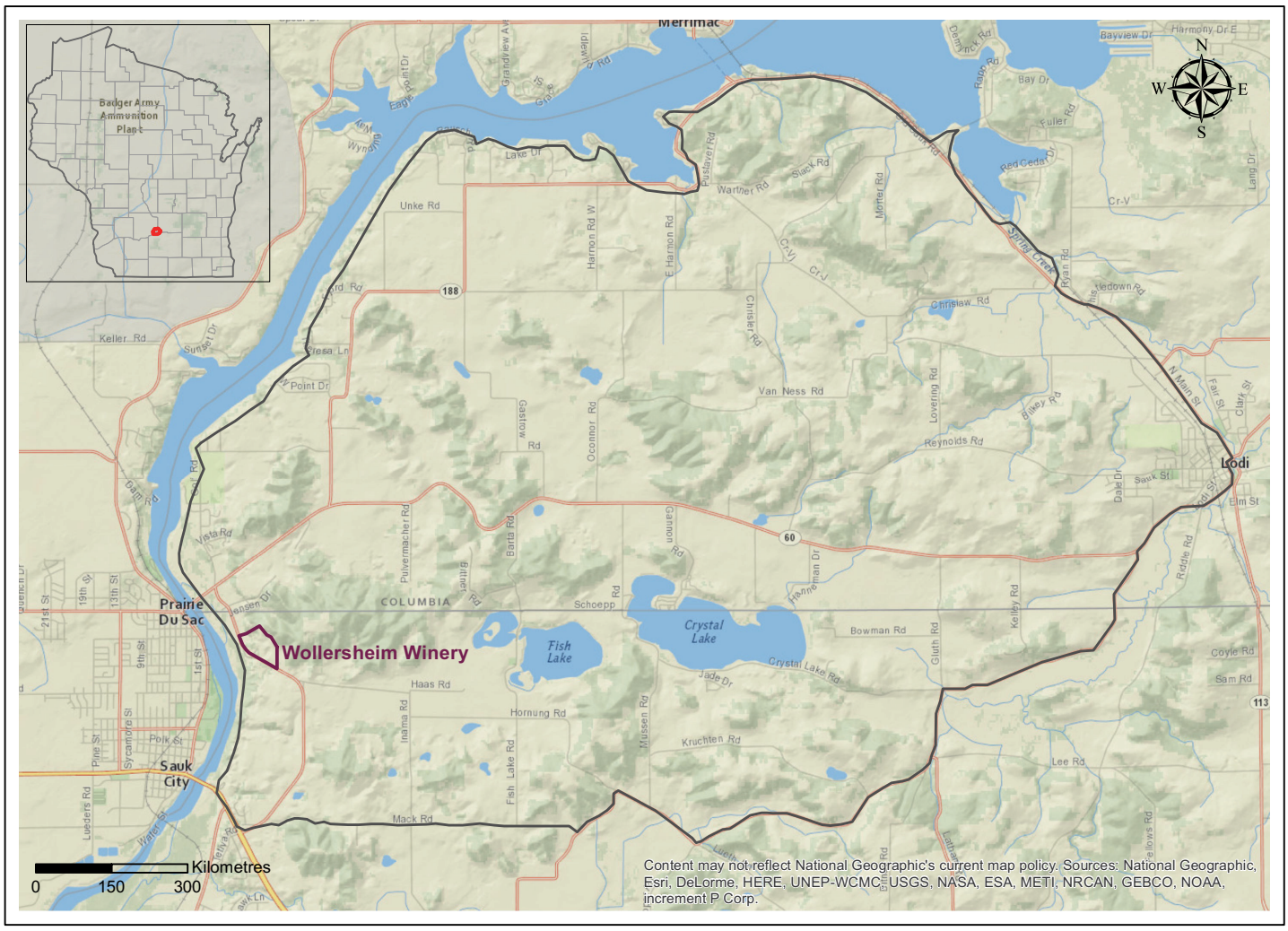

Figure 2. Map depicting the boundaries of the Lake Wisconsin American Viticultural Areas (AVA) and the location of historic Wollersheim Winery, the only winery in the Lake Wisconsin AVA.

in glacial drift, but never reached the Driftless Area in the western and southern parts of the state. The Driftless Area is characterized by a lack of glacial drift and an erosional topography consisting of flat-topped hills, steep forested slopes, and a well- developed, dendritic drainage system. The landscape is dissected by a network of steeply-cut valleys developed by stream erosion during the roughly 420 million years between the Silurian and Quaternary periods. In contrast, to the east of the Driftless Area, the land was glaciated, and the topography consists of small, gently undulating hills, a less developed drainage system, and numerous lakes, wetlands, and marshes. Although glaciers never reached the Driftless Area during the Quaternary (Mickelson et al. 1982), the effects of glaciation are observed in its peripheral deposits and landscapes, which were affected by periglacial processes (Stiles and Stensvold 2008).

The Lake Wisconsin AVA is situated in the transitional zone between the glaciated topography to its east and the unglaciated, driftless topography to its west. Its landscapes are part of the glacially-derived Holy Hill Formation, comprising the Horicon and Mapleview members (Fig. 3). The deposits consist of terminal moraines – large ridges of glacial debris that accumulated at the glacial limit – and outwash deposits of stratified sand and gravel found in the valleys of rivers that carried large volumes of glacial meltwater. Generally, postglacial deposits include sand, silt, clay, and organic materials deposited in stream valleys and lowlands, whereas glacial stream deposits include outwash and hummocky sand and gravel. Silt-sized loess, windblown from the floodplains of glacial meltwater rivers, was deposited on top of the land surface during the Wisconsinan Glaciation, but was subsequently eroded from many areas, and is now present as a thin discontinuous cover on uplands and slopes (Clayton and Attig 1997). Figure 3 depicts the glacial features across the state of Wisconsin, including the extent of the Horicon and Mapleview members

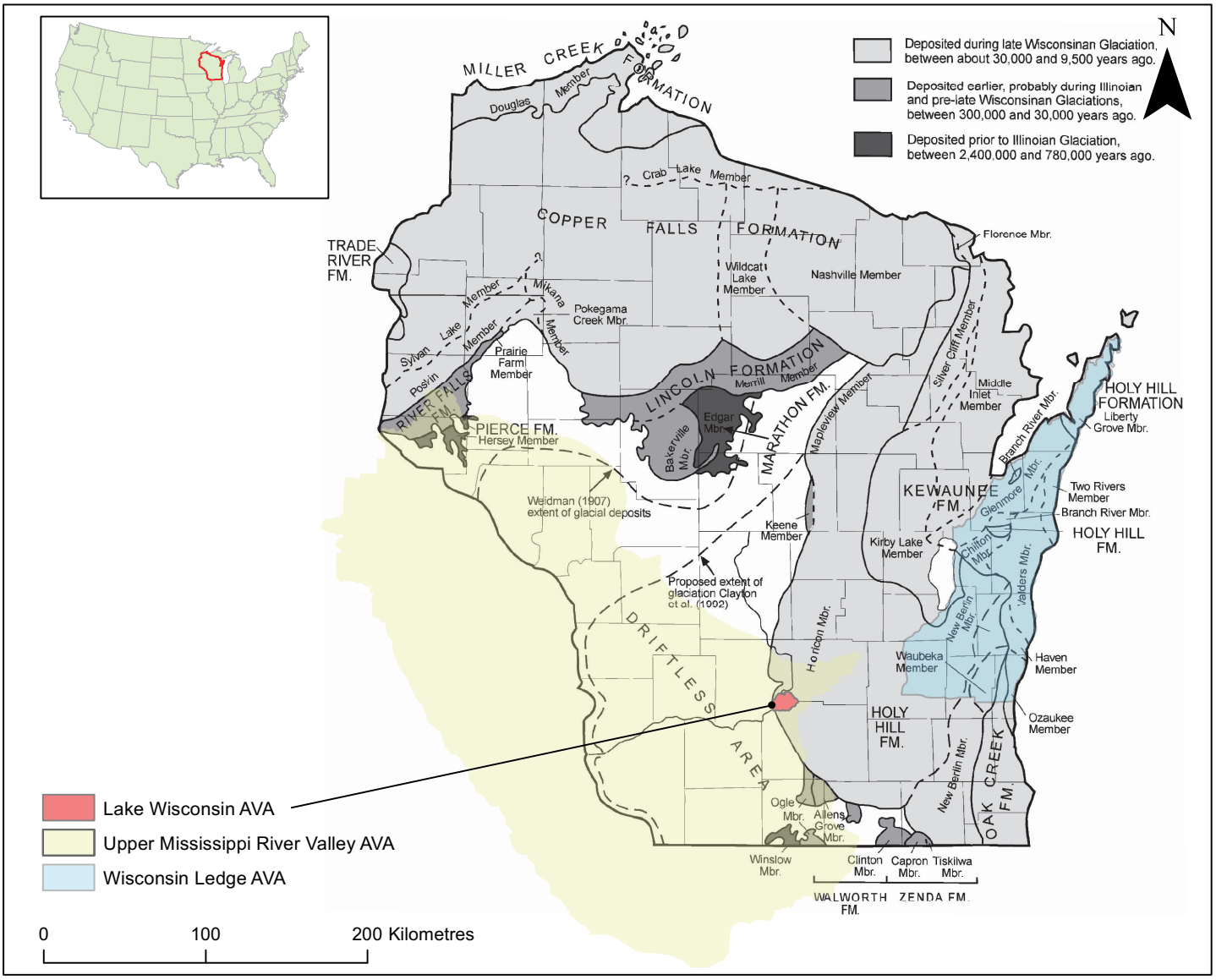

Figure 3. Map depicting the glacial features of the state of Wisconsin in relation to the locations of the state's three American Viticultural Areas (AVA). (from Syverson and Colgan 2004).

of the Holy Hill Formation, as well as the non-glaciated Driftless Area, in relation to the locations of the state's three AVAs.

The soils across the Lake Wisconsin AVA were developed on top of various types of parent materials, ranging from sandstone and dolostone bedrock to glacial till, outwash, and loess deposits. The parent materials covering the largest proportions of the AVA are calcareous sandy loam till, loess over glacial loamy till, silty sediments over stratified silts and sands, loess and/or silty slope alluvium, loess over calcareous sandy loam till, and loess over glacial till (USDA Natural Resources Conservation Service, Web Soil Survey data). Most cultivated soils in the region have developed in loess, making these windblown silt deposits the foundation of agriculture (Clayton and Attig 1997).

GLACIALLY INFLUENCED TERROIR IN OTHER VINE-GROWING REGIONS

Worldwide, many wine regions located where soils developed on glacially transported parent materials are known for producing outstanding wines. Generally, ice and glacial meltwater are the primary agents of deposition of the soil parent material, generating glacial till and glaciofluvial/ glaciolacustrine deposits, respectively. Windblown silt-sized loess deposits can also be generated from the floodplains of glacial meltwater rivers.

In New Zealand, vast portions of the North and South islands are covered by Quaternary glacial and fluvial sediments, and extensive outwash deposits are distributed across the lowlands. The majority of vineyards are planted on alluvium and

http://www.dx.doi.org/10.12789/geocanj.2016.43.107

outwash gravels. In the Central Otago region, nearly half of the planted vineyards are located on glacial gravels; in Hawkes Bay, which includes the Gimblett Gravels wine region, approximately 63% of vineyards are located on outwash deposits; and in the Marlborough and Waipara wine regions, most vineyards are planted on alluvium and outwash gravels (Imre and Mauk 2009).

In Canada, the soils of the Niagara Peninsula wine region developed on glacial till resulting from the advance and retreat of ice during Quaternary continental glaciations, and on glaciolacustrine and glaciofluvial deposits formed during interglacial periods. The Niagara vineyards planted on these soils define two distinctive terroirs: the flat area of the Lake Iroquois Plain extending between Lake Ontario and Lake Iroquois, and the Escarpment, consisting of the Lake Iroquois bench terraces and the slopes above the Niagara Escarpment (Haynes 2000). In the Canadian Okanagan and Similkameen valleys of British Columbia, many glacial advances generated soil parent materials consisting of unconsolidated glacial deposits. In the Okanagan Valley, the thickness of Pleistocene glacial deposits is nearly 100 m, and glaciofluvial deposits cover the sides of the valley (Taylor et al. 2002). Most vineyards in the Okanagan and Similkameen valleys are planted on soils derived from these glacial sediments, which include glaciofluvial, fluvial fan, and glaciolacustrine deposits (Bowen et al. 2005).

In the USA, the Columbia Valley AVA, which encompasses several other AVAs in Washington and Oregon, has soils derived from Quaternary glacial sediment and aeolian deposits. Recurring Pleistocene glacial outburst flooding events, known as the Missoula floods, generated glacial flood sediment deposits known as Touchet beds, which accumulated in river valleys and covered the landscape (Meinert and Bussaca 2000, 2002; Pogue 2009). Deposits of windblown loess of varying thickness overlie the Touchet beds. Most vineyards in the Columbia Basin are planted on soils derived from deposits of loess and glacial flood sediments (Pogue 2009). In the Finger Lakes AVA of New York state, vineyards are planted on soils consisting of varied accumulations of gravel, sand, silt, and clay produced by glacial processes (Swinchatt 2012). The Devonian bedrock, which is now covered by Pleistocene glacial deposits, was scoured repeatedly during glacial advances. The retreating glaciers generated the glacial meltwater that formed the Finger Lakes and carved a landscape of moraines, glacial till, and glacial outwash (Meinert and Curtin 2005).

In France, the landscapes of the Rhone Valley and Bordeaux wine regions have abundant glacial sediments originating from the Alps. In the Rhone Valley, alpine glaciers descended from the Alps, scouring valleys and leaving behind an assortment of glacial till and moraine deposits. Meltwater and subsequent glacial floods re-sorted some of these deposits into extensive terraces and gravel plateaus where many vineyard sites are located (Wilson 1998). In the Bordeaux wine region, Medoc and Graves vineyards are located on gravel terrace mounds. The gravel-rich soils of these areas developed on the outwash deposits associated with the Garonne River interglacial floods and the moraine deposits generated during the Pleistocene glaciation (Wilson 1998).

These glacially influenced wine regions produce exceptional wines in a unique terroir consisting of soils developed on transported, glacially derived parent materials. The glacial soils provide distinct vineyard sites and are characterized by good internal drainage and moderate fertility and water-holding capacity, controlling vine vigor and promoting grape ripening.

TERROIR CHARACTERIZATION OF WOLLERSHEIM WINERY

Historic Wollersheim Winery Background

Wollersheim Winery is a National Historic Site, with a history extending back to the 1840s, when the legendary Hungarian nobleman Agoston Haraszthy first settled on the estate. One of Wisconsin's largest wineries, top wine producers, and a leader in the Midwestern wine industry, Wollersheim Winery produces approximately 240,000 gallons or 1.2 million bottles annually, which corresponds to approximately 1410 tons of grapes. Most are custom-grown grapes, including Sangiovese, Chardonnay, Riesling, Pinot Noir, Seyval Blanc, Carignan, and Muscat from Washington (335 tons), California (10 tons), and New York (783 tons); however, approximately 20% (282 tons) are Wisconsin-grown grapes, including 25 acres of vineyards located on site. Four winter-hardy hybrid grape varieties are cultivated on the Wollersheim Winery estate, including two French-American red hybrids (Marechal Foch and Leon Millot) and two Wisconsin-native American white hybrids (St. Pepin and LaCrosse), producing eight different estate wines made entirely from Wisconsin-grown grapes. Specifically, the grapes grown in the young, flat vineyards produce light-bodied wines (Prairie Blush, Eagle White, Prairie Sunburst Red, and Ice Wine); grapes from the medium-aged vines planted on medium-sloped vineyards produce medium-bodied wines (Ruby Nouveau, Bon Vivant, and Domaine du Sac); and grapes from the oldest and steepest-sloped vineyard produce the rich, full-bodied Domaine Reserve wine.

Best known for its distinctive regional wines, Wollersheim Winery has received numerous medals and awards in national and international wine competitions. Some of the most recent Wollersheim Winery accolades include the 2012 Winery of the Year award at the San Diego International Wine Competition and the 2015 Small Winery of the Year award at the Riverside International Wine Competition. It has also won many awards for its estate wines, such as the 2015 Prairie Blush, which most recently was awarded the Chairman's Trophy at the 2016 Ultimate Wine Competition in Hawthorne, New York, and gold medals at the 2016 New World International Wine Competition in Ontario, Canada, the 2016 Winemaker Challenge International Wine Competition in San Diego, California, and the 2016 Dan Berger's International Wine Competition in Sonoma County, California. Other estate wines, including Domaine Reserve, Domaine du Sac, Eagle White, and Prairie Sunburst Red, have consistently won awards at numerous competitions; a listing of the various awards can be found on the winery's website (http://www.wollersheim.com).

This research study provides a terroir characterization of the Wollersheim Winery vineyards, and utilizes analyses of soil

type, texture, geochemistry, and mineralogy to understand the interaction of environmental factors influencing the character and quality of Wollersheim wines. The study further examines local-scale vineyard variability between two plots (Domaine Reserve and Lot 19) that are cultivated with the same grape variety (Marechal Foch) to determine the controls on small-scale variability in grape quality and Wollersheim wines.

Materials, Methods, and Data Acquisition

Total major and select minor and trace element compositions were determined on powdered rock samples and on the fine fraction of vineyard soil samples, which were powdered and fused for x-ray fluorescence (XRF) analysis. Loss on ignition (LOI) was determined by heating 1 gram of sample for 10 minutes in a muffle furnace at 1050°C and calculating the mass difference. The major element and select minor and trace element compositions were obtained from glass disks fused at 1050°C in a Claisse M4 fluxer and analyzed using a Bruker S4 Pioneer XRF in the Department of Geosciences, University of Wisconsin–Milwaukee. Plant-available soil chemistry analysis was conducted by the University of Wisconsin Soil Testing Laboratory in Madison, Wisconsin, to determine concentrations of phosphorus, potassium, calcium, magnesium, sulfur, zinc, manganese, and boron, as well as pH, cation exchange capacity, and organic matter. Soil texture was determined by grain size analysis using a Malvern Mastersizer 2000E laser diffraction particle-size analyzer. In the laser diffraction method, a laser beam is passed through a sample to measure the angular variation in scattered light intensity, which is used to evaluate the particle size distribution within a sample. Soil and rock mineralogy were determined non-quantitatively on a portion of each powdered sample by x-ray diffraction (XRD) analysis. Random mounts were prepared by packing the fine powders to a flat surface onto a cavity mount sample holder capable of assuming different orientations. Samples were analyzed in the Department of Geosciences at the University of Wisconsin–Milwaukee using a Bruker D8 Focus XRD system (Cu Ka radiation, 4 s per 0.01° 2θ, 2°–60° range, Sol-X energy dispersive detector). Minerals were identified by searching the International Centre for Diffraction Data (ICDD) database of standard X-ray powder diffraction patterns for a match with the pattern of the unknown.

Vine trunk circumferences were measured at two plots, Lot 19 and Domaine Reserve, on September 14, 2014. Vine trunk circumference measurements can be used as an indicator of vine vigor variation (Imre and Mauk 2011). The measurements were collected from every vine at every other row, approximately 20 cm from the ground surface at the narrow part of the vine.

Geophysical surveys, including electromagnetic induction (EMI) and electrical resistivity tomography (ERT) were conducted at two plots, Lot 19 and Domaine Reserve, on May 18, 2014. The EMI surveys were carried out with a Geonics EM-31-MK2 ground conductivity meter, which has a fixed coil spacing (3.66 m) and a single frequency (9.8 kHz) generating the primary magnetic field, with depths of exploration of 3 m in the horizontal dipole mode and 6 m in the vertical dipole mode. The Geonics EM-31-MK2 ground conductivity meter is calibrated for a standard operating height of 1 m above the ground, which is approximately waist height. The EMI surveys were performed at walking speed, and apparent electrical conductivity (ECa) measurements were collected from 104 locations at each plot along alternating transects between every other row of vines, for a total of 9 transects completed at each plot. ECa measurements in the horizontal and vertical dipole modes were read directly from the integrated data logger, and the measurement locations were georeferenced by means of a GPS receiver. The ECa datasets for both plots were downloaded with the Geonics DAT31W software program and interpolated using the ordinary kriging method with the Esri ArcGIS Desktop software program.

The ERT survey was conducted using a GF Instruments ARES-G4 unit, with a standard survey line of 115 m consisting of three cables and a total of 24 electrodes. The electrodes were spaced 3 m apart in the Wenner array, attaining a maximum exploration depth of 14 m. The Wenner array consists of four electrodes spaced equally in a straight line at ground surface; current is applied to the two outer (current) electrodes and the potential difference measured at the two inner (potential) electrodes. The ERT method records the contrast in apparent electrical resistivity (ER) in soil, providing an estimate of the horizontal and vertical lithological variations. Two profiles were completed at each plot, one near the top row and one near the bottom row of vines. The profiles were used to determine lateral changes in resistivity, identifying the lateral continuity of layers. The ER data for all profiles were downloaded with the GF Instruments ARES v5.0 program and exported into RES2DINV (Geotomo) inversion program for processing. A common logarithmic scale was applied to all profiles for appropriate comparison.

Results and Discussion

The Wollersheim Winery vineyards are located on a hill overlooking the Wisconsin River, at elevations between approximately 213 and 306 m, on south and southwest-facing gentle slopes. The vines are planted 2 m apart and the distance between rows is 3 m, which allows sufficient space for farming equipment. The 25 acres of bearing vineyards consist of approximately 700 vines per acre for a total of 17,500 vines on site. The landforms are streamlined hills and valleys shaped by glaciers and glacial stream deposits consisting of outwash and hummocky sand and gravel (Mickelson 2007). The glacial deposits are part of the Horicon Member of the Holy Hill Formation, which is characterized by glacial till comprising brown gravelly, clayey, silty sand, and dolomite derived from Ordovician formations; these glacial deposits are overlain by loess (Clayton and Attig 1997).

The climate is moderated by the Wisconsin River, and air drainage in the river valley inhibits frost in the vineyards. In the Wollersheim Winery area, where the average growing season ranges from April 1st to October 31st, a total of 2382 (base 50°F) GDD were recorded in 2014. Based on a 30-year climatological temperature average (1981−2010), Wollersheim Winery falls in the low range of the Winkler Region II (2501−3000 GDD) with an average of 2652 GDD. In comparison, Napa, California falls in the middle range of the Winkler Region III

http://www.dx.doi.org/10.12789/geocanj.2016.43.107

Figure 4. Location map of Wollersheim Winery vineyards illustrating the distribution of soil types, and soil sample and resistivity profile locations.

(3001−3500 GDD) with an average of 3297 GDD, and Walla Walla, Washington falls in the high range of the Winkler Region II (2501−3000 GDD) with an average of 2959 GDD.

Vineyard Soil Properties

To characterize the terroir and assess vineyard variability at Wollersheim Winery, a total of 12 soil profiles were examined and sampled throughout the vineyards (Fig. 4). Two rock samples were also collected in the vicinity of the vineyards. The first was from a sandstone outcrop exposed along Highway 60, approximately two kilometres to the north-northeast of the Wollersheim vineyards; the second was from a representative dolostone boulder (approximately 2 x 4 x 2 m) at the top of the Domaine Reserve plot that was transported from the Ordovician Prairie du Chien Group dolostone bedrock bordering the east boundary of the vineyards. The elevations of the soil sample locations range from 236 to 286 m, and the maximum depths of the soil profiles range from 50 to 70 cm below ground surface, across horizons A, E, and B.

Based on the USDA taxonomic classification, the vineyard soils are Alfisols, which is a soil order characterized by moderately weathered and leached clay-rich soils having high to medium base saturation, relatively high native fertility, and abundant iron and aluminum. The soils are further classified as the subgroup Udalfs (Alfisols found in humid climates) and the great group Hapludalfs (Udalfs with minimum horizonation). Specifically, the soils are Typic and Mollic Hapludalfs in a mesic soil temperature regime and udic soil moisture regime, indicating that the soils are similar to other Alfisols (Typic) or have a darkened and organic-rich surface horizon (Mollic). Based on a water budget analysis using the National Oceanographic and Atmospheric Administration's National Climate Data Centre climate normals and the USDA Official Soil Series descriptions (textures and profile thicknesses) to determine the water status of soils over the growing season, the soils are seasonally moist in normal years, and generally experience a surplus throughout the year. Recharge periods extend from April through October, when temperatures are generally above 5°C. Although droughts

likely alter the water balance, drought years do not represent 'normal years' in this region.

Based on the USDA Official Soil Series descriptions, the soils are part of the Gaphill–Rockbluff complex, and Boyer, Kegonsa, and Seaton Series, which are characterized by very deep, well-drained soils. Based on the grain size analysis, silt- and sand-sized grains dominate the soil samples collected throughout the vineyards, with average silt and sand compositions of 59% and 34%, respectively. The soils plot in the silty loam and sandy loam fields of the USDA soil texture triangle (Fig. 5), and these textures are in general agreement with the USDA taxonomic classification for these soils. Soil samples collected from the highest elevations in the northern and eastern parts of the property (DR-1, DR-2, and Lot 10A/B) contain the highest silt content (79–80%) and correspond to areas of steeper slope, thinner soil, and shallower depth to bedrock.

Most of the vineyard soils are silty loams developed on parent materials consisting of windblown loess deposits; these soils are represented by 8 of the 12 soil samples collected and cover approximately 42% of the property. The vineyard soils in the northern and central parts of the property, represented by soil samples Lot 10A/B, Lot 14, and Lot 20, underlie approximately 27% of the property, and consist of sandy loams derived from loamy outwash and glaciofluvial deposits underlain by outwash. Along the eastern property boundary, in a small area covering approximately 4% of the property and characterized by the highest elevations and steepest slope, soil sample DR-1 is a sandy loam developed on loamy colluvium and sandy deposits overlying sandstone bedrock. The remainder of the property (approximately 25%) consists mostly of a centrally located gravel pit developed in gravelly outwash.

Vineyard Soil Chemistry and Mineralogy

Soil chemical analyses were carried out for organic matter, cation exchange capacity, and pH, along with plant-available macronutrients (potassium, calcium, magnesium, phosphorus, and sulfur) and micronutrients (boron, manganese, and zinc) that are essential elements necessary for completion of the plant life cycle (Table 2). All these elements have important roles in the metabolic functions of vines and require that minimum levels be maintained. The physical and chemical characteristics of the vineyard soils, such as texture, pH, organic matter, and cation exchange capacity, affect the nutrient pool, availability, adsorption, and retention potential. Fine-grained, clayey soils can reduce the availability of potassium to vines, whereas coarse-grained, sandy soils are prone to leaching and can drain nutrients from the soils (Lambert et al. 2008). The silty loam and sandy loam vineyard soil samples are dominated by silt- and sand-sized grains, providing a good balance between drainage and water holding capacity. The pH values of the vineyard soil samples, ranging from 5.6 to 7.6, indicate moderately acidic to slightly alkaline conditions, which provide good nutrient availability and balance for the health of the vines. Soils rich in organic matter are generally high in available nutrients, as decomposition of organic matter adds nutrients to soil and improves water-holding capacity. Cation exchange capacity, which is influenced by the soil's organic matter and clay content, affects the ability of soil to hold positively charged nutrients for plant uptake (Dami et al. 2005). The highest organic matter percentages and cation exchange capacities, ranging from 1.1–1.3% and 12–13 cmol/kg, respectively, correspond to vineyard soil samples containing the highest silt content collected from the vineyards located in the northern and eastern parts of the property.

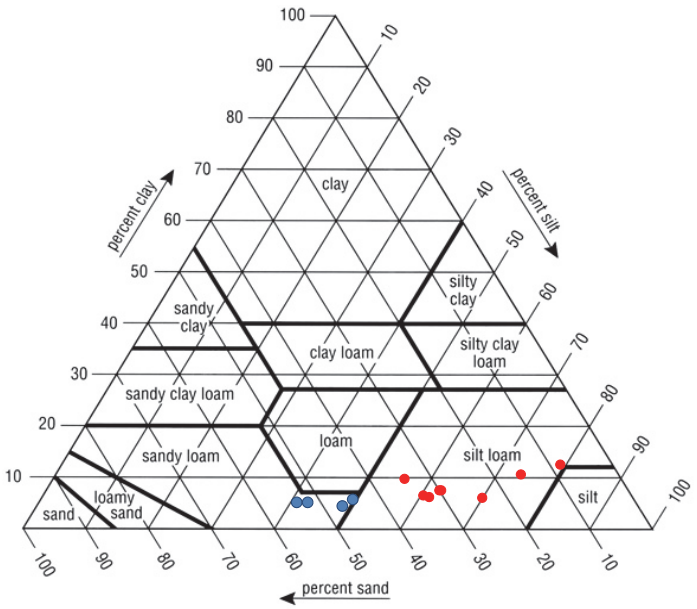

Figure 5. Ternary diagram showing the vineyard soil textures plotting in the silt loam and sandy loam fields of the United States Department of Agriculture (USDA) Soil Texture Triangle.

The concentrations of plant-available macronutrients potassium (24–112 ppm), calcium (278–1587 ppm), magnesium (62–658 ppm), phosphorus (7–49 ppm), and sulfur (1–5 ppm), and micronutrients boron (0.2–0.6 ppm), manganese (13–89 ppm), and zinc (0.4–2.1 ppm), indicate significant variability in the vineyard soils. Some of these nutrient concentrations are outside the ranges specified by Moyer et al. (2014) in their pre-plant soil fertility guidelines for establishing productive vineyards, and by Dami et al. (2005) in the Midwest Grape Production Guide. However, when assessing the nutrient requirements of established vineyards, analyzing vine tissue samples in conjunction with soil samples is critical in determining vine nutrient status and identifying potential deficiencies (Moyer et al. 2014). Overall, the plant-available soil chemistry shows the most variability for calcium, magnesium, and potassium; the highest concentrations of these elements are found in soils having the highest silt content in the northern and eastern parts of the property, i.e. in areas of steeper slope, thinner soil, and shallower depths to bedrock, where the vineyards producing the lowest yields and highest quality grapes are planted.

The XRF total elemental analysis conducted on the fine fraction (silt and clay) of the soil samples indicates some variation in the chemical composition of the vineyard soils (Table 3). These elemental abundances represent the total concentrations in the soil and are indicative of the general vineyard soil conditions, whereas plant-available essential elements (Table 2), which are necessary for the completion of the plant life

Table 2. Summary of plant-available soil chemistry and texture. The variability in nutrient levels is influenced by the vineyard soil properties, which affect the nutrient pool, availability, adsorption, and retention potential.

Sample ID	DR-1	DR-2	Lot 5	Lot 6	Lot 7	Lot 8	Lot 9	Lot 10A/B	Lot 14	Lot 19-1	Lot 19-2	Lot 20
Depth (cm)	50	50	65	65	70	60	55	50	55	50	50	50
Soil Type	1145F	SmC2	SmB	SmB	SmB	SmB	SmC2	BoD2	BoD2	KeB	KeB	BoC2
Parent Material (USDA WSS)	Loamy colluvium over sandy residuum weathered from sandstone	Loess and/or silty slope alluvium	Loess and/or silty slope alluvium	Loess and/or silty slope alluvium	Loess and/or silty slope alluvium	Loess and/or silty slope alluvium	Loess and/or silty slope alluvium	Loamy outwash over sandy and gravelly outwash	Loamy outwash over sandy and gravelly outwash	Loess over sandy and gravelly outwash	Loess over sandy and gravelly outwash	Fine-loamy fluvial deposits over sandy-gravelly outwash
Clay	5.8	12.3	7.3	7.3	5.0	5.5	4.2	10.4	6.3	4.9	6.0	9.5
Silt	70.3	79.6	62.4	63.0	41.0	49.7	48.7	74.2	60.6	42.7	61.7	56.0
Very Fine Sand	10.0	4.2	10.8	7.8	12.4	12.5	12.9	8.3	10.0	7.1	11.7	7.6
Fine Sand	8.7	2.0	14.6	12.0	26.4	20.5	20.0	5.0	9.9	17.3	11.0	12.7
Medium Sand	5.0	1.8	4.8	9.3	14.7	11.5	13.0	2.1	6.8	21.4	7.3	11.3
Coarse Sand	0.21	0.1	0.0	0.59	0.46	0.34	1.2	0.006	5.9	6.4	2.2	2.9
Very Coarse Sand	0.00	0.00	0.00	0.00	0.00	0.00	0.00	0.00	0.56	0.06	0.10	0.03
pH	7.6	5.6	5.7	6.0	6.1	5.9	5.9	6.0	7.1	7.0	7.3	7.0
OM %	1.3	1.1	0.7	0.6	0.3	0.4	0.7	1.1	1.0	0.7	1.0	1.3
CEC (cmol/kg)	12	9	3	4	2	2	2	13	9	4	9	10
P (ppm)	7	28	35	28	34	28	49	8	28	24	16	8
K (ppm)	70	95	50	49	34	24	37	112	79	44	63	79
Ca (ppm)	1587	994	465	567	278	354	482	1384	1234	689	1172	1211
Mg (ppm)	469	373	96	150	68	62	66	658	442	225	515	586
B (ppm)	0.5	0.3	0.3	0.3	0.2	0.2	0.2	0.4	0.4	0.3	0.4	0.6
Mn (ppm)	13	27	36	25	14	21	89	35	30	43	29	28
Zn (ppm)	0.9	0.4	1.5	0.7	0.4	0.4	2.1	0.5	1.2	1.5	1.0	1.0
S (ppm)	3.5	2.0	3.3	1.2	1.0	2.3	3.5	2.3	5.0	2.3	2.3	1.8

Notes:
1145F - Gaphill-Rockbluff complex, 30 to 60% slopes; SmC2 - Seaton silt loam, 6–12% slopes, eroded; SmB - Seaton silt loam, 2–6% slopes; BoD2 - Boyer sandy loam, 12–20% slopes, eroded; KeB - Kegonsa silt loam, 2–6% slopes; BoC2 - Boyer sandy loam, 6–12% slopes, eroded; USDA WSS - United States Department of Agriculture Web Soil Survey (http://websoilsurvey.nrcs.usda.gov); OM - Organic matter; CEC - Cation exchange capacity

cycle, must be dissolved in an ionized water solution to allow uptake into the metabolism of the vines. Overall, the most variability in total concentrations is noted for SiO_2 (45.16–78.73%), CaO (0.67–9.82%), MgO (0.5–.94%), Al_2O_3 (8.13–13.30%), and Fe_2O_3 (2.36−7.22%). The vineyard soils contain average total concentrations of K_2O, CaO, MgO, and P_2O_5 of 2.55%, 2.03%, 1.64%, and 0.14%, respectively; and Fe_2O_3, MnO, Ni, and Zn are present in the vineyard soils in average total concentrations of 38,650 parts per million (ppm), 1200 ppm, 25.2 ppm, and 67.5 ppm, respectively. The dolostone rock sample consists primarily of CaO (32.77%), MgO (20.72%), and SiO_2 (2.25%), whereas the sandstone sample is dominated by SiO_2 (53.77%), CaO (14.12%), and MgO (9.51%). The variation in the chemical composition of the vineyard soils reflects the diversity of parent materials in which the soils have developed.

The XRD analysis indicates that the soil mineralogy is dominated by quartz, plagioclase (albite/anorthite/laboradorite), orthoclase (microcline/sanidine/adularia), dolomite, and minor biotite, hornblende, and various clay minerals (vermiculite, montmorillonite). The dolostone consists primarily of dolomite, along with minor quartz and clay minerals, whereas the sandstone is composed of quartz and dolomite, and minor clay minerals, indicating that it is a dolomite-rich sandstone. Unpublished field notes from Road Materials Investigations Reports prepared by the Wisconsin Geological and Natural History Survey show that dolomite is the most common pebble lithotype in the Holy Hill Formation, based on analyses of rock types present in deposits of sand and gravel throughout Dane County. East of Sauk City (Fig. 2), more than 50% of the pebbles in glacial till consist of coarse-grained, mafic igneous rock to depths of at least 15 m (Clayton and Attig 1997). Consistent with chemical analyses indicating elevated MgO and CaO, soil samples DR-1, Lot-19-2, and Lot 20 contained dolomite, which may indicate the influence of weathered dolostone and dolomite-rich sandstone in the soils located in closest proximity to the bedrock outcrops. The relatively high Fe_2O_3 content in the soils relative to the rock samples may result from the oxidation of ferromagnesian minerals such as hornblende and biotite from mafic igneous rocks.

The compositional variation of the soils is illustrated graphically on plots of major element oxides versus SiO_2 (Fig. 6), and spatially on maps depicting interpolated concentrations across the study area (Fig. 7). The plots show that SiO_2 has a strong inverse correlation with CaO and MgO; high coefficients of determination explain 80% of the variation. The soils are highly depleted in CaO and MgO relative to the dolostone sample and slightly depleted relative to the dolomite-rich sandstone sample. Fe_2O_3, P_2O_5, and MnO are also inversely correlated with SiO_2, and have lower coefficients of determination that account for 40–60% of the variation. The soils are highly enriched in Fe_2O_3, slightly enriched in P_2O_5, and have similar

Table 3. Summary of total elemental soil analysis and mineralogy. The variation in the chemical and mineralogical composition of the vineyard soils is indicative of the diversity of parent materials in which the soils have developed and the influence of the dolostone and dolomite-rich sandstone weathering in the soils located in closest proximity to the bedrock outcrops.

Sample ID	DR-1	DR-2	Lot 5	Lot 6	Lot 7	Lot 8	Lot 9	Lot 10A/B	Lot 14	Lot 19-1	Lot 19-2	Lot 20	Dolostone	Sandstone
Elevation (m)	286	276	275	274	272	272	264	276	261	236	236	244	286	286
Al_2O_3	9.70	11.18	9.18	9.83	9.49	9.27	8.13	11.60	10.47	10.08	8.96	13.30	0.62	0.59
TiO_2	0.57	0.73	0.76	0.74	0.77	0.71	0.72	0.74	0.65	0.79	0.47	0.75	0.02	0.06
Fe_2O_3	3.63	3.77	2.70	3.13	3.15	2.90	2.36	4.21	3.87	4.47	4.97	7.22	0.32	0.88
K_2O	3.14	2.55	2.46	2.48	2.57	2.51	2.37	2.52	2.40	2.68	2.21	2.73	0.27	0.19
MgO	4.01	0.85	0.67	0.77	0.74	0.70	0.50	0.99	1.32	0.90	6.94	1.27	20.72	9.51
CaO	5.43	0.67	0.72	0.69	0.78	0.77	0.83	0.79	1.61	1.08	9.82	1.14	32.77	14.12
Na_2O	0.65	1.04	1.14	1.16	1.18	1.23	1.20	1.05	1.20	0.97	0.62	0.72	0.0	0.0
P_2O_5	0.16	0.11	0.12	0.10	0.12	0.10	0.13	0.07	0.14	0.17	0.21	0.20	0.03	0.09
MnO	0.10	0.10	0.08	0.08	0.06	0.08	0.14	0.12	0.10	0.19	0.21	0.19	0.09	0.05
Zr	427.28	441.49	490.58	510.92	556.97	526.00	617.09	497.27	484.21	509.67	250.06	458.42	<10.9	62.48
V	75.20	81.36	57.73	68.01	64.95	71.75	47.08	100.57	63.27	77.14	80.58	150.72	<14.0	<14.6
Zn	47.04	68.15	66.26	69.20	58.09	58.73	49.77	59.41	72.86	66.39	86.83	115.75	<16.9	<16.3
Ni	32.50	31.76	14.71	35.01	11.11	6.41	7.20	28.08	35.15	30.07	18.89	51.61	<13.2	<14.2
Cr	59.37	79.62	68.24	68.55	61.57	67.43	67.04	54.60	55.52	51.27	61.96	96.12	18.54	18.36
Ce	123.08	143.75	146.38	131.08	125.58	141.23	77.48	138.92	235.29	237.17	181.14	161.72	<49.6	107.36
Sr	143.69	129.88	125.59	121.99	175.41	192.21	123.04	128.12	139.22	118.17	118.96	110.97	125.73	50.02
Ba	410.43	587.53	647.02	614.41	626.27	605.32	684.42	519.50	499.99	541.91	369.69	492.74	<47.1	<47.0
Quartz	xxx	xxx	xxx	xxx	xxx	xxx	xxx	xxx	xxx	xxx	xxx	xxx	x	xxx
Plagioclase[1]	x	x	xx	xx	x	x	xx	xx	x	xx		x		
Orthoclase[2]	xx	xx	x		x	xx	x	xx	x	xx	x	xx		
Dolomite	xx										xx	x	xxx	xxx
Biotite	x	x	x	x	x	x	x	x	x	x		x		
Hornblende		x						x	x		x	x		
Clay[3]	x	x	x	x	x	x	x	x	x	x	x	x	x	x

Notes:
Concentrations are in weight % for oxides and ppm for elements.
[1]Plagioclase - Albite, Anorthite, Labradorite
[2]Orthoclase - Microcline, Sanidine, Adularia
[3]Clay - Vermiculite, Montmorillonite
Relative mineral abundance based on visual evaluation of peak height and intensity (xxx = most abundant; x = least abundant)

http://www.dx.doi.org/10.12789/geocanj.2016.43.107

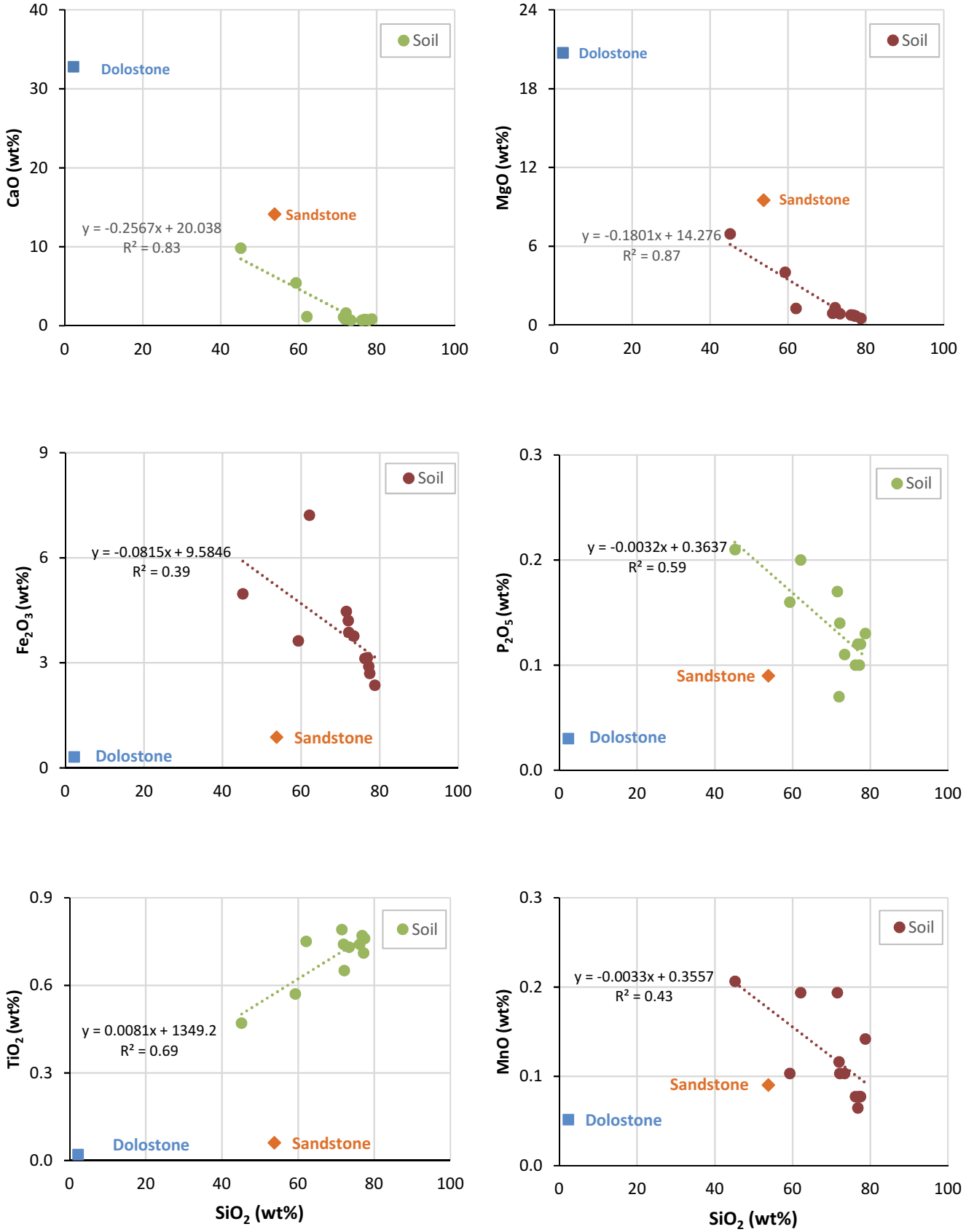

Figure 6. Harker diagrams depicting the compositional variation of selected major elements in soils relative to bedrock samples, reflecting the diversity of soil parent materials and the influence from the dolostone and dolomite-rich sandstone bedrock.

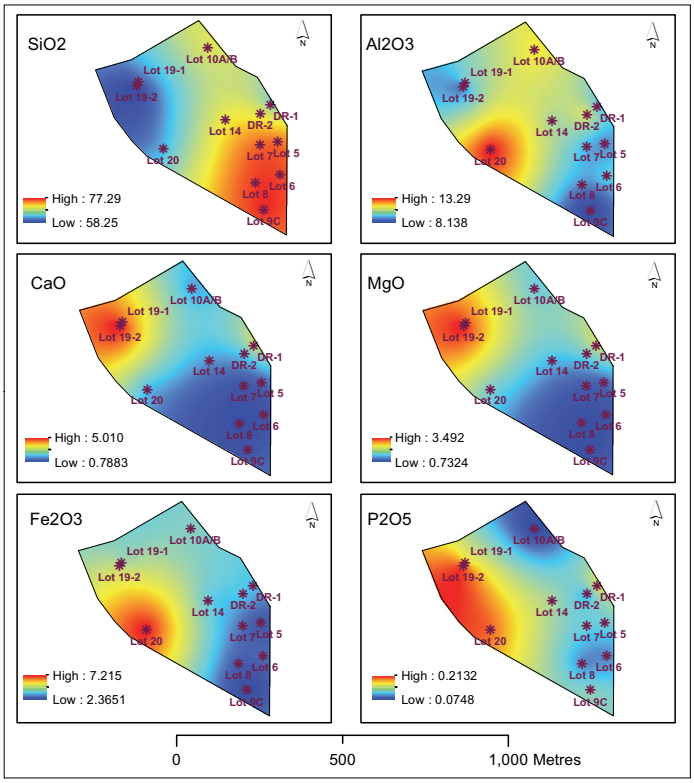

Figure 7. Map showing the spatial distribution of selected major elements in the Wollersheim Winery vineyards (see Figs. 2, 4), reflecting the variety of parent materials in which the soils formed.

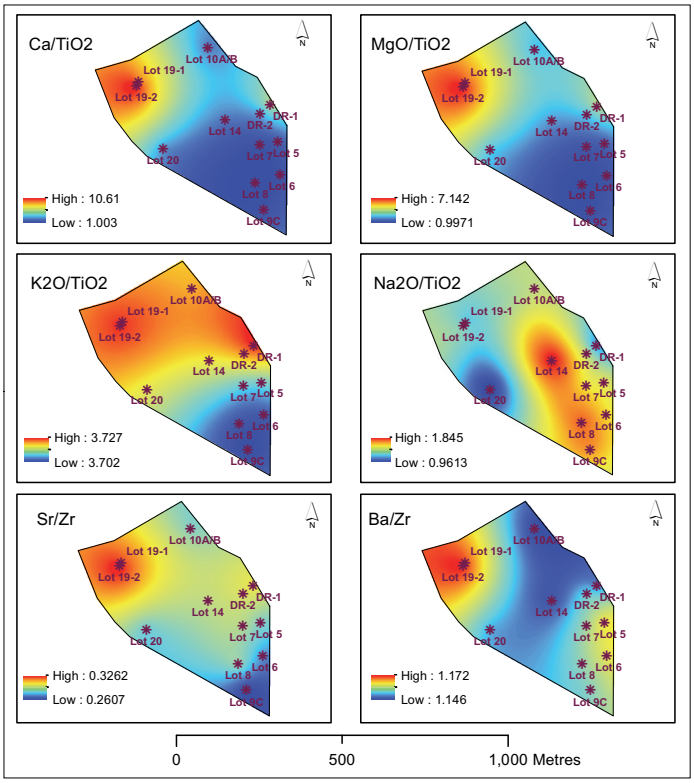

Figure 8. Map showing the spatial distribution and degree of chemical weathering in the Wollersheim Winery vineyards (see Figs. 2, 4), using ratios of selected mobile to immobile elements. More extensive chemical weathering is associated with vineyards in the north, east, and south.

MnO compositions relative to the dolostone and sandstone samples. TiO_2 and SiO_2 are positively correlated, with a coefficient of determination that accounts for 70% of the variation. The soils are significantly enriched in TiO_2 relative to the bedrock samples. Additionally, SiO_2 has a strong positive correlation with Zr and Ba; high coefficients of determination explain 80–90% of the variation (not shown). Again, these compositional differences reflect the diversity of parent materials, which include windblown loess, loamy outwash and glaciofluvial deposits underlain by outwash, and loamy colluvium and sandy deposits overlying sandstone bedrock.

Figure 7 depicts the spatial compositional variability in soils, based on interpolated concentrations across the study area. Overall, the soils with the highest SiO_2 contents are found in the southern half, whereas the lowest SiO_2 contents occur in the northwest corner of the study area. Conversely, the soils with the highest CaO and MgO contents are present in the northwest corner and the lowest CaO and MgO contents are in the southern half of the study area. The highest Fe_2O_3 and Al_2O_3 compositions are found in soils from the west and north-central parts of the study area, and the highest P_2O_5 contents are located in the west and northwestern corner. Of note are soil samples DR-1, Lot-19-2, and Lot 20, which contain the lowest percentages of SiO_2 (62.09−45.16%), the highest LOIs (7.95−19.09%), and elevated concentrations of MgO (1.27−6.94%) and CaO (1.14−9.82%) relative to the rest of the soil samples. These compositions reflect the dolostone and dolomite-rich sandstone bedrock influence on the soils of these vineyard plots, caused by dissolution of primary minerals during rock weathering. Forested ridges underlain by dolostone of the Ordovician Prairie du Chien Group border the east boundary of the vineyards, and weathered outcrops of dolomite-rich sandstone are observed approximately 2 km to the northeast, along Highway 60.

The major element chemistry was used to assess the general spatial distribution and degree of chemical weathering at the local scale in the vineyard soils (Fig. 8). Ratios of mobile elements (Ca, Mg, K, Na, Sr, and Ba used as proxies for primary minerals) to the immobile elements Ti and Zr were calculated and interpolated across the study area. Generally, the ratios of CaO/TiO_2, MgO/TiO_2, Sr/Zr, Ba/Zr, and to a lesser degree K_2O/TiO_2, representing minerals such as calcite, dolomite, plagioclase, hornblende, and mica, increase toward the northwest, indicating greater chemical weathering in the northern, eastern, and southern areas of the property. In the north and east, greater chemical weathering correlates with areas of steeper slope, thinner soil, shallower depth to bedrock, and highest soil silt content, where the vineyards producing the lowest yields and highest quality grapes are located. Wollersheim Winery winemaker, Philippe Coquard, states that the grapes from these vineyard plots (Lots 10A/B, 11 [not sampled], and Domaine Reserve) consistently produce the lowest yields and reach the highest sugar levels. With average Brix (estimated concentration of dissolved sugar) values of 21.5, average pH values of 3.31, and average yields of approximately

5 to 6 tons per acre, these grapes consistently achieve a perfect balance of sugar and pH levels at harvest, and produce wines with robust fruit flavors and concentrated aromas (P. Coquard personal communication March 15, 2016). In the southern part of the property, the vineyards are characterized by soils with higher sand content, intermediate elevations, and flatter slopes; these vineyards produce the highest grape yields (approximately 7 to 8 tons per acre) and softer wines with delicate, lighter flavours (P. Coquard personal communication March 15, 2016). Overall, these are typical economic crop yields for hybrid grapes that have been optimized and proven successful for Wollersheim Winery in terms of maintaining a balance between profitability and grape and wine quality, while meeting the demand for sensible local wines.

Vineyard Variability Study at Domaine Reserve and Lot 19

The 1.6-acre Domaine Reserve and 1.4-acre Lot 19 plots, both planted with Marechal Foch grapes, were selected for further investigation by means of geophysical methods and vine trunk circumference measurements. Both plots have a southwesterly aspect, with slopes of 21% at Domain Reserve and 10% at Lot 19. The geophysical surveys provide measurements of apparent ECa and its inverse, ER, which are correlated with soil moisture, clay content and mineralogy, rock fragments, bulk density, porosity, and other soil properties (André et al. 2012). Vine trunk circumference measurements can be utilized to assess subsurface variability at the plot level and as a proxy for vine vigor, which can be correlated with grape characteristics (Imre and Mauk 2011).

Vine Trunk Circumferences

Vine trunk circumferences were measured at Domaine Reserve and Lot 19 in September 2014. The Domaine Reserve vines were planted in 1974, and the Lot 19 vines were planted in 1987. Measurements were collected from every vine on every other row, for a total of nine rows at each plot. The number of measurements collected was 437 at Domaine Reserve and 477 at Lot 19. Generally, vine trunk circumferences were similar between the two plots: median circumferences were 170 mm at Domaine Reserve and 190 mm at Lot 19 (Fig. 9). The Domain Reserve vine circumference data displayed slightly more variation, with a range of 300 mm compared to a range of 260 mm for the Lot 19 data.

Smaller vine trunk circumferences were observed at the uppermost three rows, at higher elevations near the top of the slope at Domaine Reserve. As uniform management practices are implemented at both plots, the variation in vine trunk circumferences between them reflects vine age, soil conditions (type, texture, and drainage), and topographic conditions (slope, elevation); it is also observed in grape yields, which are approximately 5 tons per acre at Domaine Reserve and 6 tons per acre at Lot 19. Wollersheim Winery's Philippe Coquard considers the age of the vines to be the dominant factor in the variation of vine trunk circumferences, although he insists that it is the combination of these factors (vine age, soil conditions, and topographic conditions) that ultimately creates these differences (personal communication, March 15, 2016). Larger circumferences in older vines may be expected if vine age alone were a determining factor, but the actual average measurements indicate that the younger vines of Lot 19 have the larger circumferences; it is clear, therefore, that the effects of age, soil, and topographic conditions combined outweigh the effects of vine age by itself.

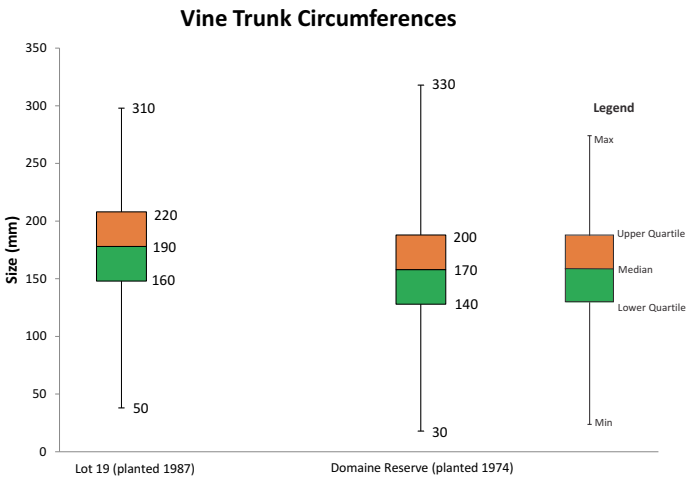

Figure 9. Box and whisker plots showing the trunk circumference measurements collected from Domaine Reserve and Lot 19; variations between the plots are a result of different vine ages, soil conditions, and topographic conditions.

Geophysical Surveys

EMI and ERT surveys were completed at Domaine Reserve and Lot 19 in May 2014. The survey measurements were utilized to determine spatial variations in the subsurface that can be used to map soil variations within each plot. The soils were likely saturated by spring precipitation at the time of the survey.

Figure 10 presents the horizontal (3 m) and vertical (6 m) soil ECa at 9.8 kHz measured in May 2014. Overall, the ECa values were relatively low, ranging from 7 to 68.75 millisiemens per metre (mS/m), and spatially correlated areas of similar ECa were noted at both plots. These areas generally coincide with the distribution of different soil types, as established by the USDA. The horizontal ECa measurements were generally similar between the two plots, ranging from 5 to 27.25 mS/m at Lot 19 and from 7 to 30.75 mS/m at Domaine Reserve, indicating relatively sandy surficial soils. Vertical ECa values ranged from 7.25 to 18 mS/m at Lot 19 and from 8 to 68.75 mS/m at Domaine Reserve. The highest vertical ECa values were encountered at Domain Reserve in the northeastern corner of the plot, which is underlain by the Gaphill – Rockbluff complex (well-drained sandy loams developed from loamy or sandy colluvium), and has steeper slopes and shallower soil (Fig. 11). An inverse relationship between ECa and depth to bedrock is observed here because soils developed from the underlying bedrock are generally more conductive than the bedrock, and groundwater at or above the bedrock interface may also increase conductivity. Philippe Coquard of Wollersheim Winery confirms that the shallow depth to bedrock restricts rooting depth and limits grape yields in this northeast

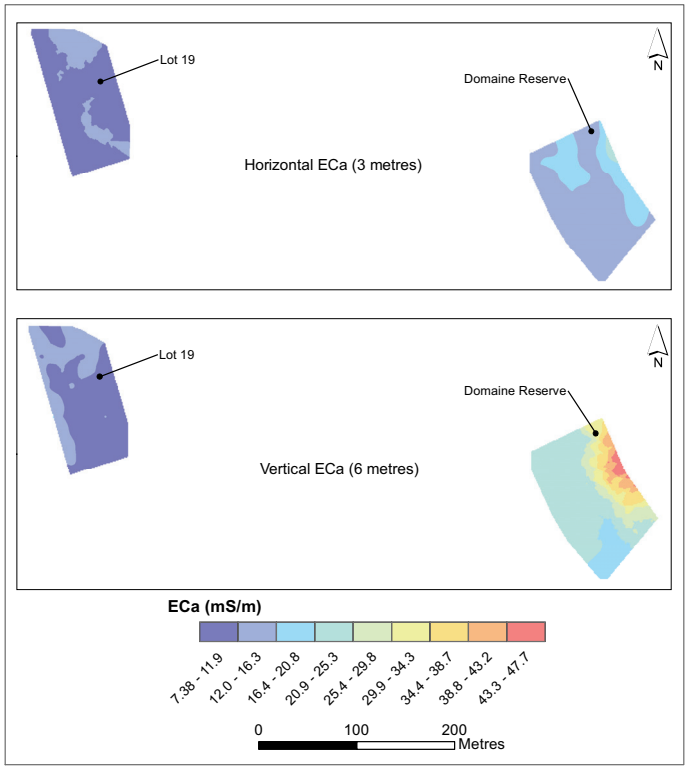

Figure 10. Map depicting the horizontal (3 m) and vertical (6 m) apparent electrical conductivity (ECa) measurements in soils at Domaine Reserve and Lot 19, demarcating areas of similar soil type at each plot. mS/m: millisiemens per metre.

portion of the plot, which also coincides with smaller vine trunk circumference measurements in this area.

Figures 12 and 13 illustrate the two resistivity profiles completed at each plot: one profile near the top row, and one profile near the bottom row of vines. Overall, the ER measurements can be correlated with the ECa data of the plots, with areas of high conductivity corresponding to low resistivity and vice versa. At Lot 19, the ER values were generally similar between the top (53–7433 ohm-m) and bottom (51−3850 ohm-m) rows. Although the top row of the Domaine Reserve plot revealed ER measurements (26−2821 ohm-m) similar to those observed at Lot 19, much higher resistivity values (25−31,551 ohm-m) were noted for the bottom row of vines, indicating the presence of a more resistive layer at lower elevations, near the foot of the slope. This highly resistive layer is encountered at a depth of approximately 12 m near the bottom row of vines at Domaine Reserve, indicating an increase in coarser soil textures with depth. These coarser textures at depth coincide with the centrally located gravel pit, consisting of stratified sand and gravel, and covering approximately 25% of the property. Based on well-log information from private wells drilled on the property, the stratified sand and gravel layer is laterally continuous and extends from 2 to 29 m below ground surface in the centre of the property and from 9 to 15 m below ground surface in the northeast part of the property. Based on the ER data, Lot 19 has a more homogeneous subsurface, compared to the Domaine Reserve plot, which shows much more variability between the top and bottom rows.

Overall, the ECa data corroborate the ER data at the Domaine Reserve plot, depicting more conductive/less resistive soils near the top row of vines, proximal to the Gaphill−Rockbluff complex, and more resistive/less conductive soils approximately 12 m deep near the bottom row of vines at Domaine Reserve. This indicates an increase in coarser soil textures with depth and coincides with the location of the stratified sand and gravel pit.

In addition to the differences established by geoelectrical methods, other plot characteristics such as elevation, slope, and vine age variations further differentiate the two plots. Specifically, the Domaine Reserve plot is situated at elevations of 259−305 m, has an average slope of approximately 20%, more soil textural variability across the plot, higher average clay and silt content, and vines approximately 42 years old. The grapes from Domaine Reserve have consistently higher sugar levels, with average Brix values of 21.13, average pH values of 3.29, and average yields of approximately 5 tons per acre, producing the best wines with robust fruit flavors and bold, concentrated aromas. In contrast, Lot 19 is located at lower elevations (213−259 m), has a gentler average slope of ca. 10%, less soil textural variability across the plot, higher average sand content, and younger vines approximately 29 years old. The grapes from Lot 19 attain intermediate sugar levels, have average Brix values of 20.07, average pH values of 3.28, average yields of approximately 6 tons per acre, and produce medium-bodied wines with pleasant fruit flavors and balanced aromas.

CONCLUSIONS

Wollersheim Winery is the birthplace of Wisconsin viticulture, a National Historic Site, and a leader in the Midwestern USA wine industry. Its location on a hill bordering the Wisconsin River marks the transition zone from glaciated terrain to the east to non-glaciated terrain to the west. The Wollersheim vineyards, with south and southwest-facing slopes and good air drainage, have well-drained soils dominated by silt- and sand-sized grains (silty loams and sandy loams). The vineyard soils are developed on parent materials consisting of windblown loess deposits, loamy outwash and glaciofluvial deposits underlain by outwash, and loamy colluvium and sandy deposits overlying sandstone bedrock.

The plant-available chemistry of the vineyard soils shows that the most variability and highest concentrations of calcium, magnesium, and potassium correspond to vineyard soils having the highest silt content in the northern and eastern parts of the property. The XRF total elemental chemistry of the vineyard soils reveals the most variability in SiO_2, CaO, MgO, Al_2O_3, and Fe_2O_3, reflecting the variety of parent materials in which the soils have developed. The soil mineralogy consists primarily of quartz, plagioclase, orthoclase, and dolomite, minor biotite and hornblende, and various clay minerals. The soil samples with the lowest SiO_2 compositions and the highest LOIs have elevated MgO and CaO contents, indicating a contribution from the weathering of dolostone or dolomite-rich sandstone bedrock in the soils of these plots, which are located in closest proximity to the bedrock outcrops. Based on a preliminary evaluation of chemical weathering

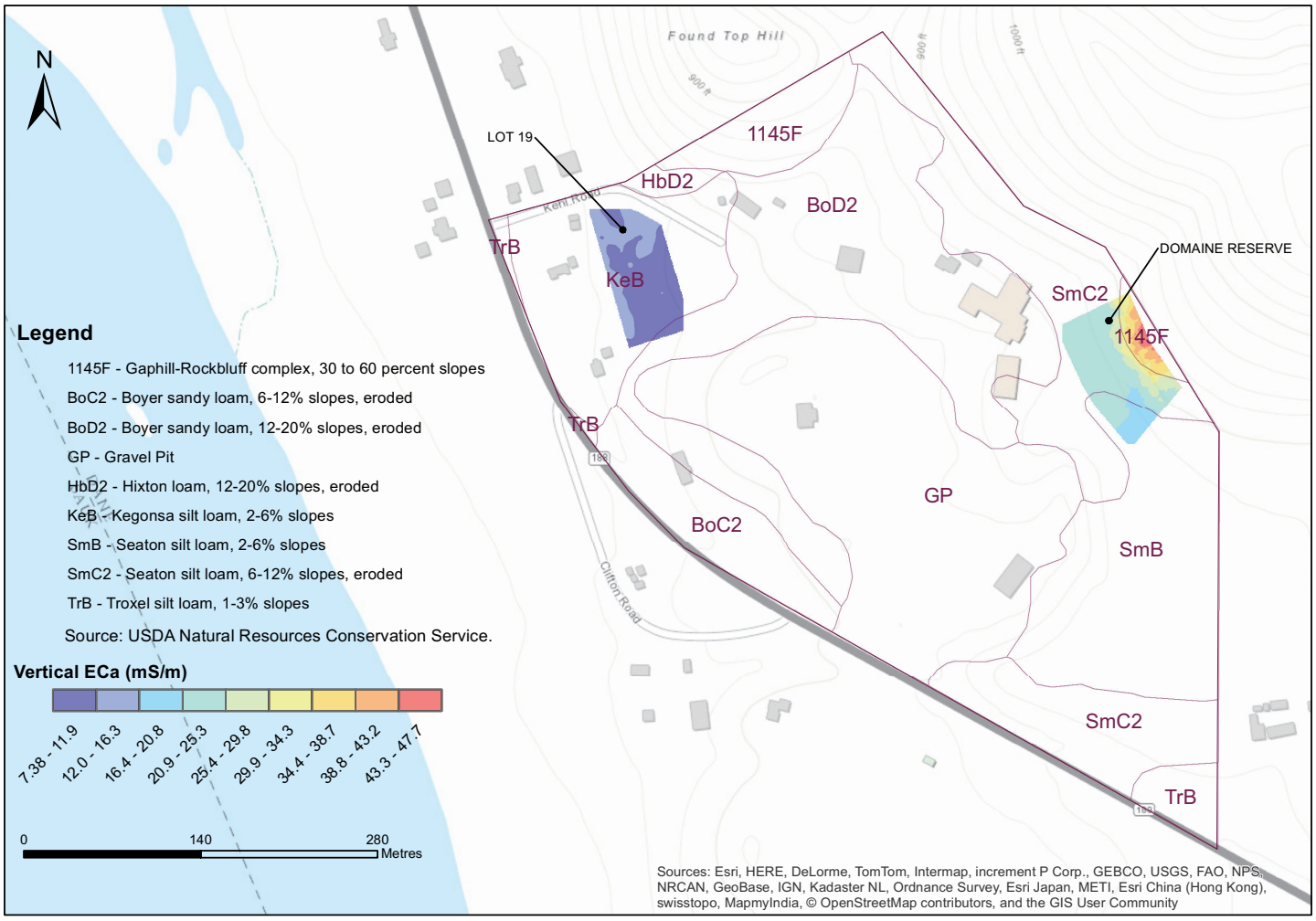

Figure 11. Map depicting the vertical (6 m) apparent electrical conductivity (ECa) measurements and soil types at Domaine Reserve and Lot 19; the area of highest ECa (the Domaine Reserve plot) coincides with steeper slope and shallower soil depth, restricting rooting depth and limiting crop yields in this area. mS/m: millisiemens per metre.

using ratios of mobile to immobile elements in the vineyard soils, an overall increase in chemical weathering is noted in the northern, eastern, and southern parts of the property. The areas of greater chemical weathering in the north and east are characterized by steeper slope, thinner soil, shallower depth to bedrock, and most silt-rich soils. They also display the highest plant-available calcium, magnesium, and potassium, and coincide with the location of vineyards producing the highest quality grapes.

Vineyard geophysical surveys at the Domaine Reserve and Lot 19 plots demonstrate spatial variations within the subsurface at the plot level, demarcating soil variations within each plot. The ECa data corroborate the ER data, indicating more soil textural variability and higher average clay and silt content for the Domaine Reserve plot, and less textural variability and higher average sand content for Lot 19. Additional characteristics, such as elevation, slope, and vine age variations further differentiate the two plots. Thus, the terroir of the Domaine Reserve plot, consisting of more heterogeneous soils with a greater degree of chemical weathering, higher elevation, steeper slope, and older vines, produces the lowest yields, the best quality grapes, and the rich, full-bodied Domaine Reserve wine, whereas the terroir of Lot 19, comprising more homogeneous soils with the lowest degree of chemical weathering, lower elevation, gentler slope, and younger vines, produces slightly higher yields, good quality grapes, and the medium-bodied Domaine du Sac wine.

With an increasing demand for wine and an expanding local consumption movement across the state, the future of viticulture in Wisconsin looks promising, with new wineries opening and larger acreage of grapes being cultivated throughout the state to meet the demand for Wisconsin wine. As climate change continues to affect the selection of cultivated grape varieties, Wisconsin holds a great potential for cultivating quality cool-climate European varieties, in addition to the American and French–American hybrids currently dominating the state's grape production. Future work focused on selecting the proper hybrid not only for the appropriate climatic conditions, but also for the specific soil type, will aid in further refining our understanding of the optimal terroir conditions for cultivating quality cold-climate grapes.

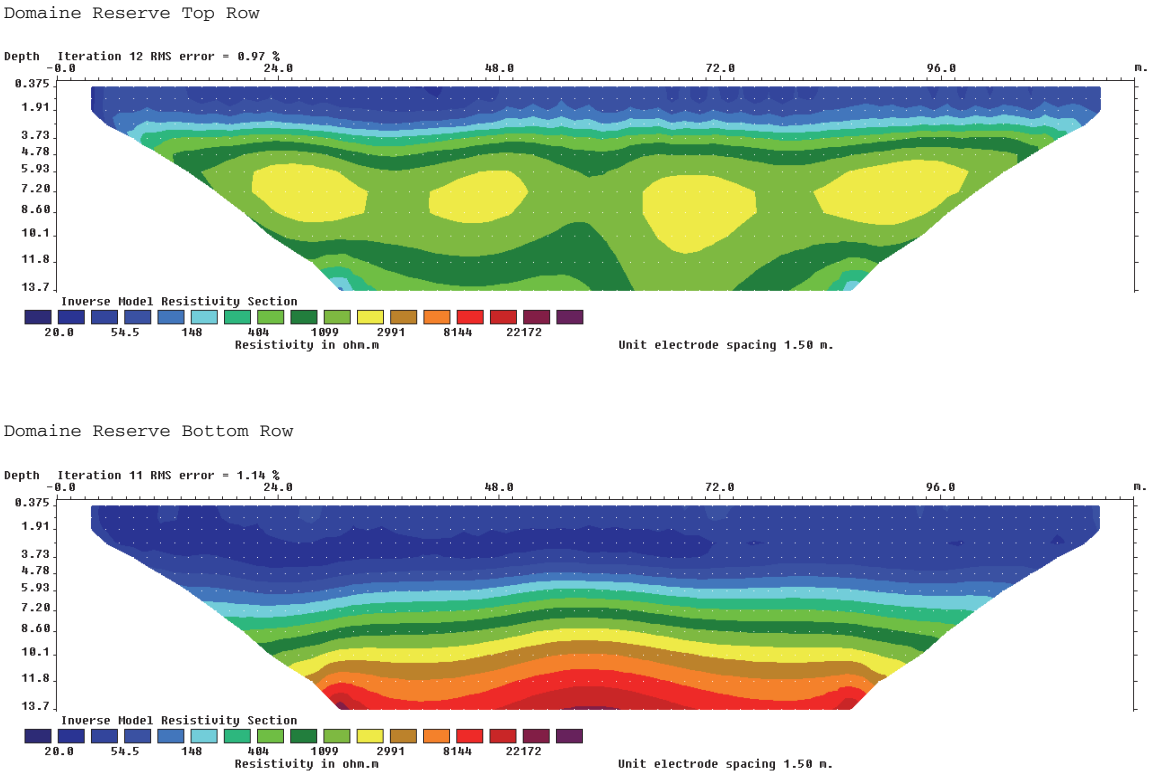

Figure 12. Figure illustrating the soil apparent electrical resistivity (ER) measurements (in ohm-m) for the two resistivity profiles completed at Domaine Reserve; the highly resistive layer at Domaine Reserve's bottom row indicates an increase in coarser soil textures with depth.

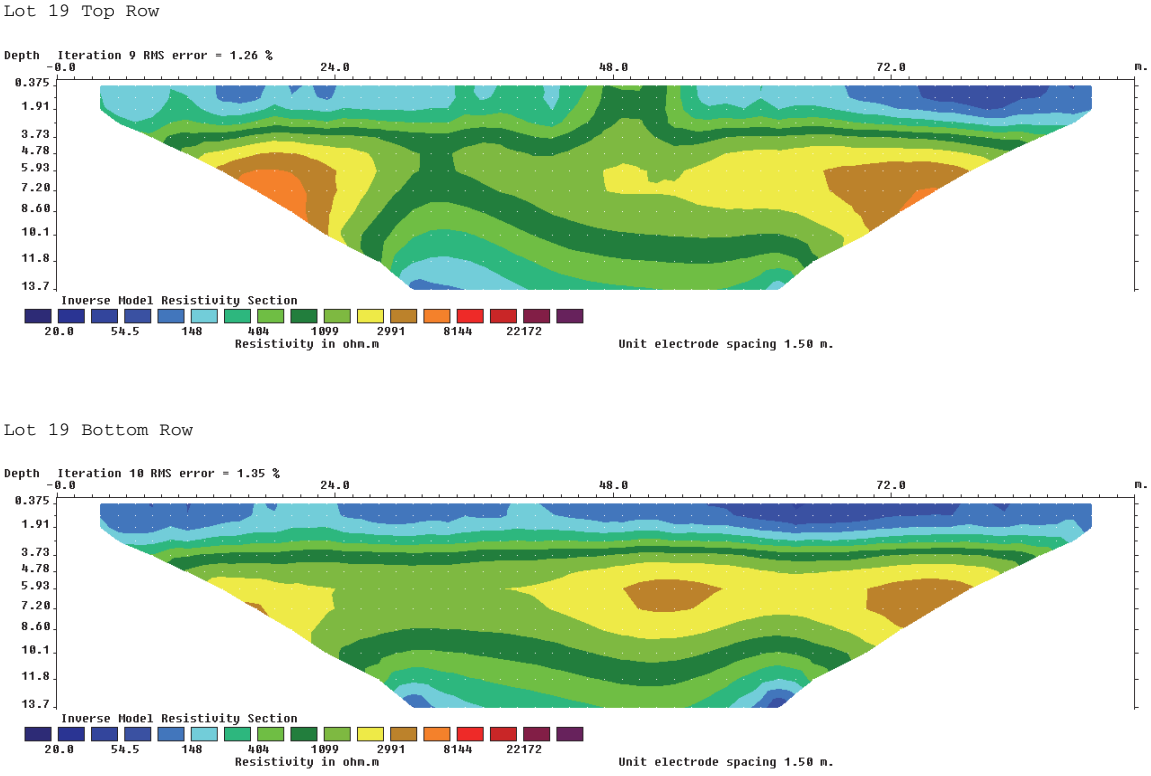

Figure 13. Figure illustrating the soil apparent electrical resistivity (ER) measurements (in ohm-m) for the two resistivity profiles completed at Lot 19; similar ER values between the top and bottom rows indicate a homogeneous subsurface.

ACKNOWLEDGEMENTS

The authors acknowledge Philippe Coquard, winemaker at Wollersheim Winery, and the Wollersheim team for sharing our passion for terroir, providing vineyard access and soil samples, stimulating terroir discussions, and great tastings. We wish to express our appreciation to Michael Baierlipp for his assistance in the field with the geophysical surveys and sharing his knowledge of geophysics and geoelectrical methods. Many thanks to Lindsay McHenry for guidance on the XRF and XRD analyses, and to Elmo Rawling for the laser grain size analysis. We gratefully acknowledge critical reviewers Roger Macqueen and Larry Meinert for their insight, thoughtful comments, and valuable suggestions that considerably improved the original manuscript.

REFERENCES

André, F., van Leeuwen, C., Saussez, S., Van Durmen, R., Bogaert, P., Moghadas, D., de Rességuier, L., Delvaux, B., Vereecken, H., and Lambot, S., 2012, High-resolution imaging of a vineyard in south of France using ground-penetrating radar, electromagnetic induction and electrical resistivity tomography: Journal of Applied Geophysics, v. 78, p. 113–122, http://dx.doi.org/10.1016/ j.jappgeo.2011.08.002.

Attig, J.W., Bricknell, M., Carson, E.C., Clayton, L., Johnson, M.D., Mickelson, D.M., and Syverson, K.M., 2011, Glaciation of Wisconsin [fourth edition]: Wisconsin Geological and Natural History Survey, Educational Series, v. 36, p. 4.

Bowen, P.A., Bogdanoff, C.P., Estergaard, B.F., Marsh, S.G., Usher, K.B., Smith, C.A.S., and Frank, G., 2005, Geology and Wine 10. Use of geographic information system technology to assess viticulture performance in the Okanagan and Similkameen valleys, British Columbia: Geoscience Canada, v. 32, p. 161–176.

Clayton, L., and Attig, J.W., 1997, Pleistocene geology of Dane County, Wisconsin: Wisconsin Geological and Natural History Survey Bulletin, v. 95, p. 64.

Dami, I., Bordelon, B., Ferree, D.C., Brown, M., Ellis, M.A., Williams, R.N., and Doohan, D., 2005, Midwest grape production guide: Ohio State University Extension, Bulletin 919, Columbus, OH, 155 p.

GPO Electronic Code of Federal Regulations, 2015, Approved American Viticultural Areas: 9.146 Lake Wisconsin: Electronic Code of Federal Regulations, U.S. Government Publishing Office, Washington, DC. Accessed 05/10/2015.

Haynes, S.J., 2000, Geology and Wine 2. A geological foundation for terroirs and potential sub-appellations of Niagara Peninsula wines, Ontario, Canada: Geoscience Canada, v. 27, p. 67–87.

Imre, S.P., and Mauk, J.L., 2009, Geology and Wine 12. New Zealand Terroir: Geoscience Canada, v. 36, p. 145–159.

Imre, S.P., and Mauk, J.L., 2011, Geophysics and wine in New Zealand, *in* Dar, I.A., *ed*., Earth and Environmental Sciences: InTech, online access: http://cdn.intechweb.org/pdfs/24548.pdf.

Jordan, T.D., Pool, R.M., Zabadal, T.J., and Tompkins, J.P., 1981, Cultural practices for commercial vineyards: New York State College of Agriculture and Life Sciences, A statutory college of the State University, at Cornell University, Miscellaneous Bulletin 111, 70 p.

Lambert, J.-J., Anderson, M.A., and Wolpert, J.A., 2008, Vineyard nutrient needs vary with rootstocks and soils: California Agriculture, v. 62, p. 202–207, http://dx.doi.org/10.3733/ca.v062n04p202.

Meinert, L.D., and Busacca, A.J., 2000, Geology and Wine 3. Terroirs of the Walla Walla Valley appellation, southeastern Washington State, USA: Geoscience Canada, v. 27, p. 149–171.

Meinert, L.D., and Busacca, A.J., 2002, Geology and Wine 6. Terroir of the Red Mountain appellation, central Washington State, U.S.A.: Geoscience Canada, v. 29, p. 149–168.

Meinert, L.D., and Curtin, T., 2005, Terroir of the Finger Lakes of New York (Abstract): The Colorado College, Extended Abstracts, 18th Keck Symposium, Colorado Springs, p. 34–40.

Mickelson, D.M., 2007, Landscapes of Dane County: Wisconsin Geological and Natural History Survey Educational Series v. 43, p. 36; map (07-6).

Mickelson, D.M., Knox, J.C., and Clayton, L., 1982, Glaciation of the Driftless Area: An evaluation of the evidence, *in* Knox, J.C., Clayton, L., and Mickelson, D.M., *eds*., Quaternary history of the Driftless Area: Wisconsin Geological and Natural History Survey Field Trip Guidebook, v. 5, p. 155–169.

Moyer, M., Moulton, G., and Henick-Kling, T., 2014, Growing winegrapes in maritime western Washington: Washington State University Extension, EM068E, 29 p.

Pinney, T., 1989, A history of wine in America: From the beginnings to prohibition: University of California Press, Berkeley, CA, p. 269–285.

Pogue, K., 2009, Folds, floods, and fine wine: Geologic influences on the terroir of the Columbia basin, *in* O'Connor, J., Dorsey, R., and Madin, I., *eds*., Volcanoes to Vineyards: Geologic Field Trips through the dynamic landscape of the Pacific Northwest: Geological Society of America Field Guide 15, p. 1–17.

Stiles, C.A., and Stensvold, K.A., 2008, Loess contribution to soils forming on dolostone in the Driftless Area of Wisconsin: Soil Science Society of America Journal, v. 72, p. 650–659, http://dx.doi.org/10.2136/sssaj2007.0112.

Swinchatt, J., 2012, Finger Lakes a new-found source of great intrigue: The world of fine wine, v. 38, p. 60–66.

Syverson, K.M., and Colgan, P.M., 2004, The Quaternary of Wisconsin: A review of stratigraphy and glaciation history, *in* Ehlers, J., *ed.,* The glacial stratigraphy of the northern U.S.: Elsevier, p. 289–305.

Taylor, V.F., Longerich, H.P., and Greenough, J.D., 2002, Geology and Wine 5. Provenance of Okanagan Valley wines, British Columbia, using trace elements: Promise and limitations: Geoscience Canada, v. 29, p. 110–120.

Tuck, B., and Gartner, W., 2014, Vineyards and wineries of Wisconsin: A status and economic contribution report: Regents of the University of Minnesota, Extension Center for Community Vitality, 51 p.

USDA. United States Department of Agriculture Natural Resources Conservation Service, Web Soil Survey data, http://websoilsurvey.nrcs.usda.gov/. Accessed 03/29/2015.

Wilson, J.E., 1998, Terroir: The role of geology, climate and culture in the making of French wines: University of California Press, 336 p.

Received August 2016
Accepted as revised September 2016

COMMENTARY

MARKING 50 YEARS OF THE WILSON CYCLE

Tuzo Wilson: An Appreciation on the 50th Anniversary of His 1966 Paper

John F. Dewey

University College Oxford
High Street, Oxford OX1 4BH, United Kingdom
E-mail: jfdeweyrocks@gmail.com

John Tuzo Wilson probably had a greater influence on the development of the earth sciences than any geologist since William Smith and Charles Lapworth. Prior to the early 1960's, he was a staunch anti-drifter but, in 1965, he pulled together many threads to create a cohesive paradigm that embraced continental drift, sea-floor spreading, subduction, and very large motions on transcurrent faults that defined the boundaries of and sites of relative motion between plates, the basis of what would come to be known as plate tectonics. Implicit in his analysis was the torsional rigidity of plates. Torsional rigidity means that plates have sufficient strength to avoid distortion in map view although they may be distorted along their edges (plate boundaries) and are more easily distorted by flexure in cross-section. Apart from the well-known contributions of Wegener (1929), Holmes (1931), Griggs (1939), Creer et al. (1958), Hess (1962), Runcorn (1962), Heezen (1960), Dietz (1961), and Vine and Matthews (1963), two lesser known and appreciated observations were instrumental in the formulation of plate tectonics. First, Harry Wellman (1955) already recognized that the Alpine Fault in New Zealand joined trenches with opposite polarities and is elongating. Secondly, Bert Quennell (1958) described the sinistral relative motion of Africa with respect to the Arabian Plate along the small circle of the Dead Sea Fault around a rotation pole near Gibraltar, implying torsional rigidity of the adjacent blocks. Simultaneously with Tuzo's 1965 paper, Bullard et al. (1965) assumed torsional rigidity to make finite difference rotations around poles of rotation, to achieve fits and minimizing misfits, between the continents around the Atlantic. McKenzie and Parker (1967) described the relative motion among the torsionally rigid Pacific, North American, and Gorda plates and the theory of plate tectonics was born. Tuzo's fundamental role

Figure 1. There are many 'official' pictures of Tuzo Wilson, but it seems more appropriate to use this lovely photograph by renowned Canadian photographer Harry Palmer, and we reprint it with his kind permission. Harry took splendid and candid photographs of many 'Companions of the Order of Canada,' and Tuzo was awarded this honour in 1969, three years after his famous paper.

came between 1962 and 1965 in his papers on the Cabot Fault (1962), and interpretations of oceanic islands (1963a) and Hawaii (1963b) as hot-spot tracks, culminating in his definitive 1965 paper that founded plate tectonics and his clever paper (1966) on the Caribbean and Scotia plates moving through gaps between continents and invading 'innocent' oceans with rifted margins. Strangely, Tuzo did not use rotation poles to describe relative motion among his global plate mosaic, in spite of the implicit rigidity of plates, even though used, explicitly, by Wellman, Quennell, and Bullard et al. Within a few years, plate tectonics was developed as a quantitative, integrated theory by McKenzie and Parker (1967), Morgan (1968), Le Pichon (1968), and Isacks et al. (1968).

Of great importance in tectonics, during this period, was Tuzo's 1966 paper, "Did the Atlantic close and then re-open?" (Tuzo enjoyed framing his papers as questions, which many journals no longer allow). In 1965, I was a young lecturer in Cambridge deeply absorbed in developing new courses in

Geoscience Canada, v. 43, http://www.dx.doi.org/10.12789/geocanj.2016.43.108 pages 283–285

structural geology and working on the geology of western Ireland, Nova Scotia, and Newfoundland. Both Harry Hess and Tuzo were on sabbatical leave in Madingley Rise, the then Department of Geophysics in Cambridge presided over by Teddy Bullard. I owe these three earth scientists more than I can say in transforming my approach to geology, in their advice to expand my horizons to include a global tectonic scale. Tuzo came into my room in the Sedgwick Museum many times for morning coffee and chats about regional and global geology, especially the relationship between structural geology and tectonics. One morning, with that inscrutable gentle smile that usually characterized his face, he announced "I have discovered a new class of fault." I confess that I was sceptical until he drew from his bag his now-classic paper model of a ridge-to-ridge transform and repeatedly opened and closed it under my nose. I was transfixed by the spectacle of a spreading ridge offset by a transcurrent fault that had the opposite sense of motion to that intuitively thought of as displacing the ridge axis along a classic transcurrent fault. Once seen, the pattern is obvious but was the most exciting thing in geology that I had witnessed in my short career thus far. It was even more fulfilling and instructive as Tuzo spent the next hour with me cutting up cards to illustrate the offsets along faults that connected trenches with the same and opposite polarities, ridges to trenches with ridge-facing and ridge-opposed polarities and several kinds of triple junction. Tuzo told me that he was about to publish all this as a coherent global model (his 1965 paper) and that he would introduce the term 'transform' for large-offset lithosphere-cutting faults that terminate at a ridge, trench or triple junction. Thus, he established the global pattern of continuous plate boundaries. I still have that model and the pieces of card (Bristol Board upon which I drew most of the illustrations for my papers until the digital revolution of Adobe Illustrator) as one of my most treasured possessions. As if all this was not enough, the following month Tuzo strode into my room and (paraphrasing) announced "my global model means that continents are carried around as passengers that oceans open with trailing rifted margins and close with collisions that make mountain belts. It seems to work for the Appalachian–Caledonian Orogenic Belt in relation to the Atlantic Ocean. The Orogen was probably developed by the closing of a Lower Palaeozoic ocean and split to form the present Central and North Atlantic leaving bits of the margins of the Lower Palaeozoic ocean (now termed Iapetus) on both sides of the present Atlantic." In 1973, Burke and Dewey coined the term 'Wilson Cycle' to describe the opening and closing of oceans. Tuzo showed me a draft of a paper that he had begun to write that appeared in *Nature* in 1966. This, together with my work with Art Boucot and Stuart McKerrow in Nova Scotia and Marshall Kay in Newfoundland in 1964, Bob Jastrow's Goddard Conference in New York in 1965 and further work in Newfoundland in 1966, developed my interest in trying to understand the Northern Appalachians and the British and Irish Caledonian Orogen. By serendipity, Chuck Drake was on sabbatical leave in Cambridge in 1966 and, knowing of my Appalachian interests, invited me to Lamont for a six month sabbatical leave in the second half of 1967. While in Lamont, the whole picture of plate tectonics was solidifying as a 'complete' theory with the work of Morgan, McKenzie and Parker, Le Pichon, Isacks et al., and Pitman. During the sabbatical, I developed a tectonic map of the Appalachian and Caledonian Chain, on a massive roll of tracing linen, upon which I plotted Lower Palaeozoic continental shelves/platforms, ophiolites, island arcs, subduction zones, collision zones and all the geological corollary hallmarks of

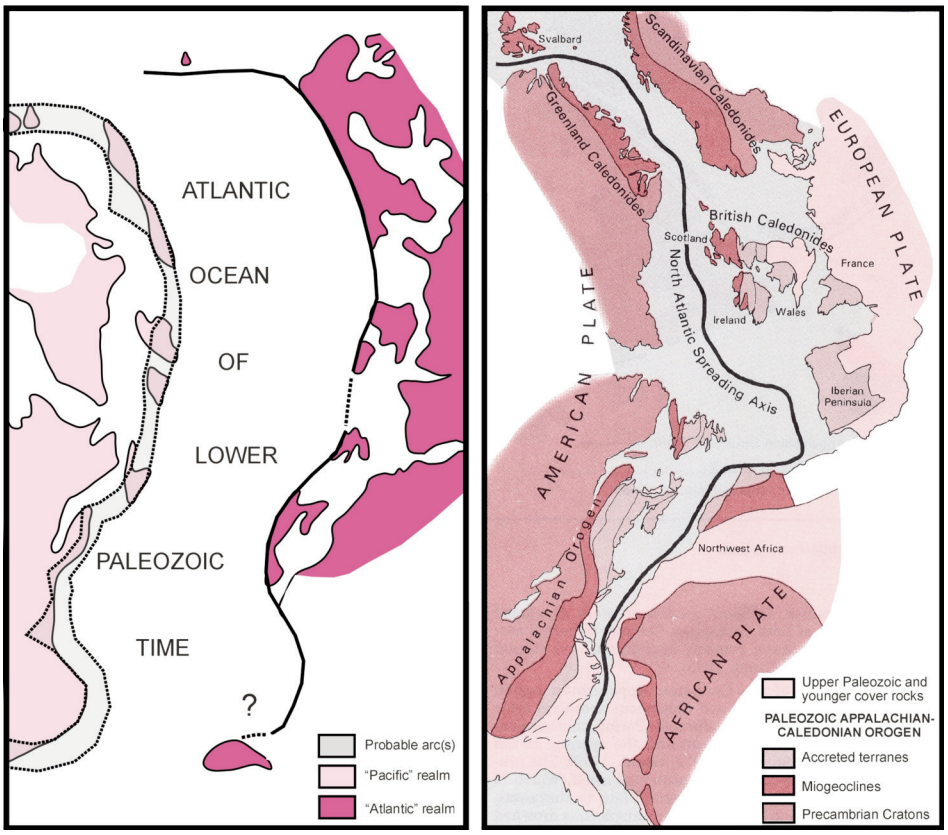

Figure2. The changing views of the North Atlantic borderlands.
On the left is a redrawn coloured version of the hand-drawn Figure 3 from Tuzo's 1966 paper in *Nature*, showing the concept of his "Atlantic Ocean of Lower Paleozoic time." We see the inference that parts of Scandinavia and the British Isles were once part of the North American continent, and that parts of eastern North America more properly belong with Europe or Africa. On the right is a later reconstruction of the Appalachian–Caledonian Orogen by Hank Williams, from the Decade of North American Geology volume (Williams 1995), showing the spreading axis of the modern North Atlantic. It incorporates more detail on the components of what we now call 'Iapetus,' but its heritage remains clear. This analysis remains a cornerstone of regional geology and tectonics in our 21st century, and it is a direct descendant of Tuzo's prescient thinking in 1966. Wilson's (1966) paper, "Did the Atlantic close and then re-open?" surely deserves recognition as one of the most influential contributions to geological science.

plate tectonics, which led to a string of papers, e.g. Dewey and Kay (1968), at the same time as those of many others, such as Atwater (1970), Hamilton (1969), and Smith (1971).

In all this, Tuzo was my main influence, inspirer, and principal encourager for which he has my eternal gratitude and respect. Like Bullard and Hess, Tuzo was a kind and generous man with his time, ideas, and encouragement of the young. His mind was quick, fertile, and imaginative with an astonishing capacity for organizing, analyzing, and synthesizing huge amounts of data. Above all, he was prepared to admit that he was wrong and changed his mind in a flash. He was brilliant at asking the right question and following it up with a prodigious amount of reading and plotting, seeing through and casting aside irrelevance, and linking apparently disparate notions and data coherently. He was always well-dressed in suit and tie with a polite but confident demeanor, seemingly happy and contented. He is remembered as a brilliant and original synthesizer who formulated global plate tectonics. He remarked to me and to Kevin Burke that, if he had known Euler's Theorem (a method of finding the simplest paths between once contiguous points), he would have 'nailed' plate tectonics cold. It is significant that Harold (Hank) Williams gained his PhD at the University of Toronto in 1961 under the supervision of Tuzo Wilson. Williams unleashed a productive period in our understanding of the geology of Newfoundland (e.g. Williams 1979) and the opening and closing of Iapetus. One might fairly say that Tuzo's 1965 paper changed the course of global tectonics and that his 1966 paper led to a complete new understanding of the implications of his 1965 paper for the origin of mountain belts resulting from super-continent cycles, the most important paradigm change in the history of geology.

REFERENCES

Atwater, T., 1970, Implications of plate tectonics for the Cenozoic tectonic evolution of western North America: Geological Society of America Bulletin, v. 81, p. 3513–3536, http://dx.doi.org/10.1130/0016-7606(1970)81[3513:IOPTFT]2.0.CO;2.

Bullard, E., Everett, J.E., and Smith, A.G., 1965, The fit of the continents around the Atlantic: Philosophical Transactions of the Royal Society London, v. A 258, p. 41–51, http://dx.doi.org/10.1098/rsta.1965.0020.

Burke, K., and Dewey, J.F., 1973, Plume-generated triple junctions (Abstract): EOS Transactions American Geophysical Union, v. 54, p. 239.

Creer, K.M., Irving, E., Nairn, A.E.M., and Runcorn, S.K., 1958, Palaeomagnetic results from different continents and their relation to the problem of continental drift: Annales de Geophysique, v. 14, p. 492–501.

Dewey, J.F., and Kay, M., 1968, Appalachian and Caledonian evidence for drift in the north Atlantic, *in* Phinney, R.A., *ed.,* The history of the Earth's crust: Princeton University Press, p. 161–167.

Dietz, R.S., 1961, Continent and ocean basin evolution by spreading of the sea floor: Nature, v. 190, p. 854–857, http://dx.doi.org/10.1038/190854a0.

Griggs, D., 1939, A theory of mountain-building: American Journal of Science, v. 237, p. 611–650, http://dx.doi.org/10.2475/ajs.237.9.611.

Hamilton, W., 1969, Mesozoic California and the underflow of Pacific mantle: Geological Society of America Bulletin, v. 80, p. 2409–2430, http://dx.doi.org/10.1130/0016-7606(1969)80[2409:MCATUO]2.0.CO;2.

Heezen, B.C., 1960, The rift in the ocean floor: Scientific American, v. 203, p. 98–110, http://dx.doi.org/10.1038/scientificamerican1060-98.

Hess, H.H., 1962, History of Ocean Basins, *in* Engel, A.E.J., James, H.I., and Leonard, B.F., *eds.,* Petrologic studies: A volume to honor A.F. Buddington: Geological Society of America, Boulder, CO, p. 599–620, http://dx.doi.org/10.1130/petrologic.1962.599.

Holmes, A., 1931, Radioactivity and Earth movements: Transactions of the Geological Society of Glasgow, v. 18, p. 559–606, http://dx.doi.org/10.1144/transglas.18.3.559.

Isacks, B., Oliver, J., and Sykes, L.R., 1968, Seismology and the new global tectonics: Journal of Geophysical Research, v. 73, p. 5855–5899, http://dx.doi.org/10.1029/JB073i018p05855.

Le Pichon, X., 1968, Sea-floor spreading and continental drift: Journal of Geophysical Research, v. 73, p. 3661–3697, http://dx.doi.org/10.1029/JB073i012p03661.

McKenzie, D.P., and Parker, R.L., 1967, The North Pacific: an example of tectonics on a sphere: Nature, v. 216, p. 1276–1280, http://dx.doi.org/10.1038/2161276a0.

Morgan, W.J., 1968, Rises, trenches, great faults, and crustal blocks: Journal of Geophysical Research, v. 73, p. 1959–1982, http://dx.doi.org/10.1029/JB073i006p01959.

Quennell, A.M., 1958, The structural and geomorphic evolution of the Dead Sea rift: Quarterly Journal of the Geological Society, v. 114, p. 1–24, http://dx.doi.org/10.1144/gsjgs.114.1.0001.

Runcorn, S.K., 1962, Palaeomagnetic evidence for continental drift and its geophysical cause: International Geophysics, v. 3, p. 1–40, http://dx.doi.org/10.1016/B978-1-4832-2982-9.50006-1.

Smith, A.G., 1971, Alpine deformation and the oceanic areas of the Tethys, Mediterranean, and Atlantic: Geological Society of America Bulletin, v. 82, p. 2039–2070, http://dx.doi.org/10.1130/0016-7606(1971)82[2039:ADATOA]2.0.CO;2.

Vine, F.J., and Matthews, D.H., 1963, Magnetic anomalies over oceanic ridges: Nature, v. 199, p. 947–949, http://dx.doi.org/10.1038/199947a0.

Wegener, A., 1929, Die Entstehung der Kontinente und Ozeane, 4th ed.: Braunschweig, Friedrich Vieweg and Sohn Akt. Ges., 231 p.

Wellman, H.W., 1955, New Zealand quaternary tectonics: Geologische Rundschau, v. 43, p. 248–257, http://dx.doi.org/10.1007/BF01764108.

Williams, H., 1995, Temporal and spatial divisions, *in* Williams, H., *ed.,* Geology of the Appalachian–Caledonian Orogen in Canada and Greenland: Geological Survey of Canada, Geology of Canada, 6, p. 21–44.

Williams, H., 1979, Appalachian Orogen in Canada: Canadian Journal of Earth Sciences, v. 16, p. 792–807, http://dx.doi.org/10.1139/e79-070.

Wilson, J.Tuzo, 1962, Cabot Fault, an Appalachian equivalent of the San Andreas and Great Glen faults and some implications for continental displacement: Nature, v. 195, p. 135–138, http://dx.doi.org/10.1038/195135a0.

Wilson, J.Tuzo, 1963a, Evidence from islands on the spreading of ocean floors: Nature, v. 197, p. 536–538, http://dx.doi.org/10.1038/197536a0.

Wilson, J.Tuzo, 1963b, A possible origin of the Hawaiian Islands: Canadian Journal of Physics, v. 41, p. 863–870, http://dx.doi.org/10.1139/p63-094.

Wilson, J.Tuzo, 1965, A new class of faults and their bearing on continental drift: Nature, v. 207, p. 343–347, http://dx.doi.org/10.1038/207343a0.

Wilson, J.Tuzo, 1966, Did the Atlantic close and then re-open?: Nature, v. 211, p. 676–681, http://dx.doi.org/10.1038/211676a0.

Wilson, J.Tuzo, 1966, Are the structures of the Caribbean and Scotia arc regions analogous to ice rafting?: Earth and Planetary Science Letters, v. 1, p. 335–338, http://dx.doi.org/10.1016/0012-821X(66)90019-7.

COMMENTARY

Did the Atlantic close and then reopen?: A commentary

Harold (Hank) Williams*

Department of Earth Sciences
Memorial University
St. John's, Newfoundland and Labrador, A1B 3X5, Canada

*Passed away September 28, 2010.

Tuzo Wilson's 1966 *Nature* paper entitled "Did the Atlantic close and then re-open?" is truly the major turning point in the history of ideas on the evolution of the Appalachian Orogen. For a hundred years, the Appalachian Orogen was the type geosyncline, and Appalachian evolution was viewed in fixist models of geosynclinal development. Contrasting faunal realms were always enigmatic and never properly explained by notions of land barriers. Equally enigmatic was the symmetry and two-sided nature of the Newfoundland cross-section that refuted the fixist idea that continents grew like trees by the outward addition of asymmetric peripheral rings. The Wilson Cycle of closing a proto-Atlantic Ocean, then re-opening the Atlantic Ocean provided an elegant and simple solution to these enigmas.

Wilson realized that island arcs existed on the North American side of the proto-Atlantic, such as the present Notre Dame Subzone in Newfoundland, and that the major faunal boundary lay to the east of these volcanic rocks. He also realized that the early Paleozoic continents may have touched in the middle Ordovician, "…*for thereafter the distinction between the Atlantic and Pacific faunal realms ceases to be marked."* One continent encroaching upon another in the middle and late Ordovician explained the former borderland concept of Charles Schuchert and Marshall Kay. Likewise, Kay's island arcs were most in evidence during the early Ordovician, the time of major proto-Atlantic closing.

Wilson also recognized irregularities in ocean closing, which occurs first at promontories, then at re-entrants, with resulting clastic wedges, and an overall change from early Paleozoic marine conditions to middle and late Paleozoic terrestrial conditions. The Taconic allochthons were also part of his ocean closing scenario. The proto-Atlantic was completely closed by the end of the Paleozoic, and major spreading of the Atlantic began in the Cretaceous.

Wilson then went on to trace the former course of the proto-Atlantic along the length of the Appalachian–Caledonian chain from Spitsbergen to Florida. This is no small task. It is encouraging to see that the contemporary Newfoundland analysis supported his views, and that even Tuzo had trouble finding a suture along the New England segment of the system. Northwest Africa was accommodated with ease as a Hercynian orogenic belt, in some respects symmetrical to the southern Appalachians.

An important corollary of the Wilson Cycle is that the assembly and eventual breakup of Pangaea must have been an event of major significance in world geology. This is certainly true in North America, where major orogenesis and accretion in the Cordilleran Orogen on the Pacific Margin corresponds to Atlantic opening.

Since the 1966 Wilson paper, we have emerged from fixist geosynclinal models that were entrenched in the literature for 100 years. Still, the Appalachian Orogen is full of surprises and there are many secrets yet to be revealed. As so aptly expressed by David Baird, how strange it is that the more we seem to find out, the horizon is still there, always inviting us to go closer. We have more problems now than our predecessors, before the advent of the Wilson Cycle. And where will the horizon be teasing us to approach in 25 or 50 or the next 100 years? Will we be then as far away from where we stand now as our present position is from the world of pre-Wilson Cycle practitioners?

Editor's Note

Hank wrote this eloquent commentary for a local conference held in St. John's in early 1992, to mark the 25th anniversary of Tuzo Wilson's landmark paper. Tuzo himself was of course the guest of honour. Those of us who were involved in the event remember it well, and a diverse assortment of guest speakers gave their own perspectives on the paper, and its influence upon later work in the Appalachians and elsewhere. I had actually forgotten about Hank's commentary until I found the 1992 conference program whilst fruitlessly searching for another document. After reading it again, it seemed only appropriate to include it here and provide it wider circulation. The current executive of the Newfoundland Section of GAC are thanked for giving permission to reprint a short piece that surely will demonstrate longevity.

Andrew Kerr

GAC-MAC: FIELD GUIDE SUMMARY

Kingston 2017: GAC–MAC Joint Annual Meeting Field Trips

Dawn A. Kellett[1] and Laurent Godin[2]

[1]Geological Survey of Canada
1 Challenger Drive, Dartmouth, Nova Scotia, Canada
E-mail: dawn.kellett@canada.ca

[2]Department of Geological Sciences and Geological Engineering
Queen's University, Kingston, Ontario, K7L 3N6, Canada
E-mail: godinl@queensu.ca

BACK TO WHERE IT BEGAN

The Department of Geological Sciences and Geological Engineering of Queen's University, in Kingston, Ontario, will host the 2017 Annual meeting of the GAC–MAC. The meeting will coincide with the 175th anniversary of the founding of the Geological Survey of Canada, which was established by the legislature of the Province of Canada in 1842, in Kingston, and with Canada's 150th anniversary celebrations. The local geology surrounding Kingston, commonly called the Limestone City, does not disappoint and multiple field trips associated with the meeting will take advantage of its unique location. Kingston is located at the eastern end of Lake Ontario, where the St. Lawrence River begins, draining the waters of the Great Lakes into the Gulf of St. Lawrence. The transition from lake to river occurs east of Kingston Harbour, where the nearly flat-lying Early Paleozoic limestone, rimming the eastern Lake Ontario basin, border against a NW-SE trending, low ridge of Grenvillian Precambrian basement rocks, locally known as the Frontenac Arch, which connects the southeastern Ontario part of the Canadian Shield with the Adirondack Massif of northern New York State. The crystalline basement rocks form a resistant ridge over which the St. Lawrence River flows northeastward from Lake Ontario, creating the 'Thousand Islands,' a well-known tourist and cottage region along the international border that now also includes a National Park.

The 2017 Kingston GAC–MAC meeting will provide seven field trip opportunities that span from Proterozoic geology to the present, and cover a wide range of Earth Sciences sub-disciplines, from geomorphology to hydrology, from Quaternary geology to metallogeny, and from tectonics to sedimentology. Trips range in length from one to five days, as homegrown as a day trip touring the local geology highlights of Kingston's environs, and as far-afield as a five day transect traversing the accreted terranes of the Newfoundland Appalachians.

Figure 1. Highly deformed tonalitic gneiss cross-cut by pegmatite dykes in the Grenville Province north of Kingston (Photo: Laurent Godin).

The one-day 'Bedrock to Beaches' field trip will take participants from Kingston to Prince Edward County and back. Along the way, participants will track one billion years of evolution of the Kingston region. They will contemplate metasedimentary rocks that were heated, squeezed, and intruded by granite ca. 1170 million years ago, sandstone deposited by rivers and wind ca. 490 million years ago, limestone and shale deposited in tropical seawater ca. 455 million years ago, faults that displaced the limestone perhaps 176 million years ago, drumlins shaped by a continental ice-sheet about 20,000 years ago, a shoreline created by a giant proglacial lake ca. 13,200 years ago, and a thin soil full of frost-heaved limestone nodules that nowadays nourishes many of the best vineyards in 'the County.'

Another one-day trip will explore local shallow neritic marine carbonate rocks on a tropical Ordovician Earth. Shallow water marine carbonate rocks are beautifully exposed in the Kingston area and many buildings in 'the limestone city' are made of these rocks. The easily accessible outcrops have been little altered since they were deposited ca. 450 million years ago and the components are easily visible making aspects of sedimentology, paleoecology, and diagenesis understandable to everyone. The carbonate rocks are world famous in this regard and have been studied for more than 150 years. The field excursion will visit sections exhibiting a range of paleoenvironments with plenty of time for illustration and discussion. Paleoceanography will range from arid tidal flats, through the paleothermocline, into interpreted cool water outer ramp storm and slope deposits. Fossils range from scarce to profuse reflecting changes in paleoseawater salinity and bottom paleotemperature. This trip has been used for many decades as a

Geoscience Canada, v. 43, http://www.dx.doi.org/10.12789/geocanj.2016.43.110 pages 287–289

Figure 2. Paleozoic boulder conglomerate unconformably resting on Grenvillian quartzite (Photo: Doug Archibald).

Figure 3. Precambrian–Paleozoic angular unconformity exposed in the Kingston area. The Grenvillian quartzite below is cross-cut by an offset mafic dyke, overlain by flat-lying Middle Ordovician limestone (Photo: Doug Archibald).

teaching tool for Queen's undergraduates and will be designed for participants who are neophytes, those who want to know more about carbonate rocks or those who are fascinated by this period in deep time. Travel will be by bus and ferry, with perhaps a libation stop.

Located adjacent to Highway 7, the Maberly shear zone is one of the most accessible structural features in the Grenville Orogen. It is also one of the oldest (*circa* 1162 Ma) and represents the boundary between the Composite Arc and the Frontenac–Adirondack belts. Beginning and ending in Kingston, this one-day trip will highlight the results of recent research along this boundary by the Ontario Geological Survey. The field trip will examine key outcrop exposures providing evidence of the tectonic, magmatic and metamorphic history of this boundary, including stops in the Sharbot Lake domain, Frontenac terrane, and the shear zone itself. Field trip discussions will focus on styles of metamorphism, magmatism, and metasomatism, complementing both the session on the *Metamorphic Architecture of Orogenic Belts* and the post-meeting trip on the *Tectonic and metamorphic architecture of the northeastern Composite Arc Belt and the Central Metasedimentary Belt boundary tectonic zone, Grenville Orogen*.

New modelling of the Laurentide Ice Sheet reveals the presence of more than 100 fast flowing ice streams. GAC–MAC 2017 will offer a three-day field trip travelling through the superbly exposed glacially-streamlined 'hard' and 'soft' beds of the former Ontario Ice Stream in southern Ontario and upper New York State. Participants on this trip will examine rock drumlins and mega-grooved limestone surfaces of the 'hard bed' seen immediately south of the border of the Canadian Shield and the down-glacier change to classic 'drift' drumlins composed of sediment of the ice stream's 'soft bed.' Participants will review variations in drumlin morphology using new imagery such as LiDAR, together with the stratigraphy where exposed along the Lake Ontario shoreline. The field trip will foster field discussion of the role of fast flowing ice streams in the subglacial evolution of rock and sediment bedforms in general, the relationship with landforms such as eskers and moraines, and implications for mineral exploration projects.

Another field trip will examine surficial processes in southern Ontario through a hydrogeology lens. This trip will traverse the Canadian Shield and Paleozoic geology of the eastern Lake Ontario Basin to highlight its contrasting style of erosion and sedimentation. The tour will review field evidence of the influence of bedrock lithology and structural control on micro/macro scales of erosional and depositional regimes. From the eroded shield and limestone terrains near Kingston, the tour will complete a loop to the northwest to the thick sediment terrain of the Peterborough drumlin field with its associated tunnel valleys and eskers. Sedimentary deposits, landforms and landscape architecture are integrated into regional conceptual models relevant to groundwater supply and management in the transitional sediment setting (thin to thick) of eastern Ontario.

What better way to follow through on the discussions from the theme session on the *Metamorphic Architecture of Orogenic Belts* than to examine a major tectonic boundary in the Grenville Orogen less than two hours drive from Kingston? This three-day field trip will begin and end in Kingston, and will highlight the results of detailed mapping, new airborne geophysical surveys, and geochemical and geochronological studies conducted by the Ontario Geological Survey between 2011 and 2015 along the northeastern part of the Composite Arc Belt and its boundary with the Central Gneiss Belt in Ontario. The field trip will examine key outcrops providing evidence of the tectonic, magmatic and metamorphic history of this notable area in terms of understanding the linkage between the gneisses of the Laurentian Margin (infrastructure) to the northwest and the Composite Arc Belt (both the suprastructure and the Ottawan orogenic lid) to the southeast. A key goal of the trip will be to foster field discussions on topics including its complex thrusting history, the recognition of ca. 1150 Ma metamorphism and magmatism in parts of the area, and the history of syenite magmatism, metasomatism, and rare element mineralization between 1080 and 1030 Ma.

The Newfoundland Appalachians trans-island field trip will take participants to some of the best-preserved ophiolites, mélanges and island arc terranes in the Appalachian mountain

belt. Crossing several suture zones, including the main Iapetus suture, participants will explore the tectono-stratigraphy of the various oceanic and micro-continental terranes and their complex tectonic interactions during successive accretion to a progressively expanding composite Laurentia from the Early Ordovician to Devonian. The trip will take participants from Stephenville to Gander, showing spectacular geology framed by the beauty and ruggedness of Newfoundland.

We do hope this menu of field trips will appeal to the broad geoscientific community and that you will visit Kingston for GAC–MAC 2017. See you next spring! Further information can be found at: http://www.kingstongacmac.ca/.

The 2017 Annual meeting of the GAC/MAC in Kingston will coincide with the 175th anniversary of the founding of the GSC in Kingston. The Geological Survey of Canada, Canada's oldest scientific agency, was established by the legislature of the Province of Canada in 1842, in Kingston, Canada West.

The Department of Geological Sciences & Geological Engineering at Queen's and the GSC will be hosting this celebratory event at Queen's University May 14-18, 2017.

www.kingstongacmac.ca See the website for further information on the program and events

http://www.dx.doi.org/10.12789/geocanj.2016.43.110

In Appreciation

2015–2016 GUEST EDITORS

Jaroslav Dostal
John Greenough
Stephen T. Johnston
Fran Haidl
Jeff Harris
Jim Hibbard
Roger Macqueen
Brendan Murphy
Jeff Pollock
Dolores Pereira
Brian Pratt
David Rudkin
Cees van Staal
Boswell Wing
Graham Young

2015–2016 REVIEWERS

Sandra Barr
Jean Bédard
Antony Berger
Peter Betts
Matthew Boyd
John Clague
Barrie Clarke
Ronald Clowes
Roy Coish
Maurice Colpron
Joel Cubley
Robert Dalrymple
Lawson Dickson
Jaroslav Dostal
Richard Ernst
Carol Evenchick
Timothy Fisher
Félix Gervais
Edward Ghent
Martin Gibling
Dan Gibson
Alan Glaner
John Greenough
Daniel Harlov
James Harrell
Robert Hildebrand
Paul Hoffman
Peter Hollings
Steven Hollis
Andrew Hynes
Rebecca Jamieson
Andrew Kerr
Roger Macqueen
Brian Marker
Franco Ajmone Marsan
Phil McCausland
Sandy McCracken
James McLelland
Lawrence Meinert
Dejan Milidragovic
Randy Miller
David Moynihan
Brendan Murphy
Godfrey Nowlan
Brian R. Pratt
Rob Raeside
Pierre-Simon Ross
Scott Samson
James Scoates
Ian Spooner
Cliff Stanley
H. Scott Swinden
Phillips Thurston
Loyc Vanderkluysen
John Waldron
Chris Yakymchuk

Thank you to the guest editors and reviewers who have contributed their valuable time and expertise to the scientific publishing and peer review process on behalf of the journal. We are very appreciative of your efforts and volunteered time in assisting the editor to make timely and informed decisions on the submissions published in 2015 and 2016.

REVIEW

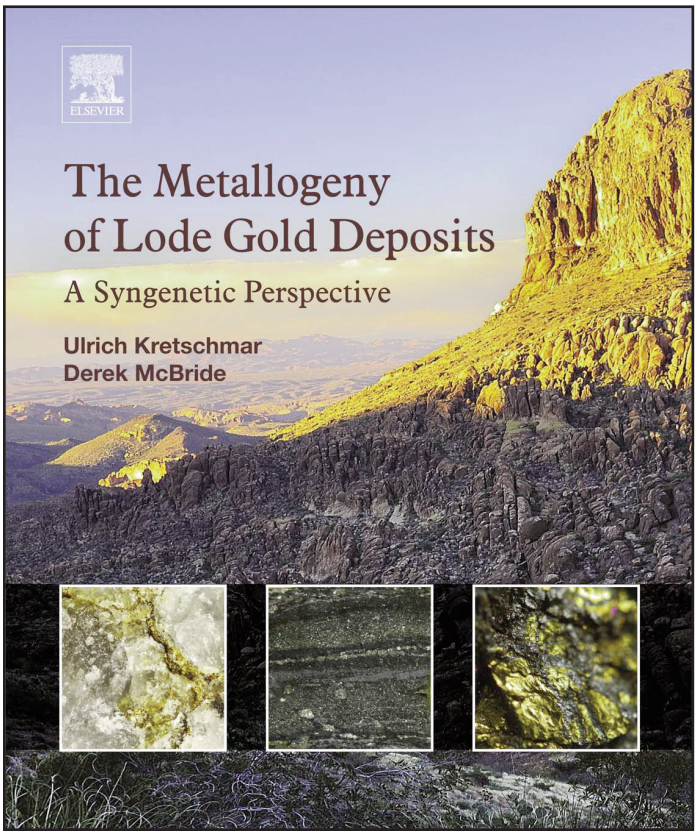

The Metallogeny of Lode Gold Deposits: A Syngenetic Perspective

Ulrich Kretschmar and Derek McBride

Publisher: Elsevier
Published: 2016; 350 p.
Print or eBook: $153 (USD)

Reviewed by Tony Christie
GNS Science
PO Box 30-368
Lower Hutt 5040, New Zealand
E-mail: t.christie@gns.cri.nz

The publisher's synopsis of this abundantly illustrated and colourful book of 350 pages claims that it "*presents a ground-breaking formation theory for lode vein gold deposits coupled with practical exploration guidelines*." The book is written by two Canadian exploration geologists Ulrich Kretschmar (who passed away in 2014) and Derek McBride, and their thesis is that lode gold deposits are syngenetic and were formed by hydrothermal fluids emanating on the seafloor and ponding in depressions. These fluids deposited ore minerals in a silica gel that later crystallized as quartz laminations conformable within the local sedimentary sequence. The main quartz veins of lode gold deposits, now mostly steeply dipping, were therefore originally flat lying, and their previously interpreted 'crack-seal' laminations represent sedimentary or diagenetically developed lamina. An underlying premise throughout the book is that the authors' approach is primarily based on field evidence that they have seen in outcrop and that they consider as not explained adequately by other genetic models.

As requested by the authors, I started reading this book with an open mind as I went through the various chapters that present the authors' evidence for syngenesis. Their evidence is mostly personal observations made whilst exploring lode gold and Volcanogenic Massive Sulfide (VMS) deposits in eastern Canada, along with some supporting information based on reviews of selected literature on these types of deposits and on modern seafloor massive sulphide systems. As a Kiwi geologist I was disappointed that the reviews made no mention of the New Zealand orogenic/mesothermal shear-zone lode gold deposits, particularly of the Reefton Goldfield, which clearly do not fit a syngenetic model because most of the quartz veins crosscut bedding, and bedding-parallel veins are rare. Nevertheless, I continued with an open mind rationalizing that maybe the authors were not suggesting that all lode gold deposits were syngenetic and that I should try and see the possibilities for some deposits in other parts of the world. Unfortunately, there is no world map included showing the lode gold deposits that the authors include in their syngenetic class.

Chapter 1 provides a review of various models for lode gold formation in an historical context, in some instances with the authors' comments on their views on the inadequacies of the models and how their syngenetic model would better explain specific characteristics. The chapter finishes with a discussion on syngenetic gold formation concepts, listing some factors that most geologists would consider to negate a syngenetic origin and then attempts to counter these. For example, radiometric dates of mineralization that are much younger than the sedimentary host rocks are dismissed as dating errors resulting from non-representative sampling or resetting of

ages by later thermal events such as igneous intrusions. I immediately thought of the extensive Ar–Ar dating done on the deposits in Victoria, Australia by Denis Arne, Frank Bierlein and others, that shows several periods of gold mineralization many millions of years after host rock deposition. Also, there is an enormous volume of literature on structural controls and development of lode gold deposits (e.g. contributions by Rick Sibson, Francois Robert and Stephen Cox) that is ignored or given only passing reference in review sections of the book, because the structural aspects are considered to postdate vein formation.

Chapter 2, *Interpreting Textures in Outcrop*, describes several features of lode gold deposits in the Ordovician turbidite rocks of the Meguma Group of Nova Scotia emphasizing the bedding-parallel nature of the main veins and suggesting that they are bedding-concordant. Crosscutting veins are considered as feeders to the bedding-concordant veins. The Archean deposit in the Kenty mine, Ontario, is also included to show an example of crosscutting 'feeder' veins and a link to Youtube videos on the Stawell and Morning Star mines in Victoria, Australia, both of which are definitely not syngenetic deposits. Chapter 2 also introduces the term 'gold cycle' that is explained in Chapter 3, *Introduction to Gold Cycles*. In this very short Chapter 3, the gold cycle concept envisages the quartz veins as part of sedimentary cycles such as Bouma-sequence turbidite units, with the quartz veins primarily associated with the fine sediment of pelagic or abyssal mud, ash or crystal tuff, and carbonate. Lamprophyres noted in many lode gold deposits are suggested to be mistakenly identified and to actually represent dark green or black chlorite-rich, fine-grained interflow sediments or tuff. Examples of gold cycle stratigraphy are given from Larder Lake and Timmins.

Chapter 4, *Field Examinations in a Variety of Gold Settings in Canada: The Meguma, Nova Scotia; Chester Twp and Beardmore, Ontario; Maskwa, Manitoba, and Nugget Pond, Newfoundland* is, as the title states, a series of geological descriptions of the above-named gold deposits. Many of the intrusive rocks of the Chester Complex are reinterpreted as basaltic to rhyolitic volcanic rocks and these enclose 'Gold Cycle' units. The descriptions of disseminated sulphides, sulphide bands and siliceous bands in some of the prospects do indeed conjure up images of VMS deposits. Mapped intrusive rocks of the Maskwa Pluton that host some large veins are also interpreted as originally volcanic rocks that have been metamorphosed to resemble plutonic rocks. Mafic dykes, lamprophyres and shear zones are reinterpreted as former pelagic-pelitic sedimentary units. I was impressed by photos of the Golden Mile vein in the Beardmore area that is 1.5 m thick, extends for > 1 km, and said to be hosted by mafic and felsic flows, and began to be swayed into considering a possible syngenetic origin for this one.

Chapter 5, *Why Lamprophyres Have No Role in Lode Vein Genesis*, uses examples in the Chester Complex, Maskwa Pluton and a few other locations to demonstrate that the lamprophyres in these areas studied by the authors are fine-grained 'Gold Cycle' interflow sedimentary units. This is partly done on the basis of geochemical data presented in several tables and in geochemical discrimination diagrams.

Chapter 6, *Felsic Volcanism Associated with Mineralization in the Chester Complex – Type Gold Deposits*, describes the Chester Complex volcanic rocks and their setting and then compares them to the Noranda Camp.

Chapter 7, *Understanding Hydrothermal Systems*, is a review of seafloor hydrothermal systems, the transport and deposition of silica and gold, and the role of carbon (graphite) in gold deposition. The Papua New Guinea Manus Basin and New Zealand Kermadec Arc, both of which are known to have gold-rich hydrothermal systems, are not mentioned.

Chapter 8, *The Role of Structural Geology and Remobilization*, describes the process of folding and cleavage development and then discusses shear zones as post-mineralization deformation, in contrast to accepted interpretations that the shear zone is the site of veining and mineralization in lode gold deposits. I found it confusing that the Heath Steele VMS deposit in New Brunswick was used as an example to show the negligible effects of remobilization on mineralization. A section of deformation of minerals and veins again confusingly includes some VMS examples, but has some excellent photos of folded veins in the Meguma Group. The chapter primarily aims to convince the reader that the structural aspects of lode gold deposits postdate mineralization. It didn't convince me.

Chapter 9, *Lode Gold Deposits: Their Geometry and Evidence For Seafloor Vent Systems*, uses maps, level plans and sections of lode gold deposits, mostly Canadian, taken from published and unpublished literature, to illustrate the geometry of the deposits and their geological setting. The selected deposits are ones in which the authors have 'personal experience' and hence many of the classic deposits where structural control is paramount are not mentioned.

Chapter 10, *Toward a Syngenetic Model and Vent Geometry*, develops the syngenetic model and includes sections on "Observations to aid exploration applications" and "Area selection." The titles offer promise, but the text is rather disappointing based mainly on distinguishing younging direction, stratigraphic correlation, 'vent tracing' based on the proportion of quartz (assuming this increases toward the seafloor vent), stratigraphic control, volcanic facies mapping and geochemistry to establish proximity to vents. Examples, where given, are only briefly described. Mostly this is a section of suggesting which exploration approaches might work. The area selection section is a generic list that applies to any mineral exploration so there is no specific advice in this list for syngenetic lode gold deposits. The chapter also includes a section on identifying and targeting volcanic rocks in units previously described as tonalite, trondhjemite and granodiorite, as well as a syngenetic classification of deposits and a recipe for using the model for target selection based on spatial relationships.

Chapter 11, *Comparisons, Conclusions, Suggestions for Further Work and Application of the Syngenetic Model*, summarizes many aspects of the preceding chapters and includes a table of characteristics of lode gold deposits comparing and contrasting the epigenetic and syngenetic interpretations. The chapter and book end with a short section on "The proof is in the success of the model in its positive application." It claims that application of the model was a key factor in the discovery of the

Nugget Pond deposit, the first gold find in the Bett's Cove Ophiolite Complex by a team led by McBride.

The authors' writing style is easy to read and chatty in many sections. There are a number of minor typos and errors in the text and figures, but none are critical. There is some repetition of information between sections and chapters, and three photos are produced twice in different chapters (Fig. 2.4 = Fig. 4.24; 2.5 = 4.26; 2.3 = 7.1). There are many instances of photos and tables that appear before their first mention in the text. I think the book would have benefited from more careful peer review and editing. I was supplied with a PDF version and printed it for my review. However, I found many of the field scene photos too small on the printed page to see what was illustrated and had to revert to the PDF to view the photos enlarged on screen. The review nature of some sections results in a large number of old references and many of the more recent references are unpublished exploration reports by the authors, giving the impression that the information is a bit dated. However, of the 568 reference listed in the references section 19% are from 2000–2009 and 11% are from 2010–2015. Nevertheless, references from the 1990s to recent publications on the genesis of orogenic gold deposits are limited and those included are mostly dismissed.

In conclusion, the book contains some informative photos and illustrations, some interesting but biased reviews of lode gold deposits, but an unconvincing development and description of the syngenetic model with little practical information for use in exploration. I recommend a quick look at a library copy, but I would be very disappointed if I had paid for my copy.

http://www.dx.doi.org/10.12789/geocanj.2016.43.112

ERRATUM

Magmatism and Extension in the Foreland and Near-Trench Region of Collisional and Convergent Tectonic Systems

Adam Schoonmaker, William S.F. Kidd and Tristan Ashcroft
(V. 43, no. 3, p. 159–178, http://www.dx.doi.org/10.12789/geocanj.2016.43.100)

An error occurred in the first line of the second column of page 173 concerning the subduction polarity of the Maine Acadian Orogeny. The sentence has been corrected and now reads "Here, we emphasize one inconsistent consequence of the west-dipping interpretation."

GEOSCIENCE CANADA

JOURNAL OF THE GEOLOGICAL ASSOCIATION OF CANADA
JOURNAL DE L'ASSOCIATION GÉOLOGIQUE DU CANADA

2016 VOLUME 43 GSCNA7 43 227-294
PRINT EDITION ISSN 0315-0941
ONLINE EDITION ISSN 1911-4850